国際水星探査計画ベピコロンボの最新状況と今後の計画

村上 豪 [1]; 早川 基 [2]; 藤本 正樹 [3]; BepiColombo MMO プロジェクトチーム 早川　基 [4]
[1] ISAS/JAXA; [2] 宇宙研; [3] 宇宙研; [4] -

Updated status and operations plans of the BepiColombo mission

Go Murakami[1]; Hajime Hayakawa[2]; Masaki Fujimoto[3]; HAYAKAWA, Hajime BepiColombo MMO Project team[4]
[1] ISAS/JAXA; [2] ISAS/JAXA; [3] ISAS, JAXA; [4] -

The ESA-JAXA joint mission BepiColombo is now on the track to Mercury. Two spacecraft for BepiColombo, 'Mio' (Mercury Magnetospheric Orbiter: MMO) and 'Bepi' (Mercury Planetary Orbiter: MPO), were successfully launched by Ariane-5 launch vehicle from Kourou in French Guiana on 20 October 2018. During the cruise to Mercury, in addition to two spacecraft MMO Sunshield and Interface Structure (MOSIF) and Mercury Transfer Module (MTM) are all integrated together. Commissioning operations of Mio and its science payloads, including the instruments with high-voltage power supply, have been done in November 2018 and May-August 2019. After these commissionings, we can more focus on preparing science operations for interplanetary cruise and planetry flybys. Some science instruments can be used even in the composit spacecraft configuration. The first and second flybys will happen at the Earth in April 2019 and at Venus in October 2019, respectively. We have started to discuss with wider science communities, e.g., heliospheric physics and Venus science. Here we report the updated status of BepiColombo mission, initial results of the commissioning operations, and the future strategy and plans for upcoming interplanetary cruise and planetary flybys.

太陽風イオンによるスパッタリングを利用した小型天体の遠隔質量分析

横田 勝一郎 [1]; 寺田 健太郎 [2]; 齋藤 義文 [3]; 西野 真木 [4]; 清水 久芳 [5]; 高橋 太 [6]
[1] 阪大; [2] 阪大・理・宇宙地球; [3] 宇宙研; [4] 名大 ISEE; [5] 東大・地震研; [6] 九大・理・地惑

Remote SIMS analyses of small body surface using the solar wind sputtering

Shoichiro Yokota[1]; Kentaro Terada[2]; Yoshifumi Saito[3]; Masaki N Nishino[4]; Hisayoshi Shimizu[5]; Futoshi Takahashi[6]
[1] Osaka Univ.; [2] Earth & Space Science, Osaka Univ.; [3] ISAS; [4] ISEE, Nagoya University; [5] ERI, University of Tokyo; [6] Kyushu Univ.

The ejection of the surface material is one of the unique features of airless small bodies in space. The solar wind sputtering ejects secondary ions from the surface, which reflect the abundance of the target materials. The amounts of the secondary ions are estimated to be enough compared with the sensitivities of typical spaceborne ion instruments for space plasma observations.

The KAGUYA that was equipped with ion analyzers observed the plasma environment around the Moon for 1.5 years. We used the KAGUYA data to estimate secondary ion fluxes emitted from the lunar surface. Although the mass resolution is not enough to clearly distinguish heavy metal ions from each other, the 1.5-year data provided the flux ratio and distribution maps of the secondary ions.

The abundances of the secondary ions by the sputtering do not directly reflect that in the targeted materials because the secondary ion yields depend on the ionization ratios. Therefore, standard samples are used for calibrations in laboratory SIMS analyses. However, we have no such standard samples for spacecraft observations of the secondary ions. In this study, we used the empirical model derived from experiments of secondary ions and a numerical model (SDTrimSP) to estimate the secondary ion yields. It was proposed that the ion flux ratios to Si+ are useful to investigate small bodies' surfaces. The empirical model showed that it is possible to determine whether targeted bodies are primitive or evolved by measuring the secondary ions. Indeed, KAGUYA data demonstrated the technique is possible.

Lander and rover explorations provide precise information on targeted bodies but they require larger costs and risks in their developments and operations compared to orbiter missions. Our findings show that secondary ion observation by orbiters also provide the information of the surface materials similarly to laboratory SIMS analyses. Such observations could achieve scientific results before landing operations and added wide-area data to precise data regarding limited areas obtained by landers and rovers.

天体表面物質の放出は、十分な大気や磁場を持たない宇宙空間に剥き出しの小型天体にとって特徴的かつ普遍的な現象である。特に太陽風によるスパッタリングは天体表面物質を物理的に削ることで構成物質を放出させるため、放出物が天体表面物質の情報を有することが期待されている。そのうちイオン化した放出物（二次イオン）の流量は、磁気圏観測衛星などに搭載される標準的なイオン分析器の検出限界を上回るという見積もりも提唱されている。

月周回探査機 KAGUYA にはイオン質量分析器が搭載されていて、約 1.5 年の間で月周辺のイオンが観測された。KAGUYA の観測データを用いて太陽風による天体表面起源の二次イオンの評価を行った。質量分解能 M/DM～20 は重イオンを明確に分別する上で十分ではないが、長期間の観測データを利用することで、二次イオンの組成比や流量分布を求めた。

スパッタリングという物理現象において、二次イオンの組成比は直ちに表面の組成比に変換することは出来ない。これは、二次イオンの放出には放出粒子のイオン化率が関わってくるためである。実験室の SIMS 分析ではイオン化率を求めるため標準試料を用いる。小型天体の観測において標準試料を用いることは困難であるため、経験モデルから求めた二次イオンの放出効率を今回は利用した。太陽風のエネルギー帯（～1 keV）でのスパッタリングは実験室プラズマにおける典型的なエネルギー領域（>10s keV）と比較してモデル化が遅れている。しかしながら、これまでの実験室での二次イオン放出の計測結果や最近の低エネルギー側に調整されたスパッタリングモデル（SDTrimSP）による結果から、Si ＋との比を採用することの有効性が提唱されるようになった。現時点では、二次イオンの観測から小型天体が始原的か進化を受けたかが判別できると見積もられている。今回の KAGUYA 観測データの解析からはその判別が可能であるという結果となった。

着陸機探査による観測は詳細な情報を提供するが、着陸探査は周回探査に比べて開発や観測運用により大きなコストとリスクを要する。今回の KAGUYA 観測データから、二次イオンの計測により周回軌道上から遠隔で天体表面の SIMS 分析が可能であることが示された。このことは、周回探査が着陸探査に対して事前に観測成果を保証し、かつ広域観測を着陸地に限られた詳細観測に追加する相補的な役割を果たせることも意味している。

水星の中性 Na 大気の生成に対する周辺環境の寄与

鈴木 雄大 [1]; 吉岡 和夫 [2]
[1] 東大・理・地惑; [2] 東大・新領域

Contribution of the environment for the generation of Hermann neutral sodium exosphere

Yudai Suzuki[1]; Kazuo Yoshioka[2]
[1] Earth & Planetary Science, Univ. Tokyo.; [2] The Univ. of Tokyo

Mercury has very tenuous collisionless atmosphere. Except hydrogen and helium, components of this atmosphere is thought to be emitted through four processes: thermal desorption (TD), photo-stimulated desorption (PSD), solar wind sputtering (SWS), and micro-meteorite impact vaporization (MIV). TD mainly causes where the surface temperature is high, such as perihelion and sub-solar point. Initial velocity of atoms emitted by TD follows Maxwell distribution of the surface temperature. PSD also causes around perihelion and sub-solar point, due to large UV flux. Emitted particles follow Maxwell distribution of approximately 1,500K.

SWS is likely to occur in mid- or high-latitude on the dayside, and releases atoms with Sigmund-Thomson distribution. MIV enhances in the leading hemisphere, which is dawn side, and emits particles following about 3,000K Maxwell distribution. Thanks to collisionlessness, atmospheric structure directly reflects spatial distribution and velocity distribution of released atoms. In other words, emission mechanism straightly links to the structure of atmosphere. Since contribution of each emission process is affected by surroundings such as the Sun, circumference environment can be estimated by scanning atmosphere.

From density profile assumed by the data taken by MESSENGER spacecraft, PSD is thought to be a main emission process of sodium, and MIV is thought to be that of calcium and magnesium. However, contribution of each emission process can be estimated only in low-latitude, since spacecraft gains data of line-of-sight integral of radiation, and it can observe limited range. Thus, it is necessary not only to analyze observation data but to construct theoretical model, in order to understand the emission processes of Hermann exosphere at different latitude.

In this research, global simulation of Hermann exosphere was constructed, considering above four emission processes in reference to previous experiments and observations. As a result, TD transported sodium from dayside to nightside, and prevented other processes from emitting sodium, especially around perihelion. This means that the variation of heliocentric distance or micro-meteoroid flux does not directly correlate with the emission rate by each process except TD. Based on this fact, the variation of amount and spatial distribution of Hermann exosphere is evaluated using my own model, and is compared with observation data by MESSENGER.

Sodium, calcium and magnesium was observed by MESSENGER/MASCS. In the future, my model is applied to calcium and magnesium, and compared with observation. This makes it possible to estimate precisely the contribution of MIV, which is thought to be a main emission process of these species. This research will realize the construction of general, versatile model of tenuous atmosphere.

水星は非常に希薄な無衝突大気を持つ。この大気を構成する原子のうち、水素・ヘリウム以外は主に表面から (1) 熱脱離 (2) 光励起脱離 (3) 太陽風イオンスパッタリング (4) 微小隕石衝突の 4 つの機構によって供給されると考えられている。熱脱離は特に近日点や太陽直下点等、表面温度が高い場所で生じ、放出される原子のエネルギー分布はその地点の温度に対応した Maxwell 分布に従う。光励起脱離も近日点や太陽直下点等、太陽からの紫外線フラックスの大きい場所で生じ、放出粒子のエネルギー分布は 1,500K 程度の Maxwell 分布に近似される。太陽風イオンスパッタリングは主に中高緯度で生じ、Sigmund-Thomson 分布に従って粒子が放出される。微小隕石衝突による蒸発は公転の進行方向にあたる朝方領域で生じ、放出粒子のエネルギー分布は約 3,000K の Maxwell 分布で近似できる。無衝突大気のため、大気構造には粒子が表面から放出される際の空間分布および速度分布が直接反映される。すなわち、表面からの放出機構と大気構造が直接結びつく。各放出機構の寄与は太陽等周辺環境に大きく左右されるため、大気構造から周辺環境を推定できる。

これまでに MESSENGER 探査機のデータを用いて各原子の鉛直分布が推定されており、Na は光励起脱離、Ca, Mg は微小隕石衝突が主放出機構であると考えられている。しかし、各原子の発光強度の視線方向積分のデータしか得られないことおよび探査機の軌道による観測範囲の制約から、主放出機構の推定は低緯度域に限られている。従って、他の緯度における水星大気の主生成機構を理解するためには観測データの解析のみならず、部分的な観測結果を説明できる理論モデルの構築が必要である。

本研究では最も発光強度が大きく観測データの多い Na について、これまでに行われてきた室内実験や観測結果をもとに上述の 4 つの放出機構を考慮した水星大気の全球シミュレーションを構築した。その結果、特に近日点付近では、熱脱離によって昼面の Na が夜面へ輸送され、他機構による放出量が大きく減少することが分かった。これは公転による水星と太陽との距離の変化や微小隕石フラックスの変動が、熱脱離以外の放出機構による大気生成量と直接相関しないことを意味する。これを踏まえ、太陽光強度や太陽風粒子フラックスおよび微小隕石フラックスの変化による水星大気量および大気分布の変動を自身の構築したモデルを用いて評価し、MESSENGER の観測データと比較した。

MESSENGER/MASCS では Na, Ca, Mg が観測されている。今後の研究では、本研究で構築したモデルを Ca,Mg に適用し、観測データと比較することで、水星の Na 大気への寄与は小さいが Ca, Mg の放出機構としては非常に重要で考えられる微小隕石衝突等の過程の寄与を正しく評価し、より一般的で汎用性の高い理論モデルの構築を目指す。

Sustainable dipolar morphology of a lunar dynamo driven by compositional convection

Fumi Hyodo[1]; Futoshi Takahashi[2]; Satoshi Kaneshima[2]; Hisayoshi Shimizu[3]; Hideo Tsunakawa[4]
[1] Earth and Planetary Sciences, Kyushu Univ.; [2] Kyushu Univ.; [3] ERI, University of Tokyo; [4] Dept. Earth Planet. Sci., Tokyo TECH

The paleomagnetic data of the Moon indicates that the lunar dynamo existed for a period of at least 4.2 to 3.56 Ga [Weiss and Tikoo, 2014]. As Laneuville et al. (2014) suggest that the inner core growth of the Moon is likely to last until now, we assume the lunar dynamo is caused by the chemical convection due to the ejection of light elements at the inner core boundary (ICB) upon core crystallization. In dynamo simulations, the Rayleigh number Ra and the Ekman number E are important parameters. We calculate them as a function of time with a help of thermal history model of the Moon [Sheinberg et al., 2015]. Besides, inner core size is varied discretely with respect to the radius ratio x=r_i/r_o, where r_i and r_o are the radii of the inner core and the outer core, respectively. Here, guided by our thermal history calculations, we focus on the range of x from 0.3 to 0.5, which roughly corresponds to the duration when the lunar dynamo is supposed to be in operation (i.e. 4.2 to 3.56 Ga). In this presentation, we report our dynamo simulation results in terms of two viewpoints about Ra and E. Firstly, parameters are given according to thermal evolution calculations, namely, (Ra, E) = ($1.1*10^4$, $2.0*10^{-4}$) at x=0.3, ($7.3*10^3$,$2.8*10^{-4}$) at x=0.4, and ($2.9*10^3$,$4.0*10^{-4}$) at x=0.5. Along this line, dipolar-dominant dynamos are obtained. Magnetic field strength at the lunar surface and dipolarity increase with increasing x. Secondly, only Ra is varied with E kept unchanged at $2.0*10^{-4}$ at x=0.3, $2.8*10^{-4}$ at x=0.4, and $4.0*10^{-4}$ at x=0.5. In the cases of Ra=$8.8*10^3$ at x=0.3, Ra=$6.1*10^3$ at x=0.4, and Ra=$2.4*10^3$ at x=0.5, the dipole component remains dominant at x=0.3 and 0.4, and then gives way to the non-dipole components at x=0.5. Magnetic field strength at the lunar surface and dipolarity have a maximum at x=0.4. The surface field at x=0.3 and 0.4 are about ten times stronger than that at x=0.5. These results show that the form of a lunar dynamo evolution changes greatly with the size of Ra given along our thermal history calculations.

ひさきで観測された木星オーロラの内因性準周期変動

垰 千尋 [1]; 木村 智樹 [2]; 土屋 史紀 [3]; 村上 豪 [4]; 北 元 [5]; 山崎 敦 [6]; 吉岡 和夫 [7]; 吉川 一朗 [8]; 笠羽 康正 [9]; 藤本 正樹 [10]
[1] 情報通信研究機構; [2] Tohoku University; [3] 東北大・理・惑星プラズマ大気; [4] ISAS/JAXA; [5] 宇宙科学研究所; [6] JAXA・宇宙研; [7] 東大・新領域; [8] 東大・理・地惑; [9] 東北大・理; [10] 宇宙研

Quasi-Periodic Variation of Jupiter’s Aurora Observed by Hisaki

Chihiro Tao[1]; Tomoki Kimura[2]; Fuminori Tsuchiya[3]; Go Murakami[4]; Hajime Kita[5]; Atsushi Yamazaki[6]; Kazuo Yoshioka[7]; Ichiro Yoshikawa[8]; Yasumasa Kasaba[9]; Masaki Fujimoto[10]
[1] NICT; [2] Tohoku University; [3] Planet. Plasma Atmos. Res. Cent., Tohoku Univ.; [4] ISAS/JAXA; [5] ISAS/JAXA; [6] ISAS/JAXA; [7] The Univ. of Tokyo; [8] EPS, Univ. of Tokyo; [9] Tohoku Univ.; [10] ISAS, JAXA

Quasi-periodic variation with a few day to several days is seen in energetic plasma and appearance of auroral spots in the Jupiter magnetosphere. Magnetospheric global re-configuration following periodic magnetotail reconnections is proposed for producing these periodicities. A previous work reported gradual increase and decrease of auroral power integrated over the pole region over 5-10 days with the peaks occurred during magnetotail disturbed periods. Hisaki is a space telescope launched by JAXA in 2013 and provides continuous observations of emissions from Jupiter auroral and Io plasma torus. We analyzed Jupiter aurora taken by a spectrometer EXCEED (Extreme Ultraviolet Spectroscope for Exospheric Dynamics) onboard Hisaki to investigate the statistical feature of the auroral periodic variation.

Auroral power revised by the rotational appearance shows periodic variation with gradual increase and decrease. We analyzed data observed over 2014-2016 which includes periods when Io’s volcanic activity was quiet (in 2014-2015) and high (in 2015). The auroral periodicity spreads from 1.3 to 7 days, which is comparable with the periodicity seen in other observations. The periodicity does not change significantly between the volcanic activity and quiet periods, while the association with the short-burst event increases during the volcanic active time. The periodicity does not show clear correlation with solar wind dynamic pressure, auroral power, central meridional longitude, nor Io phase angle. The periodic variation is continuously seen in the auroral modulation due to solar wind variation. A super-epoch analysis of the spectral information shows the symmetric increase and decrease trends of auroral power and magnetospheric source current, while the color ratio, which is a proxy for auroral electron energies, does not show significant variation associated with this periodic variation. Auroral power also shows asymmetric duration between increase and decrease phases as seen in the ion flux and spectral slope. We will discuss these characteristics and relationships in the presentation.

Spiral structure of hot electron in the inner magnetosphere of Jupiter

Fuminori Tsuchiya[1]; Ryo Arakawa[2]; Hiroaki Misawa[3]; Ryoichi Koga[4]; Reina Hikida[5]; Fumiharu Suzuki[6]; Kazuo Yoshioka[7]; Masato Kagitani[8]; Hajime Kita[9]; Tomoki Kimura[10]; Yasumasa Kasaba[11]; Go Murakami[12]; Ichiro Yoshikawa[13]; Atsushi Yamazaki[14]

[1] Planet. Plasma Atmos. Res. Cent., Tohoku Univ.; [2] Geophysics, Tohoku Univ.; [3] PPARC, Tohoku Univ.; [4] Geophysics, Tohoku Univ.; [5] the Univ. of Tokyo; [6] Complexity Science, Univ. of Tokyo; [7] The Univ. of Tokyo; [8] PPARC, Tohoku Univ; [9] ISAS/JAXA; [10] Tohoku University; [11] Tohoku Univ.; [12] ISAS/JAXA; [13] EPS, Univ. of Tokyo; [14] ISAS/JAXA

Io plasma torus is dense plasma region distributed around the orbit of the satellite Io and consists of sulfur and oxygen ions supplied from the satellite Io. The plasma torus persistently emits intense radiation in visible and ultraviolet wavelength ranges through electron impact ionization. This means that there exists persistent electron heating process that balances the intense radiative cooling in the plasma torus. However, the origin of the electron heating is still not resolved and has been one of outstanding problems of the Jovian magnetosphere. Here, we examined you 2-dimensional distributions of thermal electron temperature in the plasma torus based on the HISAKI satellite observation to visualize location of hot electrons injected in the torus and their subsequent transport. In this study, we used continuous data set of the plasma torus observed from Dec. 2014 to May 2015. In Jan. to Mar. 2015, a major volcanic event occurred at Io and input significant amount of mass to the plasma torus. To drive the electron temperature, we used a sulfur line ratio, SIV 65.7nm/SII 76.5nm. This is a useful proxy of not only ion density ratio, $S3^{+}/S^{+}$, but thermal electron temperature since the hotter electron temperature causes to increase charge state of ion. The radial distribution of the line ratio was obtained every $0.5R_J$ step from 5.0 R_J to 9.0 R_J from Jupiter. The azimuthal distribution was derived from rotational modulation of the line ration at each radial distance. Combining the radial and azimuthal dimensions, we obtained two-dimensional distribution of the electron temperature in the equatorial plane. Before the peak of the volcanic event (Feb. 2015), we found that high electron temperature region showed a left-handed spiral structure in the equatorial plane. This is explained by electron heating in a limited longitude range in the plasma torus and subsequent transport effect of both slow outward transport and the lagged azimuthal flow. This is consistent with a model proposed by Copper et al. (2016). On the other hand, spiral structure showed right-hand sense after the peak of the volcanic event. Further investigation is required for resolve origin of the opposite spiral.

Characteristics of Jupiter's decametric Riddle arcs observed by LWA and Juno

Kazumasa Imai[1]; Charles A. Higgins[2]; Tracy Clarke[3]; Masafumi Imai[4]; W.S. Kurth[5]
[1] NIT, Kochi; [2] Middle Tennesee State University; [3] Naval Research Laboratory; [4] University of Iowa; [5] Univ. of Iowa

The Riddle arcs were found in the dynamic spectrum of Jupiter's decametric radio emissions observed by the Voyager spacecraft [Riddle, 1983]. The Riddle arcs have the same slope at the same frequency and System III longitude on a frequency time plot. An isolated Riddle arc can be easily recognized inside of the Io-A arc structures. The emission of the Riddle arcs was determined to be from the instantaneous Io flux tube.

The modulation lane method [Imai et al., 2018] is based on the slope measurements of modulation lanes on the dynamic spectrum of Jupiter's decametric radio emissions. We usually measure the slope with a 1 MHz bandwidth and determine the most probable value of the lead angle between activated flux tubes to fit the value of the slope. We use this lead angle to calculate the longitudinal location of the magnetic field line of the radio emitting sources.

The Long Wavelength Array (LWA) is a low-frequency radio telescope designed to produce high-sensitivity, high-resolution spectra in the frequency range of 10-88 MHz [Clarke et al., 2014]. Using LWA data we analyzed the modulation lanes and the Riddle arcs and found that almost all of the Riddle arcs correspond to a zero-degree lead angle. This means that the radio sources related to the Riddle arcs are located along the instantaneous Io flux tube. This result is consistent with Riddle's conclusion.

With the advantage of Juno's unique polar orbit, the Waves instrument [Kurth et al., 2017] observed for the first time the polar beaming patterns and geometry of Jupiter's decametric radio emission sources. The dynamic spectra recorded by the Waves instrument from PJ1 (Aug. 27, 2016) to PJ16 (Oct. 29, 2018) show the Riddle arcs very clearly. The characteristics of these Riddle arcs are almost the same. The Riddle arcs occur during the time of positive jovigraphic latitude, and their existence implies sharp beaming from the northern hemisphere radio source. We consider this finding of Riddle arcs recorded by the Juno Waves instrument to be very important because it provides details of Jupiter's decametric radio emission around the instantaneous Io flux tube.

References:

Riddle, A.C., Identification of radio emissions from the Io flux tube,
Journal of Geophysical Research, Vol.88, pp.455-458, doi: 10.1029/JA088iA01p00455, 1983.

Imai, K., C.A. Higgins, M. Imai, and T.E. Clarke, Jupiter's Io-C and Io-B decametric emission source morphology from LWA1 data analysis, Planetary Radio Emissions VIII, edited by G. Fischer, G. Mann, M. Panchenko, and P. Zarka, Austrian Academy of Sciences Press, Vienna, pp.89-101, doi: 10.1553/PRE8s89, 2018.

Clarke, T.E., C.A. Higgins, J. Skarda, K. Imai, M. Imai, F. Reyes, J. Thieman, T. Jaeger, H. Schmitt, N. P. Dalal, J. Dowell, S.W. Ellingson, B. Hicks, F. Schinzel, and G.B. Taylor, Probing Jovian decametric emission with the long wavelength array station 1, Journal of Geophysical Research, Space Physics, Vol.119, pp.9508-9526, doi: 10.1002/2014JA020289, 2014.

Kurth, W.S., G.B. Hospodarsky, D.L. Kirchner, B.T. Mokrzycki, T.F. Averkamp, W.T. Robison, C.W. Piker, M. Sampl, and P. Zarka, The Juno Waves Investigation, Space Science Reviews, Vol.213, pp.347-392, doi: 10.1007/s11214-017-0396-y, 2017.

火星における宇宙放射線被ばくの予測

片岡 龍峰 [1]; 村瀬 清華 [2]; 佐藤 達彦 [3]; 塩田 大幸 [4]; 久保 勇樹 [4]; 三宅 晶子 [5]; 関 華奈子 [6]; 三好 由純 [7]
[1] 極地研; [2] 総研大・極域科学; [3] 原子力機構; [4] 情報通信研究機構; [5] 茨城高専; [6] 東大理・地球惑星科学専攻; [7] 名大 ISEE

Prediction of space radiation exposure on Mars

Ryuho Kataoka[1]; Kiyoka Murase[2]; Tatsuhiko Sato[3]; Daikou Shiota[4]; Yuki Kubo[4]; Shoko Miyake[5]; Kanako Seki[6]; Yoshizumi Miyoshi[7]
[1] NIPR; [2] Polar Science, SOKENDAI; [3] JAEA; [4] NICT; [5] Ibaraki College; [6] Dept. Earth & Planetary Sci., Science, Univ. Tokyo; [7] ISEE, Nagoya Univ.

We are setting the stage for human exploration to Mars. The purpose of this study is to quantitatively predict the radiation dose on the surface of Mars associated with galactic cosmic rays (GCRs) and solar energetic particles (SEPs). The required elements for the physics-based prediction are a) modeling GCR energy spectra in Mars orbit, b) modeling SEP energy spectra, c) air shower simulation of the Mars atmosphere with a + b as input to evaluate the radiation dose, d) Quantitative tuning by observation data set. The basic framework called WASAVIES has been developed for the Earth to combine them to realize the prediction (Kataoka et al., 2014, 2019; Sato et al., 2019). However, there are several points that require new development for adapting to Mars. One of the most challenging points is the low energy component of the SEPs, which has been neglected on Earth because of the strong geomagnetic field and thick atmosphere. It cannot be neglected on Mars because of the weak magnetic field and thin atmosphere. In other words, it is necessary to model the very complex variations of SEPs associated with the evolution of interplanetary shocks in the inner heliosphere, which has not been considered in the framework of WASAVIES. In this study, SUSANOO-CME model (Shiota and Kataoka, 2016) is introduced to solve this problem by reproducing and analyzing the interplanetary shocks in real time to find the physical limitation associated with the shock acceleration processes. In this talk, we will summarize the other potential problems of a, b, c and d, and report the current status of our development of Mars-version WASAVIES.

Kataoka, R., Sato, T, S. Miyake, D. Shiota, and Y. Kubo (2018), Radiation Dose Nowcast for the Ground Level Enhancement on 10-11 September 2017, Space Weather, 16, https://doi.org/10.1029/2018SW001874.

Sato, T, R. Kataoka, D. Shiota, Y. Kubo, M. Ishii, H. Yasuda, S. Miyake, I. Park, and Y. Miyoshi (2018), Real-Time and Automatic Analysis Program for WASAVIES: Warning System of Aviation Exposure to Solar Energetic Particles, Space Weather, 16, https://doi.org/10.1029/2018SW001873.

Shiota, D., and R. Kataoka (2016), Magnetohydrodynamic simulation of interplanetary propagation of multiple coronal mass ejections with internal magnetic flux rope (SUSANOO-CME), Space Weather, 14, 56?75, doi:10.1002/2015SW001308.

Kataoka, R., T. Sato, Y. Kubo, D. Shiota, T. Kuwabara, S. Yashiro, and H. Yasuda (2014), Radiation dose forecast of WASAVIES during ground level enhancement, Space Weather, 12, doi:10.1002/2014SW001053.

人間が火星に滞在する日も近い。本研究の目的は、銀河宇宙線や太陽プロトン現象に伴う火星表面での人体への被ばく量を、物理モデルにより定量的に予測することである。予測に必要となる要素は、a) 火星軌道における銀河宇宙線のエネルギースペクトルの物理モデル化、b) 太陽プロトン現象のエネルギースペクトルの物理モデル化、c)a+b を入力とした火星大気での空気シャワー計算による被ばく量の推定、d) 観測データによる定量チューニング、である。これらの 4 つの要素と、それらを組合わせて予測を実現するフレームワークについては、これまで我々が地球での宇宙放射線被ばく量の予測手法として開発してきた WASAVIES (Kataoka et al., 2014, 2019; Sato et al., 2019) を火星版として転用することで部分的に実現可能であるが、新規に開発が必要となる要素も複数ある。特に、b に関しては、地球では強い磁場でカットされ、厚い大気で吸収されるために無視してきた太陽プロトン現象の低エネルギー成分が、磁場の弱い火星ではカットされず、大気も薄いために火星表面にまで影響してしまうことが主な問題となる。つまり、これまで考慮してこなかった惑星間空間衝撃波による粒子加速によって太陽プロトン現象の顔ぶれが多様に変化してしまうことがモデリング上の問題である。そこで本研究では、SUSANOO-CME モデル (Shiota and Kataoka, 2016) で再現される惑星間空間衝撃波を準リアルタイムに解析し、衝撃波加速を考慮した物理的な制限をかけることで、この問題を解決することを目指す。本講演では、a,b,c,d それぞれの課題について整理し、火星版ワサビーズの開発の現状について報告する。

Internally generated ULF waves in the Martian magnetosphere

Yuki Harada[1]; Suranga Ruhunusiri[2]; Jasper S. Halekas[3]; Jared R. Espley[4]; Gina DiBraccio[4]; James P. McFadden[5]; David L. Mitchell[5]; Christian Mazelle[6]; Glyn Collinson[4]; David A. Brain[7]; Takuya Hara[5]; Masahito Nose[8]; Satoshi Oimatsu[9]; Kazuhiro Yamamoto[10]; Bruce M. Jakosky[11]

[1] Dept. of Geophys., Kyoto Univ.; [2] Univ. of Iowa; [3] Dept. Phys. & Astron., Univ. Iowa; [4] NASA GSFC; [5] SSL, UC Berkeley; [6] CNRS,IRAP; [7] LASP, Univ. of Colorado at Boulder, USA; [8] ISEE, Nagoya Univ.; [9] Kyoto Univ; [10] Geophysics, Kyoto Univ.; [11] LASP, CU Boulder

http://www-step.kugi.kyoto-u.ac.jp/members/staff/haraday.html

In contrast to relatively well studied upstream waves generated externally to the bow shock of Mars, the presence, sources, and consequences of internally generated ULF waves in the Martian magentosphere are yet to be properly identified. Here we investigate ULF waves driven by local proton instabilities in the Martian magnetosphere by utilizing magnetic field and plasma data obtained by MAVEN. In the dayside upper ionosphere and nightside magnetotail of Mars, MAVEN detected narrowband emissions in the predominantly compressional component near the local proton cyclotron frequency and its harmonics. The dayside waves are typically accompanied by ring/shell-like proton velocity distribution functions formed by injected hot protons of magnetosheath origin, and these waves are observed preferentially in the presence of dense ionospheric protons under high solar extreme ultraviolet (EUV) conditions. Meanwhile, the nightside waves tend to be observed when both of the solar wind dynamic pressure and solar EUV flux are high, leading to simultaneous enhancement of warm and cold protons in the magnetotail. The wave properties and their dependence on local and upstream conditions can be mostly explained by a proton Bernstein mode instability driven by a positive perpendicular slope in proton velocity distribution functions. We discuss potential implications of these waves for energization of ionospheric protons.

Effects of the intrinsic magnetic field on the ion loss from Mars at 3.5 Ga and 4.5 Ga

Ryoya Sakata[1]; Kanako Seki[1]; Shotaro Sakai[1]; Naoki Terada[2]; Hiroyuki Shinagawa[3]; Takashi Tanaka[4]
[1] Dept. Earth & Planetary Sci., Science, Univ. Tokyo; [2] Dept. Geophys., Grad. Sch. Sci., Tohoku Univ.; [3] NICT; [4] REPPU code Institute

Although Mars possessed a thick atmosphere in the Noachian period, Mars had lost the most part of the atmosphere and only have a thin CO_2 atmosphere today. Ion loss to space is one of the important processes of atmospheric escape from ancient Mars because the strong solar X-ray and extreme ultraviolet (XUV) flux and the harsh solar wind in the ancient day promotes the ion loss from the planet. On the other hand, ancient Mars had a global intrinsic magnetic field like the Earth. The existence of the intrinsic magnetic field changes the electromagnetic environment around the planet and thus affects processes and rates of the ion loss. However, the detailed effects are still in debate.

Our previous study investigated the ion loss from Mars under the extreme solar conditions at 4.5 Ga and the existence of dipole field with different strength based on the global multi-species magnetohydrodynamic (MHD) simulations. The solar XUV flux was 100 times higher than the present flux and the solar wind density, velocity, and the interplanetary magnetic field (IMF) strength were 1000 cm^{-3}, 2000 km/s, and 60 nT, respectively. The study indicates that the effects of the intrinsic magnetic field on the ion loss depends on whether the ionosphere is in the overpressure state. In the overpressure cases, where the solar wind dynamic pressure exceeds the sum of the maximum plasma pressure and the local magnetic pressure due to the intrinsic field in the ionosphere, the existence of an intrinsic magnetic field enhances the cusp outflow and increases the loss rates of molecular ions such as $O_2{}^+$ and $CO_2{}^+$. In the non-overpressure cases, however, the loss rates of molecular ions are reduced by two orders of magnitude. The effects on the O^+ loss rate are less pronounced than on molecular ions. This is because the mass-loading process at the extended oxygen corona created by the strong solar EUV flux contributes to the total O^+ loss and weakens the effects of the intrinsic magnetic field. We here investigated the effects of the intrinsic magnetic field on the ion loss from Mars under the more moderate solar conditions at 3.5 Ga in order to reveal how the effects of the intrinsic magnetic field depend on the solar XUV and solar wind conditions. We assumed that the solar XUV flux was 10 times higher and the solar wind density, velocity and the IMF strength were 70 cm^{-3}, 700 km/s, and 6.58 nT, respectively. We conducted simulations with different dipole field strength to compare the results in the overpressure cases and the non-overpressure cases.

Study of ion composition in the polar plume from Mars based on MAVEN observations

Kotaro Sakakura[1]; Kanako Seki[2]; Shotaro Sakai[2]; David A. Brain[3]; James P. McFadden[4]; Jasper S. Halekas[5]; Gina DiBraccio[6]; Bruce M. Jakosky[7]

[1] Dept. Earth & Planetary Sci., Science, Univ. Tokyo; [2] Dept. Earth & Planetary Sci., Science, Univ. Tokyo; [3] LASP, Univ. of Colorado at Boulder, USA; [4] SSL, UC Berkeley; [5] Dept. Phys. & Astron., Univ. Iowa; [6] NASA GSFC; [7] LASP, CU Boulder

Mars climate was warm and had water on its surface about 4 billion years ago, but there is no water on the surface at present. Escape of the atmosphere to space is considered as the main cause of this climate change. However, the mechanism of the large amount of atmospheric loss is far from understood. Ion escape is one of the important candidates of such mechanism. There are three channels of the ion escape, namely, tailward escape, pickup ion, and polar plume. Polar plume ions are accelerated by solar wind electric field and escape to +E hemisphere of the Mars-Sun-Electric field (MSE) coordinates. It is estimated by Dong et al., [2017] that the escape rate is 20-30% of the total ion escape depending on the solar EUV radiation. This is not negligible in order to understand ion escape from Mars. To fully understand the mechanism of polar plume, it is important to study the composition of the plume.

The purpose of this study is to investigate contribution of molecular ions (O_2^+ and CO_2^+) to the polar plume. The source of O_2^+ and CO_2^+ is the ionosphere only, while O^+ has the neutral corona as its source in addition to the ionosphere. Thus, contribution of molecular ions to the polar plume can be different from that of O^+. Spatial distribution of the ion number density ratio between O_2^+ and CO_2^+ is expected to change systematically if the plume is accelerated by electric field, since the trajectory of accelerated ions depends on the ion mass. We analyzed observation data by STATIC (Supra Thermal and Thermal Ion Composition), MAG (magnetometer) and SWIA (Solar Wind Ion Analyzer) onboard MAVEN (Mars Atmosphere and Volatile EvolutioN). STATIC can measure ion distribution functions with mass discrimination. We selected a few orbits, in which the plume with high CO_2^+ flux is observed continuously, from two years (from December 2014 to December 2016) of data. To derive CO_2^+ number density, we used a fitting method invented by Inui et al., [2018]. By fitting a log-normal distribution to O_2^+ count data, we eliminated O_2^+ contamination in the CO_2^+ mass range.

In the event on August 28, 2015, MAVEN moved from the nightside induced magnetosphere to dayside solar wind region in the +E hemisphere of the MSE coordinates. During this event, CO_2^+/O_2^+ number density ratio increased with increasing sunward distance in the main plume region. This tendency is consistent with the plume acceleration by the solar wind electric field as previously proposed. In this event, maximum O_2^+ and CO_2^+ fluxes are 1.2×10^6 and 3.6×10^6, respectively. These fluxes are about one order of magnitude higher than the average O^+ flux in the polar plume reported by Dong et al., [2017]. It should be noted that higher CO_2^+ flux than O_2^+ is partly caused by limited coverage of FOV (field of view) of STATIC during the plume event. In the event on December 17, 2016, in which the STATIC FOV was good, the maximum O_2^+ and CO_2^+ fluxes are 7.2×10^6 and 2.2×10^6, respectively. The higher maximum flux of O_2^+ than CO_2^+ is qualitatively consistent with ion species ratio in the source ionosphere. In order to discuss the acceleration and transport mechanism of the molecular ion plumes, we will also report on the results of ion trajectory tracings in the electric and magnetic field configuration obtained by multi-species global MHD simulation.

References:

Dong, Y., et al. (2017), *J. Geophys. Res. Space Physics, 122*, 4009-4022, doi:10.1002/2016JA023517

Inui, S., et al. (2018), *Geophysical Research Letters, 45*, 5283-5289, doi:10.1029/2018GL077584

Study of proton escape from Mars based on MAVEN observations

Yuki Mori[1]; Kanako Seki[1]; Shotaro Sakai[1]; Takuya Hara[2]; David A. Brain[3]; James P. McFadden[2]; Jasper S. Halekas[4]; Gina DiBraccio[5]; Francis G. Eparvier[6]; Bruce M. Jakosky[6]
[1] Dept. Earth & Planetary Sci., Science, Univ. Tokyo; [2] SSL, UC Berkeley; [3] LASP, Univ. of Colorado at Boulder, USA; [4] Dept. Phys. & Astron., Univ. Iowa; [5] NASA GSFC; [6] LASP, CU Boulder

Mars is considered to have had water on surface in ancient days, while there is no surface water at present. Escape of atmospheric gases to space is considered to play an important role in this climate change. Especially, hydrogen loss has substantially affected the water content on Mars. Its main mechanism is thought to be Jeans escape of hydrogen atoms. Hydrogen molecules, which are sourced from odd-hydrogen reactions with near-surface water vapour, diffuse to the upper atmosphere. Some of them are dissociated, diffuses to the exobase as hydrogen atoms and escape. Since this molecular hydrogen is long-lived, the seasonal variation of neutral hydrogen escape is predicted to be typically less than a factor of two (Krasnopolsky, 2006). However, Halekas (2017) provided quantitative estimates of the hydrogen exosphere for over one Mars year (MY), revealing about one order of magnitude seasonal changes in column density with a peak slightly after perihelion, approximately at the southern summer solstice. Lower atmospheric dynamics such as dust storms might be one cause of this peak. It was suggested by Heavens et al. (2018) that the transport of water vapour and ice to the middle atmosphere by deep convection in Martian dust storms can enhance hydrogen escape. Chaffin et al. (2017) suggested by using their photochemical model that hydrogen escape flux can increase by one order if there is water vapour in the middle atmosphere around 80km altitude.

If the Martian dust storms can enhance the hydrogen corona and escape by one order of magnitude, the proton escape sourced by neutral hydrogen will also increase. In order to assess the hypothesis, we will investigate proton escape from Mars based on MAVEN (Mars Atmosphere and Volatile EvolutioN) observations from November 2014 to March 2019. We will also investigate if the seasonal variation depends on size of the dust storms by comparing MY32, 33 and 34, since Martian global dust storm occurred only in MY34.

For this purpose, we implemented methods to separate planetary-origin protons from solar-origin protons. The separation methods utilize characteristics of phase space density (PSD) observed in investigated regions, i.e., solar wind, magnetosheath, and magnetotail wake, by STATIC (Supra Thermal and Thermal Ion Composition) instrument. For identification of each region, we used data from MAG (magnetometer) and SWIA (Solar Wind Ion Analyzer) onboard MAVEN. STATIC can measure ion distribution functions with energy and mass discrimination. In the magnetotail wake region, we divided the energy range in three parts: less than 20eV, between 20eV and 100eV, and greater than 100eV. The lowest energy one was assumed to be planetary protons. The result shows that planetary proton density in the wake region had a seasonal variability which was more than one order, while variations in MY32, 33 and 34 were similar. Therefore, it is thought that the size of dust storm does not affect proton escape in the magnetotail wake. The method to separate planetary protons from solar wind protons needs to be different from that in the wake region. In this study, we calculated partial moments of picked up protons originated from hydrogen corona to derive parameters of planetary protons in the solar wind and magnetosheath. The obtained variations of the planetary protons are compared with EUV flux at Mars as well as with dust storm activities in order to understand the cause of seasonal variations of protons.

References:
Krasnopolsky (2006), *Icarus*, doi: 10.1016/j.icarus.2006.06.003
Halekas (2017), *J. Geophys. Res. Planets*, doi: 10.1002/2017JE005306
Heavens et al. (2018), *Nat. Astron.*, doi: s41550-017-0353-4
Chaffin et al. (2017), *Nat. Geosci.*, doi: 10.1038/NGEO2887

中間赤外線中空ファイバーの低温環境下での透過率測定

伊藤 良太 [1]; 平原 靖大 [2]; 松浦 祐司 [3]; 高見 康介 [4]; 中川 広務 [4]; 笠羽 康正 [5]; 山崎 敦 [6]
[1] 名大・環; [2] 名大・院・環境・地球惑星; [3] 東北大・医工学; [4] 東北大・理・地球物理; [5] 東北大・理; [6] JAXA・宇宙研

Transmittance measurement of mid-infrared Hollow core fiber at cryogenic temperature

Ryota Ito[1]; Yasuhiro Hirahara[2]; Yuji Matsuura[3]; Kosuke Takami[4]; Hiromu Nakagawa[4]; Yasumasa Kasaba[5]; Atsushi Yamazaki[6]
[1] Environmental Studies, Nagoya Univ.; [2] Earth&Planetary Sciences, Nagoya Univ.; [3] Biomedical Engineering, Tohoku University; [4] Geophysics, Tohoku Univ.; [5] Tohoku Univ.; [6] ISAS/JAXA

We aim at the long-term spectroscopic observation of the planetary atmosphere in the mid-infrared wavelength region for the purpose of clarifying various phenomena of atmosphere physics and atmospheric chemistry of solar system planets and satellites by 1.8m off-axis telescope PLANETS (Polarized Light from Atmospheres of Nearby Extra-Terrestrial Systems), which is planned to be constructed at Mt. Haleakala of Maui. The PLANETS will be equipped with high dispersion cooled echelle spectrograph GIGMICS (Germanium Immersion Grating Mid-Infrared Cryogenic Spectrograph), which can observe N-band (wavelength 8-13um) with R˜40,000. In this research we report the development of the new cooled fiber system for optical guiding to GIGMICS from PLANETS. By using the mid infrared HCW (hollow core waveguide) developed in recent years, we can realize simultaneous observation with other observing instruments such asMILAHI, and improvement of optical throughput by abbreviation of a large number of guide mirrors.

In the present study, we report on the development of a new hollow core waveguide (HCW) fiber for installing and operating GIGMICS on PLANETS. There are commercially available single mode optical fibers for communication band for short wavelength infrared region up to 2.5 um wavelength, and it is used on the European Mars Lander ExoMars Mission 2020, but transmission efficiency is low in the wavelength longer than 3 um wavelength (<70% / m) AgS polycrystalline fiber only. Mid-infrared hollow fiber developed in Tohoku University Graduate School of Medical Science and Technology in recent years has a metal and dielectric double-layer thin film with high reflectivity near a wavelength of 10 um is embedded inside the tube with an inner diameter of about 1 mm. It is being applied to high efficiency transmission of carbon dioxide gas laser light and in vivo spectroscopy. We are working on the evaluation of the permeability of hollow fiber in low temperature and vacuum environment with the aim of developing a new astronomical observation device utilizing the characteristics of this hollow fiber and the development of future planetary exploration equipment.

We adopted a HCW with an inner diameter of 0.8 mm, in which a thin glass material on the inner surface of a polyimide pipe was clad with a metal (Ag) coated with AgI. Since the reflective layer is metal, it is expected that the loss can be reduced as the resistivity decreases in cryogenic temperature region. Therefore, we developed a Wilson seal to keep the vacuum shield, and the fiber cooling mechanism that satisfies three conditions for (1) holding the vacuum inside of the hollow fiber, (2) cooling with liquid nitrogen, and (3) keeping the low temperature by vacuum insulation. The small Pt-100 temperature sensors were attached to several places where the fiber was introduced, and a cooling test using a liquid nitrogen pump system was carried out. As a result, within 10 minutes after the start of cooling, reached 78K within the distance of 2m uniformly. In addition, we developed a flow rate controller of liquid nitrogen in order to keep cooling for a long time with 20L liquid nitrogen container. For the measurement of the HCW transmittance at cryogenic temperature, we constructed an optical system for measurement that using a 1mm x 1mm detector (Vigo Systems PVMI-4TE Photoelectric MCT), and a 10.4um QC laser (Daylight Unicorn II, 100mW CW). The QC laser have a fluctuation of about 5% of the beam intensity in the long time measurement. In the future, we will construct a double-beam optical system with a Ge half mirror, to sequential intensity calibration of incident infrared light, and measure the transmittance of the hollow fiber with high accuracy.

多様な太陽系惑星・衛星の大気物理・大気化学の諸現象を観測的に明らかにする目的で、我々は、マウイ島ハレアカラ山頂に建設予定の 1.8m 軸外し型グレゴリアン式望遠鏡 PLANETS(Polarized Light from Atmospheres of Nearby Extra-Terrestrial Systems) に、赤外線領域の「大気の窓」である N-band(波長 8-13um) 全域を観測域とする高分散 (R˜40,000) 冷却エシェル分光器 GIGMICS(Germanium Immersion Grating Mid-Infrared Cryogenic Spectrograph) を搭載することで、中間赤外域での惑星大気の連続的な観測を目指す。

本研究では、GIGMICS を PLANETS に搭載・運用するための新型のファイバーの開発について報告する。従来、波長 2.5um までの短波長赤外域の通信バンド用シングルモード光ファイバーが存在し、欧州火星着陸機 ExoMars Mission2020 搭載機器に採用されているが、波長 3um より長波長の領域では透過効率が低い (70%/m 未満)AgS 多結晶ファイバーのみであった。近年、東北大学医工学研究科において開発された中間赤外線中空ファイバーは、内径 1mm 程度のチューブ内面に、波長 10um 近辺で高反射率となる金属と誘電体の 2 層薄膜を内装した構造を持つ新しいデバイスであり、炭酸ガスレーザー光の高効率伝送や、生体内の分光計測に応用されつつある。我々はこの中空ファイバーの特性を活かした新たな天文観測装置の開発や将来の惑星探査機器の開発を目指し、低温・真空環境での中空ファイバーの透過率の評価に取り組んでいる。

本研究では、ポリイミドパイプの内面の薄いガラス材を AgI でコートした金属 (Ag) をクラッドした内径 0.8mm の

中空ファイバーを用いた。反射層に金属が用いられているため、冷却環境下では抵抗率低下に伴う低損失化が期待される。そこで、多重真空を保持するためにウィルソンシールを開発し、更に (1) ファイバー内の真空の保持 (2) 液体窒素による冷却 (3) 真空断熱による低温の維持、の 3 つを満たすファイバー冷却機構を製作した。ファイバー導入部分数か所に Pt-100 温度センサーを取り付け、液体窒素ポンプシステムを用いた冷却試験を行ったところ、冷却開始後 10 分で 2m の距離内が均一に 78K に到達した。また、液体窒素の流量自動調節機構を製作し、20L の液体窒素で長時間の冷却保持が可能となった。このファイバーについて低温での透過率測定を行うため、波長 10.4um の QC レーザー (Daylight 社製 Unicorn II, 100mW CW) を光源とし、1mm X 1mm の検出器 (Vigo Systems 社製 PVMI-4TE 光電型 MCT 検出器) を用いた測定用光学系を構築した。光学系に用いる QC レーザーは、長時間の測定においておよそ 5%のビーム強度の揺らぎがあることがわかった。今後、Ge ハーフミラーを使ったダブルビーム光学系を構築し、入射赤外光の逐次強度較正を行えるようにし、高い精度の中空ファイバーの透過率測定を行う。

赤色矮星周りの系外惑星の外圏大気における酸素原子のエネルギー状態とトランジット観測による検出可能性

村岡 徹 [1]; 亀田 真吾 [1]
[1] 立教大

Energy state of oxygen atoms in the exosphere of exoplanets around red dwarfs and detectability by transit observation

Toru Muraoka[1]; Shingo Kameda[1]
[1] Rikkyo Univ.

An exoplanet is a planet that orbits a star other than the sun. Since the widespread recognition of their existence in the 20th century, approximately 4,000 exoplanets have been found. Current work features the detection of these exoplanets and their environments, such as their atmospheres.

Transit observation is an exoplanet detection method based on the light absorbed by a planet as it passes in front of its host star; it is expected that the atmospheric components of exoplanets can be detected by applying spectroscopy to this observation. The discovery of a planet where life activities can be expected is one of the most featured themes in this field of research. In recent years, seven planets the size of the Earth have been discovered around the M-type red dwarf TRAPPIST-1 using the transit method. Furthermore, it is thought that three of them exist in the habitable zone of their host star; the habitable zone is the area where liquid water can exist on the surface of the planet. However, it is difficult to determine whether life activity can be expected on these planets simply because they were detected.

Previous research has predicted that the Earth’s atmosphere will spread to very high altitudes as the Earth receives 10 to 100 times the amount of extreme ultraviolet (EUV) radiation that it receives at present, which is comparable to the amounts emitted when the sun was younger. This is mainly because high EUV radiation heats and expands the thermosphere, where locates Earth’s upper atmosphere. In contrast, because the atmospheres of Mars and Venus contain carbon dioxide at high mixing ratios, a cooling effect impedes atmospheric spreading.

Exoplanets in the habitable zones around red dwarfs such as TRAPPIST-1 receive EUV radiation from their host stars that is significantly stronger than the radiation that the Earth currently receives from the sun. By modeling the atmosphere expansion of th Earth under conditions such as those in the habitable zone of TRAPPIST-1, it is expected to detect oxygen levels on TRAPPIST-1 exoplanets via transit observation using telescopes equipped for ultraviolet spectroscopy.

However, ground state atomic oxygen is believed to be useless in detecting such absorption, as the absorption of interstellar ground state atomic oxygen is much larger than that of the modeled planetary atmosphere. Therefore, our research investigates what the energy state of the atomic oxygen distributed in the upper atmosphere of the Earth would be if the latter was placed in a high EUV environment and reexamines the possibility of detecting atomic oxygen in exoplanet atmospheres.

太陽以外の恒星の周りを回る惑星を系外惑星という。20 世紀にその存在が広く認められるようになってから現在に至るまで約 4000 もの数が見つかってきており、現在では惑星の検出にとどまらず、惑星大気などの諸環境への興味が開拓されつつある。

系外惑星の検出方法の 1 つに、惑星が恒星前面を通過する際の減光を利用するトランジット観測がある。このトランジット観測を分光観測に応用することで、系外惑星の大気成分などを検出できることが期待されている。

系外惑星の環境への興味という点で代表的なものとして、生命活動が期待できる惑星の発見が挙げられる。近年ではトランジット観測により、TRAPPIST-1 という木星ほどの大きさを持つ M 型赤色矮星の周りに地球程度の大きさをもつ惑星が次々に発見された。さらにそのうち 3 つがハビタブルゾーン（惑星表面に液体の水が存在できる範囲）に存在すると考えられている。しかしながら、それらの惑星が地球のような、生命活動が期待できる惑星なのか、そうではなく金星や火星のような惑星なのかを検出のみによって判別することは困難である。

先行研究では、太陽系ができて間もない頃のように、地球が現在の 10~100 倍の極端紫外線 (EUV) 放射を受けた場合、地球の高層大気に位置する熱圏が加熱され膨張することなどによって、地球の大気は非常に高高度まで広がるだろうと予測されている。一方、火星や金星では混合比の高い二酸化炭素による冷却が主に効果的に働き、大気はあまり広がらないと考えられている。

TRAPPIST-1 のような赤色矮星のハビタブルゾーンでは、主星から受ける EUV 放射は、現在地球が太陽から受けている放射の数 10 倍強いと考えられており、太陽系の初期の姿に似ていると考えられている。

これらの議論により、TRAPPIST-1 のような恒星のハビタブルゾーンに地球があった場合を仮定しその大気の広がりを計算した上で、大気に含まれる酸素原子を、紫外線分光宇宙望遠鏡を用いたトランジット観測によって検出する計画が検討されている。

しかしながら、基底状態の酸素原子については、輝線の吸収量は惑星大気のトランジットによるものよりも星間空間の酸素原子によるものの方がはるかに大きいため観測できないと考えられている。そのため本研究では、高 EUV 環境においた地球の高層大気における酸素原子がどのようなエネルギー状態の分布をもつかを検討し、改めて酸素原子検出の可能性について議論する。

大学規模の太陽系地上観測所、その将来計画：東北大の場合

笠羽 康正 [1]; 坂野井 健 [2]; 鍵谷 将人 [3]; 平原 靖大 [4]; 三澤 浩昭 [5]; 熊本 篤志 [6]; 土屋 史紀 [7]; 村田 功 [8]; 中川 広務 [9]; 木村 智樹 [10]; 小原 隆博 [11]; 岡野 章一 [12]; Zarka P.[13]
[1] 東北大・理; [2] 東北大・理; [3] 東北大・理・惑星プラズマ大気研究センター; [4] 名大・院・環境・地球惑星; [5] 東北大・理・惑星プラズマ大気研究センター; [6] 東北大・理・地球物理; [7] 東北大・理・惑星プラズマ大気; [8] 東北大院・環境; [9] 東北大・理・地球物理; [10] Tohoku University; [11] 東北大・惑星プラズマセンター; [12] 東北大・理・PPARC; [13] Observatoire de Paris

A Future plan of a university-scale ground-based observatory for solar system science: The case of Tohoku University

Yasumasa Kasaba[1]; Takeshi Sakanoi[2]; Masato Kagitani[3]; Yasuhiro Hirahara[4]; Hiroaki Misawa[5]; Atsushi Kumamoto[6]; Fuminori Tsuchiya[7]; Isao Murata[8]; Hiromu Nakagawa[9]; Tomoki Kimura[10]; Takahiro Obara[11]; Shoichi Okano[12]; P. Zarka[13]
[1] Tohoku Univ.; [2] Grad. School of Science, Tohoku Univ.; [3] PPARC, Tohoku Univ; [4] Earth&Planetary Sciences, Nagoya Univ.; [5] PPARC, Tohoku Univ.; [6] Dept. Geophys, Tohoku Univ.; [7] Planet. Plasma Atmos. Res. Cent., Tohoku Univ.; [8] Environmental Studies, Tohoku Univ.; [9] Geophysics, Tohoku Univ.; [10] Tohoku University; [11] PPARC, Tohoku University; [12] PPARC, Tohoku Univ.; [13] Observatoire de Paris

http://pparc.gp.tohoku.ac.jp/

Tohoku University has supported planetary missions with small-scale but long-lasting capability of the ground-based observations dedicated to solar system. At present, our core telescopes are Vis-IR 60-cm and Vis 40-cm at Mt. Haleakala, Hawaii, and VHF-Radio 30-m (IPRT) at Iitate, Fukushima.

For future, we are running the construction of 1.8-m PLANETS Vis-IR telescope with a unique Offset-Gregorian type (with Nagoya/Kyoto Univ. in Japan and Univ. Hawaii et al. in overseas), and also investigating the participation to the NenuFAR project promoted by Obs. de Paris as the expansion of Euro LOFA (Low Frequency radio interferometer).

For the effort to expand the future observational capability toward Sun, planets, satellites, minor bodies, and exoplanets, we hope to get the participations and supports from the communities in Japan.

東北大は、1974 年の木星電波放射観測施設の開設以来、小規模ながら太陽系天体の地上観測能力を擁し、国内外の惑星ミッション群へ参画し随時・継続的な支援観測を行ってきた。現在、光赤外ではハワイ・ハレアカラ山頂 60cm 光赤外・40cm 光学、電波では福島県飯舘 VHF 帯 30m(IPRT) の各望遠鏡を中核とする。

将来に向け、オフセット・グレゴリアン型のユニークな構造を持つ 1.8m PLANETS 光赤外鏡（国内では名大・京大、国外ではハワイ大他と共同）の建設中、欧 LOFA(低周波電波干渉計) 拡張としてパリ天文台が Nancey 観測所で
進める NenuFAR 計画への参画検討中である。

この太陽、惑星・衛星群、小天体群、そして系外惑星への高頻度/任意 timing の観測能力向上に対し、国内コミュニティからのご参加・ご支援を希望する。

火星中間圏における異常昇温層の発見

中川 広務 [1]; Jain Sonal[2]; Montmessin Franck[3]; Yelle Roger V.[4]; Schneider Nicholas M.[5]; Groller Hannes[6]; 黒田 剛史 [7]; 吉田 奈央 [8]; 寺田 直樹 [9]; 関 華奈子 [10]; 今村 剛 [11]; 藤原 均 [12]
[1] 東北大・理・地球物理; [2] LASP; [3] LATMOS; [4] University of Arizona; [5] LASP, Univ. of Colorado; [6] なし; [7] 東北大・理; [8] 東北大・理・地物; [9] 東北大・理・地物; [10] 東大理・地球惑星科学専攻; [11] 東京大学; [12] 成蹊大・理工

Unexpected warm layer in the summer nightside mesosphere of Mars and its behavior during the global dust storm by MAVEN/IUVS

Hiromu Nakagawa[1]; Sonal Jain[2]; Franck Montmessin[3]; Roger V. Yelle[4]; Nicholas M. Schneider[5]; Hannes Groller[6]; Takeshi Kuroda[7]; Nao Yoshida[8]; Naoki Terada[9]; Kanako Seki[10]; Takeshi Imamura[11]; Hitoshi Fujiwara[12]
[1] Geophysics, Tohoku Univ.; [2] LASP; [3] LATMOS; [4] University of Arizona; [5] LASP, Univ. of Colorado; [6] none; [7] Tohoku Univ.; [8] Geophysics, Tohoku Univ.; [9] Dept. Geophys., Grad. Sch. Sci., Tohoku Univ.; [10] Dept. Earth & Planetary Sci., Science, Univ. Tokyo; [11] The University of Tokyo; [12] Faculty of Science and Technology, Seikei University

The Mars mesosphere and thermosphere (up to ˜100 - 200 km) is well known as an intermediate atmospheric region strongly impacted by coupling with the underlying lower-middle atmosphere (via gravity waves, planetary waves and tides, and dust storms) and coupling with the overlying exosphere and ultimately the Sun (via solar EUV radiation and solar wind particles). Information on this part of the atmosphere is vital to prepare spacecraft missions performing aerobraking, aero-capture or EDL (entry, descent and landing). On the other hand, the Martian atmosphere at this intermediate region is still poorly known due to its highly variable nature and a lack of measurements. This paper presents a new set of stellar occultation measurements made using the Imaging Ultraviolet Spectrograph (IUVS) onboard Mars Atmosphere and Volatile EvolutionN (MAVEN). We report the detection of an extensive layer of warm air at 70 - 90 km altitudes on the night side in the summer hemisphere on Mars. Our result suggests the relatively permanent peaks of atmospheric temperature around 80 km exist over the northern summer night at Ls = 0 - 180 deg. Mars Climate Database does not reproduce a warm layer around 80 km altitude, gradually declining along the height. The predicted temperature by MCD underestimates the quantities of temperature by 10 to 90 K. The longitudinal distribution of atmospheric temperature suggests a mode wave-3 structure. Such distinct layer was also found in the dusty southern summer at Ls = 249 deg, that implies 20 km-higher peaks. The saturated water amount was estimated by the observed temperature profiles by IUVS self-consistently as the possible maximum. Warm air at this altitude range can attribute to preserve the water vapor more than hundreds ppmv in the mesospheric atmosphere and prevent the water vapor condensation falling in the lower atmosphere. Our observations show that as much as more than 100 times more water vapor than expected could be present at this altitude, that will impact the water loss to space. We believe that our result highlighted the dynamical mesospheric thermal structure and upsurge of aerosol plays some role not fully considered in the current model. Although the water vapor amount is not measured by IUVS, the interaction between water, aerosol, and background thermal structure could be addressed in near future by a new observation of TGO. The response of mesospheric thermal structure during the global dust storm 2018 is shown in the paper.

非静力学全球火星大気循環モデルの開発と高解像度計算

樫村 博基 [1]; 八代 尚 [2]; 西澤 誠也 [3]; 富田 浩文 [4]; 中島 健介 [5]; 石渡 正樹 [6]; 高橋 芳幸 [7]; 林 祥介 [8]
[1] 神戸大・理・惑星/CPS; [2] 環境研・地球 C; [3] 理研 R-CCS; [4] 理研 AICS; [5] 九大・理・地惑; [6] 北大・理・宇宙; [7] 神戸大・理・惑星; [8] 神戸大・理・惑星

Development of a global non-hydrostatic Martian atmospheric model and its high-resolution simulation

Hiroki Kashimura[1]; Hisashi Yashiro[2]; Seiya Nishizawa[3]; Hirofumi Tomita[4]; Kensuke Nakajima[5]; Masaki Ishiwatari[6]; Yoshiyuki O. Takahashi[7]; Yoshi-Yuki Hayashi[8]
[1] Planetology/CPS, Kobe Univ.; [2] NIES/CGER; [3] RIKEN R-CCS; [4] RIKEN AICS; [5] Earth and Planetary Sciences, Kyushu University; [6] Cosmosciences, Hokkaido University; [7] Department of Planetology, Kobe Univ.; [8] Planetology/CPS, Kobe Univ.

In the Martian atmosphere, dust storms in various scales–from dust devils, local dust storm, to global dust storm–have been observed. However, interactions between these scales are unknown. In addition, since Mars has a thin atmosphere and no ocean, the temperature difference between day and night is large and vertical convection should play an essential role in the Martian meteorology and climate, but it is also unknown. To investigate these mysteries, global atmospheric simulations with horizontal resolution as high as few kilometers and by solving the governing equations without assuming the hydrostatic balance are required.

We are developing a non-hydrostatic global Martian atmospheric model (Martian SCALE-GM) which is suitable for large-scale parallel computation. SCALE-GM (http://r-ccs-climate.riken.jp/scale/) is being developed by using the dynamical core of NICAM (Tomita & Satoh, 2005; Satoh et al., 2008, 2014), a non-hydrostatic model for the Earth atmosphere using a finite volume method in the icosahedral grid systems (Tomita et al., 2001, 2002), and by aiming at sharing of physical process modules with the regional model (SCALE-RM) and application to other planetary atmospheres. We are developing Martian SCALE-GM by incorporating constants and physical process modules of the Martian atmosphere. The Martian physical modules are taken from DCPAM (https://www.gfd-dennou.org/library/dcpam/), an existing pan-planetary atmospheric general circulation model (GCM). DCPAM is a traditional, hydrostatic GCM using a spectral method for horizontal discretization.

We ported a Martian atmospheric radiation model (Forget et al., 1999) and a soil model from DCPAM to SCALE-GM and performed a test of temperature evolution in a vertical 1D-atmosphere and soil. The atmosphere model has 100 layers (dz = 1 km), and distribution of dust is fixed with 0.2 optical depth. The soil model has 18 layers. Soil's heat capacity and thermal conductivity are set to 9.7 x 10^5 [J K^{-1} kg^{-1}] and 0.076 [W m^{-1} K^{-1}], respectively. Surface albedo is fixed at 0.2. For the calculation of surface fluxes and vertical diffusion, BH91B95 (Beljaars & Holstang, 1991; Beljaars, 1995) and MY2.5 (Mellor & Yamada, 1982) are used, respectively. The initial condition is the 200 K constant temperature atmosphere and soil. We have confirmed that both models show almost the same temperature evolution.

Next, we performed 3D calculations under a Mars-like condition in 8 different horizontal resolutions to check the resolution dependence. Horizontal grid intervals are 240 x $(1/2)^n$ [km] (n = 0, 1, 2, 3, 4, 5, 6, 7); i.e., 1.9 km at minimum. The horizontal diffusion representing turbulent mixing in sub-grid scales is given in the 3rd order Laplacian with the relaxation time for the shortest scale given by 100 x $(1/2)^n$ [s]. The atmosphere is divided into 36 layers, which are concentrated near the surface. To avoid wave reflections at the model top, a sponge layer represented by 1st order Laplacian is set above 40 km altitude; the relaxation time for the shortest scale is given by 3600 x $(1/4)^n$ [s] except for the case of dx = 3.75 km, in which 3 s is used. The 4th order Runge-Kutta method is used for time-integration with a time step of 360 x $(1/2)^n$ [s]. The surface albedo is set to 0.5. Neither topography nor condensation processes are included.

Numerical solutions showed that the diurnal vertical convection did not appear clearly in the cases with dx larger than 15 km, whereas they appeared in higher resolution cases. Furthermore, it was confirmed that the horizontal scale and occurrence local-time of the vertical convection are highly dependent on the horizontal resolution.

(Figure: Horizontal resolution dependence of vertical wind [m s^{-1}]. Snapshots at 2 km altitude after 30 days from the spring equinox of the Northern hemisphere. Panels g, h, i are zoom-up views of Panels d, e, f, respectively)

地球大気の運動は数メートル規模から惑星規模に至るまで幅広く、様々な規模の現象が相互作用している。このことが、より高解像度の大気シミュレーションが求められる理由の 1 つである。こうした状況は、火星をはじめとした他の惑星でも同様なはずである。火星では数十から数百メートル規模のダストデビル（塵旋風）から、数十キロメートル規模のローカルダストストーム、全球を覆うグローバルダストストームまで、大小様々な規模の砂嵐が観測されているが、これらのスケール間の相互作用は未解明である。また火星は大気が薄く海がないため、昼夜間の寒暖差が大きく、鉛直対流が卓越すると考えられるが、全球規模の大気大循環に対するその役割は解明されていない。これらの謎に挑むためには、水平数キロメートル解像度の高解像度で、非静力学の方程式系による全球大気計算が求められる。

そこで我々は、大型計算機「京」の後継機、「富岳」で火星高解像度計算の実現を目指し、全球非静力学火星大気モデル (火星版 SCALE-GM) を開発している。SCALE-GM (http://r-ccs-climate.riken.jp/scale/) は、正二十面体準一様格子法

(Tomita et al., 2001, 2002) による地球大気の全球非静力学モデル NICAM (Tomita & Satoh, 2005; Satoh et al., 2008; Satoh et al., 2014) の力学コアを基に、領域モデル (SCALE-RM) との物理過程モジュールの共通化や他の惑星大気計算など、より幅広い応用を目指して開発が進められている大気大循環モデルである。我々は SCALE-GM に、火星大気用の定数や放射・地表面過程などの物理モジュールを組み込んだ火星版 SCALE-GM を開発している。開発は、既存の汎惑星大気大循環モデル DCPAM (https://www.gfd-dennou.org/library/dcpam/) の火星物理モジュールを移植する形で進めている。なお DCPAM は静力学平衡を仮定した方程式系をスペクトル法で解く、伝統的な全球大気モデルである。

本研究ではまず、DCPAM 物理モジュールのうち、火星大気放射モデル (Forget et al., 1999) と土壌モデルを移植し、テスト計算として鉛直 1 次元大気と土壌の温度変化を確認した。大気は鉛直 100 層 (dz = 1 km)、ダストは光学的厚さ 0.2 の固定分布とし、土壌は 18 層、熱容量 9.7 x 10^5 [J K^{-1} kg^{-1}]、熱伝導率 0.076 [W m^{-1} K^{-1}] とした。地表アルベドは 0.2 とし、地表面フラックスは BH91B95 (Beljaars & Holstang, 1991; Beljaars, 1995)、鉛直拡散は MY2.5 (Mellor & Yamada, 1982) で計算した。初期値は 200 K の等温静止大気・土壌とし、SCALE-GM と DCPAM で同様の時間発展が計算されることを確認した。

次に、火星的設定下における高解像度 3 次元計算のテストと解像度依存性の確認を兼ねて、水平解像度の異なる以下の 8 ケースの計算を実施した。水平格子間隔は、240 x $(1/2)^n$ [km] (n = 0, 1, 2, 3, 4, 5, 6, 7; 以下同じ) であり、最小時はおよそ 1.9 km である。サブグリッドスケールの乱流拡散を表す水平渦拡散は 3 次のラプラシアンで与え、その最小スケールに対する緩和時間は、100 x $(1/2)^n$ [s] とした。大気の鉛直層数は 36 とし、地表付近ほど層間隔が狭くなるように配置した。モデル上端での波の反射を防ぐため、高度 40 km より上空に 1 次のラプラシアンで擾乱を潰すスポンジ層を設置した。その最小スケールに対する緩和時間は 3600 x $(1/4)^n$ [s] とした。ただし計算の都合上 dx = 3.8 と 1.9 km のときは、3 s とした。時間積分には 4 段 4 次のルンゲクッタ法を用い、時間刻み幅 360 x $(1/2)^n$ [s] で計算した。地表アルベドは 0.5 とした。地形および凝結過程は導入していない。

計算の結果、水平格子間隔が 30 km 以上の場合、日周期加熱に伴う鉛直対流は明瞭には現れなかったが、15 km 以下の場合には、鉛直対流が表現された。また、鉛直対流の規模・発生時刻は、今回計算した範囲では解像度に制約されていることが確認された。

（図：高度 2 km の鉛直流 [m s^{-1}] の解像度依存性。北半球春分から 30 日後の瞬間場。g, h, i はそれぞれ d, e, f の拡大図である。）

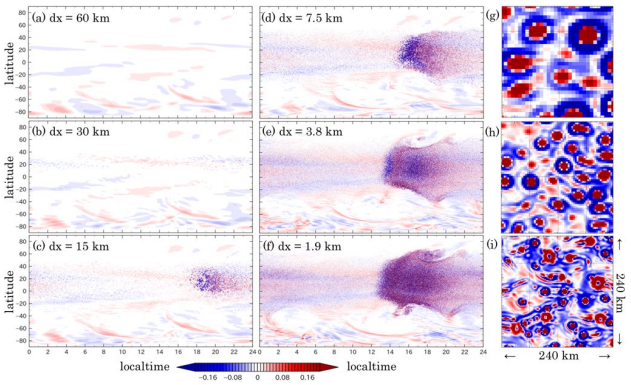

火星大気大循環モデリングの精緻化：重力波と水輸送

黒田 剛史 [1]
[1] 東北大・理

Refinement of a Mars General Circulation Model (MGCM): Gravity waves and water transport

Takeshi Kuroda[1]
[1] Tohoku Univ.

A high horizontal resolution (T106 spectral truncation, equivalent to 1.1^ox1.1^o or ˜67 km grid size) MGCM has been adopted to the calculations of current atmospheric environment on Mars for a full Martian year. In such simulations, gravity waves (GWs) with the horizontal wavelengths of down to ˜200 km, which favorably propagate to the mesosphere/thermosphere and affect the dynamical features there, can be resolved and the generations of such GWs by the orographic and dynamical effects can be reproduced. Kuroda et al. (2019, JGR Planets, doi:10.1029/2018JE005847) showed the seasonal variations of the GW activities on Mars from the simulations, indicating great variances with season and geographical location. In particular, lower-atmospheric GW activity is smaller in polar regions of the troposphere throughout all seasons, and the intensity is larger in southern spring and summer and in winter hemisphere at both solstices. In the mesosphere, the peak of GW activity shifts toward middle and high latitudes, and the interhemispheric symmetry is much larger compared to the lower atmosphere.

In addition, the comparison of MGCM results between T106 and lower horizontal resolution (T21 spectral truncation, equivalent to 5.6^ox5.6^o or ˜333 km grid size, which is conventional to most MGCMs in the world) has been made. The features of atmospheric circulation in solstitial seasons apparently differ, with up to ˜25 K higher winter polar warming and up to ˜20 m s^{-1} larger meridional wind velocity in T106 simulations. It shows that resolved GWs work to enhance the meridional circulation. Also, the resolved GWs work to weaken the zonal wind velocity above ˜50 km altitude. These features are consistent with the effects of GW drag parameterizations which have been implemented into most of MGCMs with conventional horizontal resolution (e.g. Medvedev et al., 2011, JGR Planets, doi:10.1029/2011JE003848) compensating for the abbreviation of sparse grid interval.

Simulations applying GW drag parameterizations to conventional-grid-interval MGCMs are reasonable for the reproductions of synoptic-scale atmospheric circulations, but it does not applicable for the reproductions of localized features. In fact, the GW drag parameterization implemented into Medvedev et al. (2011) has no spatial and temporal variations, which contradicts the simulated GW features by Kuroda et al. (2019). Therefore, it should be important to progress the horizontal high-resolution approaches for the atmospheric modeling on Mars towards the next step of understanding the Martian environment, with a lot of high-resolution camera data and fast many-core computing systems.

Simulations of water cycle should also be affected by the horizontal resolutions. Pottier et al. (2017, Icarus, doi:10.1016/j.icarus.2017.02.016) indicated that the significant effects of the high horizontal resolution on the simulated water cycle are seen only in local features, but I believe that the resolved GWs should affect also the global transport. In the presentation, the simulated results of water cycle with different horizontal resolutions will also be shown.

Temperature in the Venusian mesosphere observed by mid-infrared heterodyne spectrometer in 2018

Kosuke Takami[1]; Hiromu Nakagawa[1]; Hideo Sagawa[2]; Yasumasa Kasaba[3]; Isao Murata[4]
[1] Geophysics, Tohoku Univ.; [2] Kyoto Sangyo University; [3] Tohoku Univ.; [4] Environmental Studies, Tohoku Univ.

Extensive observations of the Venusian mesosphere have been performed by Venus Express (VEX) during 2006 - 2014 (e.g., Patzold et al., 2007; Mahieux et al., 2015). In terminators above 100 km in altitude, the thermal structure was reached common understandings by the comparisons between observations by the Solar Occultation at Infrared (SOIR) onboard VEX and numerical simulations by general circulation models (GCMs) . However, the temperature profiles in the altitude region of 85 - 100 km are not reproduced by GCMs, and the discrepancies have not been properly interpreted (Bougher et al., 2015; Gilli et al., 2017). Additional observational constraint for GCMs are needed to advance the understanding of the Venusian mesospheric thermal structure. In this paper, we will report the initial results of our challenge to this topic by obtaining temperature profiles in the mesosphere and its temporal and latitudinal variations utilizing the Mid-Infrared Laser Heterodyne Instrument, MILAHI (Nakagawa et al., 2016), developed by Tohoku University.

Temperature profiles in the altitude region of 70 - 100 km in the nightside are retrieved from CO_2 absorption spectra in 10 micron band. The absorption feature is formed by absorption of the thermal radiation emitted in the altitude close to the cloud top. MILAHI can resolve the spectra with the resolving power of 10^7 owing to the implementation of a CO_2 laser in 10 micron band (30 THz) as a local oscillator with a frequency stability of lower than 1 MHz. This spectral resolution has a potential to derive the temperature profiles with an accuracy of 10 K.

The observations were executed on 11 - 13, 19, and 20 November 2018 by using the Tohoku University 60 cm telescope (T60) located at the summit of Mt. Haleakala in Maui, Hawaii. Apparent diameter of Venus changed between 55.4 and 49.4 arcsec versus the spatial resolution of 4 arcsec by MILAHI with T60 in the wavelength of 10 micron. CO_2 absorption spectra were obtained at the equator on 11 - 13 Nov, 33N degrees on 19 Nov, and 33S degrees on 20 Nov at the evening terminator (local time of 20 h) with integration times of 80 - 105 minutes. In current tentative results, relative temperature differences are investigated by analyzing the day-to-day and latitudinal changes in relative intensity and line shape. The relative intensities on 11 and 12 Nov are similar level while that on 13 Nov is lower. This means that the temperature above the cloud top decreased on 13 Nov. The CO_2 absorption core at 33N degrees is sharper than that at 33S degrees. This can be interpreted as temperature in high altitude around 90 - 100 km at 33N degrees is lower. In presentation, we will show quantitative results in comparison with previous the radio occultation experiments by Akatsuki.

Wind field at the cloud top of Venus covering all local time obtained from thermal infrared images

Kiichi Fukuya[1]; Takeshi Imamura[2]; Makoto Taguchi[3]; Tetsuya Fukuhara[4]; Toru Kouyama[5]
[1] School of Science, Univ. of Tokyo; [2] The University of Tokyo; [3] Rikkyo Univ.; [4] Rikkyo Univ.; [5] AIST

Knowledge of the structures of the mean meridional circulation and the thermal tides is important for understanding the dynamics of the Venus atmosphere. Measurements of the wind field at a specific altitude covering all local time are essential to such studies. However, cloud tracking has been possible only for the dayside cloud top or the nightside middle/lower cloud region depending on the wavelength, except the southern polar region observed by Venus Express (Peralta et al., 2012).

Venus' cloud-top temperature distribution is now continuously mapped by LIR (Long-wave Infrared camera) mounted on the Venus orbiter Akatsuki, which can potentially be used for studying the dynamics in all local time regions. LIR images have not been used for cloud tracking because of the relatively low S/N ratio and the existence of stationary features induced by topographic gravity waves that obscure passive tracers.

Here we conduct cloud tracking using LIR data with a new method. Multiple images taken in ˜4 hours sliding windows are averaged successively in the coordinate system that rotates with the background superrotation. In the resultant images, random noises were suppressed and stationary features were smoothed out, enabling detection of detailed cloud morphologies. By the combination of this method and the cross-correlation method (Ikegawa and Horinouchi 2016), we derived the wind field both on the dayside and the nightside for the first time. As a result, the structures of the thermal tides and the mean meridional circulation at the cloud top were revealed. Predominant equatorward flows on the nightside and an equatorial convergence of the mean meridional flow were discovered.

大気大循環モデルを用いた金星雲分布の再現

安藤 紘基 [1]; 高木 征弘 [2]; 杉本 憲彦 [3]; 佐川 英夫 [4]; 松田 佳久 [5]
[1] 京産大; [2] 京産大・理; [3] 慶大・日吉物理; [4] 京都産業大学; [5] 東京学芸大

Venusian cloud distribution simulated by a general circulation model

Hiroki Ando[1]; Masahiro Takagi[2]; Norihiko Sugimoto[3]; Hideo Sagawa[4]; Yoshihisa Matsuda[5]
[1] Kyoto Sangyo University; [2] Faculty of Science, Kyoto Sangyo University
; [3] Physics, Keio Univ.; [4] Kyoto Sangyo University; [5] Tokyo Gakugei Univ.

We construct a simple cloud model for a Venus general circulation model (GCM), which includes condensation, evaporation and sedimentation of sulfuric acid cloud particles and condensable gases (H2O and H2SO4 vapors). The cloud distribution reproduced in the model is the thickest and thinnest in high- and mid-latitudes, respectively. The mixing ratio of H2O and H2SO4 vapor increase with latitude in the cloud and the sub-cloud levels, which are qualitatively consistent with previous measurements. In low-latitudes, the moderately thick cloud with zonal wavenumber 1 and 2 structures is formed and changes in time significantly. These structures would be associated with atmospheric waves in the cloud layer.

金星には高度 50-70km に分厚い硫酸の雲が広がり、全球的に金星を覆っている。赤外線や電波を用いた観測によって、金星の雲分布や雲の材料物質である水蒸気・硫酸蒸気混合比の分布は良く調べられている。しかし、この硫酸雲の生成・維持されるメカニズムについては良く分かっていない。

本研究では、金星大気大循環モデル AFES-Venus に金星の雲物理過程を導入し、雲や雲材料物質の分布を決定する要因について理論的に調べた。本研究では、過去の理論研究を参考にして以下のような仮定のもとで数値計算を行なった。雲材料物質として水蒸気と硫酸蒸気のみを考える。雲は硫酸の液滴で構成されており硫酸濃度は 85%に固定した。また、水蒸気と硫酸蒸気が両方とも飽和した時にのみ生成されるとする。雲の粒径として Mode1 と Mode2 のみを考え、それぞれの粒径を固定する。水蒸気は初期に高度 30km 以下に 30ppmv 存在しているとし、この混合比値は高度 30km 以下で一定とする。また硫酸蒸気は高度 62km 周辺で光化学的に生成されるとする。モデルの分解能は T42L120 であり、高度 0-120km の範囲で計算する。そして計算は 15 地球年行い、最後の 2 地球年のデータを主に解析した。

解析の結果、雲は極域で最も分厚くなることが分かり、Pioneer Venus や Venus Express の赤外観測と整合的である。水蒸気混合比は緯度共に大きくなり、Venus Express の VIRTIS の観測結果と定性的に整合する。硫酸蒸気混合比も高緯度で極大を持ち、Venus Express の電波掩蔽観測の結果と定性的に整合している。本発表では計算結果を示すと共に、雲や水蒸気・硫酸蒸気混合比分布を決定している物理過程について詳しく議論する。

3-D thermal structure of the Venus atmosphere obtained by Akatsuki/LIR

Masahiro Akiba[1]; Tetsuya Fukuhara[2]; Makoto Taguchi[3]; Takeshi Imamura[4]; Toru Kouyama[5]; Takao M. Sato[6]
[1] Physics department, Rikkyo Univ; [2] Rikkyo Univ.; [3] Rikkyo Univ.; [4] The University of Tokyo; [5] AIST; [6] HIU

Brightness temperature of the Venus disk obtained by Longwave Infrared Camera (LIR) onboard Akatsuki shows clear limb darkening in the low and middle latitudes. Limb darkening is an apparent temperature decrease from the center to the limb of the Venus disk. It is caused by increase of the altitude sensed by LIR as an emission angle, which is a zenith angle of direction of emission from the Venus atmosphere to the sensor, increases and a negative lapse rate of the atmosphere. In higher latitudes limb brightening is observed, because an inversion layer exists at the cloud-top altitudes. In other words a profile of limb brightness reflects vertical distributions of atmospheric temperature and optical thickness of cloud particles. Taylor et al. [1980] presented local time dependence of limb darkening using brightness temperature data obtained by the Pioneer Venus orbiter, but did not mention its physical mechanism. In this study horizontal distributions of brightness temperature obtained by LIR when Akatsuki was in the altitude range from 60,000 to 100,000 km during the period from October 19, 2016 to October 2, 2018 were analyzed to investigate the vertical structure of brightness temperature distribution above the cloud-tops based on the emission angle dependence of the sensing altitude. We used LIR data obtained with an observation mode in which 32 successive images are acquired with an interval of two seconds. Each brightness temperature image with 328 x 248 pixels was divided into 3280 x 2480 sub-pixels, and 32 successive images were accumulated after precise adjustment of the Venus disk position to improve S/N. Then average brightness temperatures were derived as a function of the emission angle for 24 local time zones and 18 zonal belts with a latitudinal width of 10 degrees within plus or minus 85 degrees. Emission angles are converted to sensing altitudes by a radiative transfer calculation with nominal temperature and cloud particle distributions composed of the past Venus observations [Sato et al., 2014]. Thus, we derived a local time-altitude cross section of the brightness temperature deviation above the cloud-tops. In the equator region it shows a clear semidiurnal tide of which the phase shifts upstream as the altitude increases. The maximum positive temperature deviation appears around 10 and 21 LT at the bottom of the sensing altitudes. It is suggested that the thermal tide is generated deep in the cloud deck by solar heating and propagates upward. Ando et al. [2018] indicated that the phase of the semidiurnal tide inclines in the altitude range from 70 to 85 km by a general circulation model, and estimated a vertical wavelength of the semidiurnal tide in the altitude range from 75 to 85 km to be 10-15 km. A vertical wavelength will be also derived from our observation result by the same way, and will be compared with the simulation result to evaluate the background wind field. In the higher latitudes an inversion layer is identified in a local time-altitude cross section of the brightness temperature deviation corresponding to the cold polar collar.

金星探査機「あかつき」によって観測された中緯度帯雲頂構造

河瀬 慎一郎 [1]; 田口 真 [2]; 福原 哲哉 [3]; Lee Yeon Joo[4]; 山崎 敦 [5]; 神山 徹 [6]
[1] 立教大・理・物理; [2] 立教大・理・物理; [3] 立教大・理; [4] JAXA/ISAS; [5] JAXA・宇宙研; [6] 産総研

Cloud-top structure in the middle latitudes observed by the Venus orbiter Akatsuki

Shinichiro Kawase[1]; Makoto Taguchi[2]; Tetsuya Fukuhara[3]; Yeon Joo Lee[4]; Atsushi Yamazaki[5]; Toru Kouyama[6]
[1] Physics, Rikkyo Univ.; [2] Rikkyo Univ.; [3] Rikkyo Univ.; [4] JAXA/ISAS; [5] ISAS/JAXA; [6] AIST

Venus is covered with thick sulfuric acid clouds floating at 40-70 km altitudes. The cloud particles scatter sunlight and shine brightly. In the visible region, light reflected by the clouds are poorly absorbed and almost uniformly distributed over the dayside disk except for a geometrical effect. However, in the infrared region, we observe thermal structures such as streaks aligning from the mid-latitude to the pole, the cold collars and polar vortices in the polar regions. On the other hand, in the ultraviolet region, we observe Y-shaped structures in the low-latitude region and the streak structures like those seen in the infrared region.

The five cameras onboard the Venus orbiter Akatsuki can capture radiation from multiple altitudes using the difference of the atmospheric transmittance at their peculiar wavelengths, and light up the 3-D structure and dynamics of the Venus atmosphere. Among the cameras, the Longwave Infrared Camera (LIR) detects thermal emission from the cloud top in a wavelength region 8-12 um to map the cloud-top temperature (Fukuhara et al., 2011) and Ultraviolet Imager (UVI) is designed to map the ultraviolet contrast at 283 nm and 365 nm for observing SO2 and un unknown absorber, respectively (Yamazaki et al., 2018).

Both LIR and UVI observed the streak structures, but unlike previous observations (Titov et al., 2008), the brightness temperature and ultraviolet brightness of the streak structures show a positive correlation.

Since Akatsuki orbits in a plane close to the equatorial plane, it is difficult to determine what shape the streak structures and cold collars found in the middle and high latitudes have. Therefore, we projected images centered on the North pole or the South pole (Kouyama et al., 2017). Furthermore, we calculated the average value of thermal images and created polar maps of temperature deviations. As a result, in images obtained by LIR, we found that the streak structure may start from the latitude of 60 degree around noon to the polar region in the afternoon and that the cold collar appears at latitudes of 60-80 degree in the morning.

In addition, we analyzed frequency characteristics in the local time domain at each latitude in order to investigate the local time dependency. As a result, in the images obtained by LIR, we found that a wavenumber 2 component is dominant in the equatorial region and that a wavenumber 1 component is dominant in the middle- and high-latitudes where the streak structure and the cold collar are observed.

In the presentation, we present the comparison between the results of these analysis and numerical simulations, and discuss the dynamics of the atmospheric structures of Venus' cloud-top in the middle-latitude region.

Properties of gravity wave packets detected in radio occultation temperature profiles of the Venus atmosphere

Ryota Mori[1]; Takeshi Imamura[2]; Hiroki Ando[3]
[1] Astrobio,Complexity Science and Engineering,Frontier Sciences, Tokyo Univ; [2] The University of Tokyo; [3] Kyoto Sangyo University

Gravity waves are thought to play key roles in atmospheric dynamics by carrying momentum in the vertical direction. They induce acceleration or deceleration of the mean wind by depositing momentum on the background atmosphere while dissipating. Such processes should also affect the global structure of the high-speed zonal wind of the Venusian atmosphere. However, since the spatial scales of gravity waves are small and the wave periods are relatively short, it is difficult to capture their spatial structures by observations. Though the meridional distribution of the mean magnitude of short vertical-scale temperature disturbances (Tellmann et al. 2012) and the vertical wavenumber spectrum (Ando et al. 2015) have been investigated, the statistical properties of the wavelength, the amplitude and the vertical extent of the wave packet have not been studied.

Here we analyze temperature profiles obtained from 2016 by the radio occultation experiment in the Venus orbiter mission Akatsuki. Radio occultation is a method to measure the change of the refractive index of the atmosphere as a change of the frequency of the signal received on the ground. At the opportunity when the radio wave transmitted from Akatsuki toward the Earth passes through the planetary atmosphere, the wave is refracted and then reaches the receiving station. We can retrieve the vertical profiles of the pressure and the temperature from each refractive index profile. In the temperature profiles obtained in this way, variations due to various atmospheric disturbances are observed.

To extract spatially-localized temperature disturbances, we applied wavelet analysis to the temperature profiles obtained by radio occultation. Though there have been studies that applied Fourier transform to temperature data, Fourier transform assumes infinitely continuous waves and it is not suitable for extracting spatially localized wave packets. Wavelet analysis is an effective way of obtaining the wavenumbers and the amplitudes of waves in such finite intervals. In this presentation, we report the result of wavelet analysis applied to the temperature data obtained with high vertical resolution by radio holographic method (Imamura et al. 2018). From the obtained results, we report the statistical relationships among wave parameters such as the amplitude, the vertical wavelength and the packet length.

Restoration-by-Deconvolution 法を用いたあかつき IR2 夜面データの復元 (と科学成果)

Vun Choon Wei[1]; 佐藤 毅彦 [2]; 佐藤 隆雄 [3]; 堀之内 武 [4]; Peralta Javier[5]; McGrouldrick Kevin[6]
[1] SOKENDAI; [2] 宇宙研; [3] 情報大; [4] 北大・地球環境; [5] 宇宙研; [6] コロラド大

Akatsuki IR2 nightside data Restoration by Deconvolution and Scientific Outcomes

Anthony Vun[1]; Takehiko Satoh[2]; Takao M. Sato[3]; Takeshi Horinouchi[4]; Javier Peralta[5]; Kevin McGrouldrick[6]
[1] Space Sciences, SOKENDAI; [2] ISAS, JAXA; [3] HIU; [4] Hokkaido University; [5] ISAS/JAXA; [6] University of Colorado Boulder

IR2(2-um camera) is one of the scientific instruments onboard Akatsuki which studies Venus meteorology utilising near infrared windows of CO2 atmosphere. This presentation focuses on the data restoration work performed on IR2 data quality. IR2 observes nightsides in 1.735um, 2.26um, 2.32um filters. IR2 is a platinum silicide (PtSi) Schottky-barrier CCD detector regulated by a cryocooler to be ˜65K for operation, where it full frame covers 1024x20124 pixels. Satoh et al. 2016;2017 reported the careful image reduction performed for flat fields, temperature-dependent quadrants, and point spread function (PSF) issue.

Even after the corrections, the nightside data still suffer from both light spreading (convolution) by PSF and contamination from the dayside. The IR2 team strives to achieve highest photometric accuracy as possible. In achieving so, Restoration-by-Deconvolution (RD) method was developed to perform imagery restoration. The PSF was modelled using Moffat function where parameters have been updated. The RD method can be divided into two main processes: 1. Replace saturated pixels in the original data (See presentation for full details); 2. Perform Lucy-Richardson Deconvolution by model-PSF on the 1024x1024size image embedded in the centre of a wider canvas of 2048x2048 pixels to avoid repetition of Venus disk when FFT for deconvolution is performed.

After successful restoration performed on IR2 data, aerosol properties such as the particle size parameter (Carlson et al. 1993; Wilson et al. 2008) can be deduced from the correlation plots between the restored 1.735um and 2.26um data. The 'branch' features for interpreting size modes population requiring photometric accuracy finally appeared in the restored data, which were not visible in the original IR2 data due to contamination and artefacts. Moreover, interesting morphologies such as the discontinuity features of the enormous cloud cover (2016-08-18) appears more visible where being restored at true contrast to study both the spatial and temporal variations. To conclude, development of IR2 photometric restoration is coming to a confident stage whereby the accuracy is estimated to be below ˜10% deviation and more upcoming scientific achievements using restored data can be anticipated.

あかつきに搭載されている IR2(赤外線) カメラによる CO2 観測で金星大気の研究が行われている。本講演では、IR2 により得られたデータの復元に着目する。IR2 カメラでは 1.735um、2.26um フィルターによって夜側を、2.02um フィルターによって昼面を観測している。(冷凍機により約 65K に調整された) ケイ化白金 PtSi CCD 検出器は 1024x1024 ピクセルである。Satoh et al. (2016;2017) は flat field 処理、CCD 温度依存性の除去 (T-Dependent quadrants)、また PSF を考慮することで高精度のデータ処理を行った (実現した)。

しかし、上記の処理を行っても、夜面データは昼側の光の漏れ出しによる影響を受ける (汚染される)。IR2 チームの努力により測光データの精度向上が試みられている。そのために、RD 法が画像復元に利用されている。ここで、PSF は Moffat 関数を用いてモデル化されている。RD 法においては、1. saturate したピクセルを元データと置き換え、2. モデル化した PSF に対し LR 法によって Deconvolution することで精度向上を行うことができた。

上記によって復元されたデータを用いて、金星大気中のエアロゾルの粒子の大きさの解析を行った。この解析には高精度な測光観測が必要であり、復元前のデータからは確認できなかったが、本研究の手法で復元された画像によってより正確な結果が得られた。さらに、巨大な雲における不連続構造など、様々な興味深い形状も確認できた。

結果として、RD 法によるデータ復元精度の向上を達成することができた。

LIR で同定された金星における惑星規模大気波動の構造

神山 徹 [1]; 今井 正尭 [1]; 今村 剛 [2]; 堀之内 武 [3]; 田口 真 [4]; 福原 哲哉 [5]; 佐藤 隆雄 [6]; 村上 真也 [7]; はしもとじょーじ [8]; Lee Yeon Joo[9]; 二口 将彦 [10]; 山田 学 [11]; 秋場 聖浩 [12]; 佐藤 毅彦 [13]; 中村 正人 [14]
[1] 産総研; [2] 東京大学; [3] 北大・地球環境; [4] 立教大・理・物理; [5] 立教大・理; [6] 情報大; [7] 宇宙研; [8] 岡大・自然; [9] JAXA/ISAS; [10] 東邦大; [11] 千葉工大・惑星探査研究センター; [12] 立教大・理・物; [13] 宇宙研; [14] 宇宙研

Structures of wavenumber-1 planetary scale waves at the cloud level of Venus identified by LIR

Toru Kouyama[1]; Masataka Imai[1]; Takeshi Imamura[2]; Takeshi Horinouchi[3]; Makoto Taguchi[4]; Tetsuya Fukuhara[5]; Takao M. Sato[6]; Shin-ya Murakami[7]; George Hashimoto[8]; Yeon Joo Lee[9]; Masahiko Futaguchi[10]; Manabu Yamada[11]; Masahiro Akiba[12]; Takehiko Satoh[13]; Masato Nakamura[14]
[1] AIST; [2] The University of Tokyo; [3] Hokkaido University; [4] Rikkyo Univ.; [5] Rikkyo Univ.; [6] HIU; [7] ISAS/JAXA; [8] Okayama Univ.; [9] JAXA/ISAS; [10] Toho Univ.; [11] PERC/Chitech; [12] Physics department, Rikkyo Univ; [13] ISAS, JAXA; [14] ISAS

It has been observed planetary-scale waves, such as Kelvin wave and Rossby wave, in Venusian atmosphere by analyzing periodical signatures in variations of windspeeds and UV cloud albedo. However, because the cloud tracking with UV data and the albedo analysis can be applied only in dayside region, it is difficult to capture a whole structure of the planetary-scale wave at one time. Due to the difficultly, we usually assume that such waves have wavenumber-1 structures when we conduct a periodical analysis, though any wavenumber-1 structure has not been directly identified.

Longwave Infrared Camera (LIR) onboard Akatsuki captures thermal emission from the upper level of the cloud layer of Venus, and thus it can observe brightness temperature in both hemispheres and over the whole local time. In this study, we projected the observed brightness temperature onto a coordinate rotating with a 4-day period for detecting a Kelvin wave, or a 5-day period for a Rossby wave. By using such the rotating coordinate, we can exclude signals whose periods are not same as the assumed rotating period. We used LIR data (1) from October to December 2018 for detecting a Kelvin wave, and (2) from July to September 2017 for a Rossby wave. The data periods were determined based on the periodical analysis for the cloud tracking results from Akatsuki data. From the results, we confirmed clear wavenumber-1signatures in both cases for 4-day and 5-day waves, which is a first result of identifying wavenumber-1 waves without any wavenumber-1 assumption. The detected 4-day wave was centered at the equator, which is consistent with the Kelvin wave signature, whereas the 5-day wave had a rather latitudinally broad structure.

In this presentation, we will introduce our approach to extract the wave signatures with LIR data, and will discuss the characteristics of the waves, such as latitudinal extents and directions of vertical propagation.

金星大気に関する多くの観測で Kelvin 波や Rossby 波といった数日周期で惑星を一周する惑星規模の波動が、雲追跡結果から得られた風速変動や、紫外波長での雲明るさ変化の周期解析から同定されてきた。ただし雲追跡や雲明るさ変動解析は昼面のみにデータが限られ、惑星規模の波動構造を 1 度にとらえることが困難であった。結果、周期解析では波動の経度方向の水平スケールを暗黙のうちに波数 1 構造を仮定することが常であり、このような仮定を置かず直接的に波数 1 構造を取り出した研究事例はいまだない。

本研究ではこのような惑星規模の波数 1 構造を抽出するため、金星雲層からの熱放射を昼・夜の別なく捉えることができるあかつき/中間赤外カメラ (LIR) 温度画像を用いる。とくに数日周期で惑星を一周する構造を抽出するため、スーパーローテーションより短い周期で伝搬する Kelvin 波については 4 日、長い周期で伝搬する Rossby 波については 5 日周期で回転する座標系上を設定し、観測された温度の平均を行った。観測データとして、これまでの解析からそれぞれの波動シグナルが確認されている、Kelvin 波には 2018 年 10 月〜12 月、Rossby 波には 2017 年 7 月〜9 月のデータを用いた。解析の結果、Kelvin 波、Rossby 波両者について仮定を置くことなく波数 1 構造が初めて同定された。また Kelvin 波は赤道にトラップされたような構造が見られ、また Rossby 波は幅広い緯度に広がったような構造を持ち、理論的に予想される構造と整合的であった。

本発表ではこのような結果を得るために実施した解析手順を紹介するとともに抽出された波動を特徴づける緯度構造や伝搬特性について議論を行う。

惑星大気の筋状模様の傾きについて

今村 剛 [1]
[1] 東京大学

Orientation of streaks

Takeshi Imamura[1]
[1] The University of Tokyo

The mechanism that determines the orientation of streaks is studied. We consider two types of streak formation in a steady, axi-symmetric atmospheric circulation:

(1) Stretching of meso-scale clouds by a sheared flow

(2) Advection of tracers that are continuously supplied from a localized, moving source (by some propagating wave)

Mathematical expressions of the orientation of streaks for these cases were derived. It was found that streaks follow the streamline in the coordinates corotating with the source of the tracers in both cases. The expression explains the observed streak orientation, and furthermore, superposition of streaks having different orientations was found to be possible. Based on the expression the latitudinal distribution of the source of clouds can be constrained from the observed streak distribution.

「あかつき」紫外カメラが撮影した金星の雲頂には様々な筋状模様が存在し、緯度線に対して異なる傾きを持った筋状構造が重なり合う様子もしばしば見られる。このような筋状構造は大気循環によって流される雲や紫外吸収物質の塊が風速シアーによって引き延ばされることによって作られると考えられるが、その傾きが風速場によってどのように決まるのかはきちんと導出・定式化されておらず、またどのような場合に傾きの異なる筋状模様が重なり合うことができるのかも説明されていない。本研究では、経度依存のない定常的な東西・南北風による以下の 2 通りの筋状模様の形成について考える。

(1) 小規模なトレーサー塊が引き延ばされて筋状模様になる。

(2) 特定の緯度で波動により一定の位相速度で伝播する局所的なトレーサー源を考え、そこから流れ出すトレーサーの分布が筋状模様となる。

金星でいえば、前者は小規模な雲塊の模様を、後者は未知吸収物質の傾いた帯状構造を想定している。

それぞれについてトレーサー分布の傾きを支配する微分方程式を導いて解いたところ、いずれの場合についても、筋状模様はトレーサーの発生源の自転軸周り角速度の回転座標系における流線に一致することがわかった。得られた式をもとに金星雲頂の低緯度で供給されたトレーサーが高緯度に流されながら作る筋状模様の傾きを計算すると、観測された傾きに近い値が得られる。また、異なる緯度で発生した雲塊がそれぞれ引き延ばされながら流れていくとすれば異なる傾きを持つ筋状構造が同時に存在しうることがわかった。この理解に立ち、金星雲頂の筋状模様の分布から雲塊の起源の緯度分布の情報を得ることができると考えられる。

Development of prediction system of Mercury's magnetosphere for any solar wind parameter

Manabu Yagi[1]; Kanako Seki[2]; Yosuke Matsumoto[3]; Dominique Delcourt[4]; Francois Leblanc[5]
[1] RIKEN R-CCS; [2] Dept. Earth & Planetary Sci., Science, Univ. Tokyo; [3] Chiba University; [4] LPP, Ecole Polytechnique, CNRS; [5] LATMOS-IPSL, CNRS

The Launch of the Bepi-Colombo is a big news for all scientists studying space environment of Mercury. Observations by previous satellite 'MESSENGER' found the Mercury's magnetosphere to be analogous to the Earth's, while several issues have been remained. One of the important issue is each distribution of heavy ions' components originating the Mercury's exosphere. The Larmor radii of heavy ions are not negligible to the magnetospheric size, and kinetic effects of such ions will be important in Mercury's magnetosphere. Until 2025, Bepi-Colombo's arrival, developing the Mercury's magnetospheric model which can be used for the prediction system for any solar wind parameter is target of our work. Comparison of different types of models, such as MHD(ideal/multi-fluid), Test Particles, Hybrid, and PIC simulations, is a good approach to know a global structure of Mercury's magnetosphere and kinetic effects of exospheric ions, as is starting the SHOTS (Studies on Hermean magnetosphere Oriented Theories and Simulations) team's activities. In this study, first we performed over 1000 cases of MHD simulation solving an interaction with solar wind plasma and offset dipole of Mercury, and tracing trajectories of heavy ions in the electric and magnetic fields obtained from MHD simulation. In the realistic IMF case which comes from Parker's spiral, global configurations of magnetosphere are drastically changed from pure northward IMF case and become more complicated structures which include stronger north-south and dawn-dusk asymmetry. IMF-Bx also affects to the intensity ratio of north and south cusp pressure, while the location cusp didn't change largely. IMF-By component 'twist' the cusp region to longitudinal direction. The heavy ions' trajectories basically obey the global structure of magnetic field, so that the ions' precipitation concentrate on the 'magnetic cusp' defined from MHD simulations, but the precipitation region is wider and diffusive compared to the MHD cusp. In the presentation, we will discuss the comparison of MHD and heavy ion precipitation pattern. The identification of global structures and ions' precipitation region especially the cusp is important not only on the understanding of magnetospheric physics itself, but also making a proposal to the observational plan of spacecraft such as Bepi-Colombo.

SHOTS simulations of Mercury's magnetosphere for the BepiColombo mission

Hideyuki Usui[1]; Sae Aizawa[2]; Manabu Yagi[3]; Go Murakami[4]; Usui Hideyuki BepiColombo SHOTS simulation team[5]
[1] System informatics, Kobe Univ; [2] Geophysics, Tohoku Univ; [3] RIKEN R-CCS; [4] ISAS/JAXA; [5] -

http://shots-bepicolombo.irap.omp.eu/

We present the current activities of the SHOTS team (Studies on Hermean magnetosphere Oriented Theories and Simulations). SHOTS is an international simulation collaboration that was formed by some motivated members in Young Scientists Working Group of the BepiColombo Mercury mission. It focuses on the plasma simulations of the plasma interaction with Mercury's environment using multi-fluid/MHD, hybrid, and fully kinetic (particle-in-cell) models. SHOTS aims to figure out which model is more suitable to describe particular environments or physical processes in Mercury's magnetosphere, and how and where the kinetic effect has significant influence.SHOTS has been currently working on global simulations to examine Mercury's magnetosphere using different numerical approaches. The small size of Mercury's magnetosphere is a promising topic to compare and benchmark simulation codes based on different numerical approaches such as MHD, Hybrid particle, and Full PIC. These codes are used in numerical simulations within the BepiColombo community for specific questions needed to be investigated. However, there has never been a quantitative comparison of the existing codes in their numerical effectiveness, stability, and different approaches for the same physical problems. To demonstrate how different numerical approaches in the simulations affect our understanding of the features of Mercury's magnetosphere, we have been working on MHD and hybrid particle simulations with a common solar wind condition in terms of density, Mach number, and IMF. We will discuss how the major features of the magnetosphere are characterized by each simulation, including the bow shock, the magnetopause, and a typical current sheet crossing. We will also discuss the effect that different boundary conditions between each code can have on overall structures visible in the various simulations.

In preparation for BepiColombo observations, we plan to run all the codes with realistic physical conditions. In addition to inter-code comparisons, we will compare our simulations with available data from the MESSENGER mission.

太陽系天体の宇宙風化再現実験に向けた汎用プラズマ照射装置の開発

木村 智樹 [1]; 木村 淳 [2]; 吉岡 和夫 [3]; 村上 豪 [4]; 寺田 直樹 [5]; 臼井 英之 [6]; 西野 真木 [7]; 横田 勝一郎 [8]; 三宅 洋平 [9]
[1] Tohoku University; [2] 阪大・理・宇宙地球; [3] 東大・新領域; [4] ISAS/JAXA; [5] 東北大・理・地物; [6] 神戸大・システム情報; [7] 名大 ISEE; [8] 阪大; [9] 神戸大学

Development of Generic Plasma Irradiation System for Modeling of Space Weathering at Solar System Bodies

Tomoki Kimura[1]; Jun Kimura[2]; Kazuo Yoshioka[3]; Go Murakami[4]; Naoki Terada[5]; Hideyuki Usui[6]; Masaki N Nishino[7]; Shoichiro Yokota[8]; Yohei Miyake[9]
[1] Tohoku University; [2] Earth & Space Science, Osaka Univ.; [3] The Univ. of Tokyo; [4] ISAS/JAXA; [5] Dept. Geophys., Grad. Sch. Sci., Tohoku Univ.; [6] System informatics, Kobe Univ; [7] ISEE, Nagoya University; [8] Osaka Univ.; [9] Kobe Univ.

Surface and atmosphere of solar system bodies are continuously irradiated with the planetary magnetospheric plasma, solar wind, solar photon, cosmic dusts, and ring grains, which are responsible for long-term alteration of surface and atmospheric materials on timescales up to geological scale (Giga years) known as the 'space weathering'. The space weathering accompanies creation and destruction of molecules in the surface and atmospheric materials (see e.g., Johnson et al., in Jupiter textbook, 2004). For example, organic compounds like tholins are likely created and destroyed via the space weathering at Titan's upper atmosphere and icy moon's surfaces at Jupiter and Saturn (e.g., Waite et al., 2007; Lopez-Puertas et al. 2013). This suggests that the newly created/destroyed molecules are accumulated on the surface over the geological time scale, which are likely essential energy and material sources for evolutions of the surface, atmosphere, and possibly interior. However, the creation and destruction balance of surface/atmospheric molecules on the geological timescale are still unknown because of small irradiation doses in the previous laboratory experiments. Here we develop a new laboratory experiment system for modeling of the space weathering on geological timescales. In order to associate the space weathering with evolution of body's magnetic field, we first try to model the plasma space weathering with a high-fluence charged particle irradiation (<1e+23 particles/cm2). Now fabrication of the plasma irradiation system is going on after structural and thermal designs. The current status of development will be presented in this poster.

電子反射法を用いた太陽風中での月面磁場強度推定

#川口 友暉 [1]; 原田 裕己 [2]; 斎藤 義文 [3]; 横田 勝一郎 [4]; 西野 真木 [5]; 臼井 英之 [6]; 三宅 洋平 [7]; 高橋 太 [8]; 清水 久芳 [9]
[1] 京大・理・地惑; [2] 京大・理・地球惑星; [3] 宇宙研; [4] 阪大; [5] 名大 ISEE; [6] 神戸大・システム情報; [7] 神戸大学; [8] 九大・理・地惑; [9] 東大・地震研

Lunar surface magnetic field intensity in the solar wind inferred from electron reflectometry

Tomoki Kawaguchi[1]; Yuki Harada[2]; Yoshifumi Saito[3]; Shoichiro Yokota[4]; Masaki N Nishino[5]; Hideyuki Usui[6]; Yohei Miyake[7]; Futoshi Takahashi[8]; Hisayoshi Shimizu[9]
[1] Geophysics, Kyoto Univ.; [2] Dept. of Geophys., Kyoto Univ.; [3] ISAS; [4] Osaka Univ.; [5] ISEE, Nagoya University; [6] System informatics, Kobe Univ; [7] Kobe Univ.; [8] Kyushu Univ.; [9] ERI, University of Tokyo

The Moon is classified as a nonmagnetized, airless body that does not hold a global, intrinsic magnetic field and a thick atmosphere. Consequently, most of the solar wind particles collide with the lunar surface and get absorbed. Meanwhile, some regions of the lunar surface called magnetic anomaly are locally shielded from the solar wind by magnetic fields of crustal origin. Previous studies have focused mainly on the interaction between the solar wind and the strong magnetic anomaly. The purpose of this study is to reveal how the magnetic field strength on the dayside lunar surface varies globally, including weakly magnetized regions, by utilizing remote sensing data obtained by spacecraft.

In addition to direct measurements by magnetometers, the global distribution of crustal magnetic field strength has been investigated by electron reflectometry, which remotely infers the surface magnetic field strength from the loss cone angle of ambient electrons reflected from the lunar crustal magnetic field by the magnetic mirror effect. As the aim of the conventional electron reflectometry is measurements of the strength of the lunar crustal magnetic field itself, a standard practice is to use data obtained on the night side of the Moon and within the terrestrial magnetotail lobes with less influence of the solar wind plasma. Generally, energy dependence of the electron loss cone has to be taken into account because electrons are affected by electrostatic potential difference between the Moon and the spacecraft.

We utilized data obtained by the electron spectrum analyzers (MAP-PACE-ESA) and magnetometer (MAP-LMAG) on board Kaguya. By applying the electron reflectometry to the data obtained on the lunar day side in the solar wind, we revealed that the surface magnetic field intensity is globally enhanced, particularly under high solar wind dynamic pressure conditions. This suggests that the lunar crustal magnetic fields are compressed by the solar wind plasma. Additionally, we investigated the energy dependence of electron loss cone angles. As in previous studies, the energy dependence is evident in our data and the effect is smaller for high energy electrons. Based on this result, we utilized the 250-350 eV electron data, which are less affected by the energy dependent loss cone. We examined the response of the magnetic pressure on the lunar surface to the solar wind dynamic pressure variation and identified selenographical dependence of magnetic compression efficiency, which is better associated with the crustal magnetic field intensity at the lunar surface than that at a 30 km altitude. This suggests that the compression of lunar crustal magnetic fields is mainly caused by charged particle motion at low altitudes below a few tens of kilometers.

月は、全球的な固有磁場や大気を保持しない天体であり、太陽風のほとんどは月表面に衝突し吸収される。しかし、月面には磁気異常と呼ばれる地殻起源の磁場によって太陽風から局所的にシールドされている地域も存在する。これまでの観測及び数値シミュレーション研究では、主に強い磁気異常に着目して太陽風と月地殻磁場の相互作用について調べられてきた。本研究は、衛星による遠隔観測のデータから、比較的弱い磁気異常も含めた全球的な月面磁場強度の変動を明らかにすることを目的とする。

月地殻磁場の全球的な分布は、磁力計による直接観測に加えて、電子反射法を用いて調査されてきた。電子反射法は月周辺電子の磁気ミラー効果を利用して、月地殻磁場によって反射された電子のロスコーン角から月面での磁場強度を遠隔計測する手法である。従来、電子反射法は月地殻磁場自体の強度を計測するために、太陽風プラズマの影響が少ない月の夜側や地球磁気圏尾部ローブ内で得られたデータが用いられてきた。この手法を用いる際、電子は月と衛星間の電位差の影響を受けるため、エネルギー依存を考慮する必要がある。

今回、我々は月探査衛星「かぐや」に搭載された電子分析器 MAP-PACE-ESA-S1、-S2 と磁場観測装置 MAP-LMAG によって取得されたデータを用い、月地殻磁場により反射された太陽風電子について解析を行った。電子反射法を昼側月面が太陽風に曝されている時に計測されたデータに応用すると、太陽風動圧が高くなると月面磁場強度が全球的に強くなる傾向が見られた。これは月地殻磁場が太陽風によって圧縮されたためであると考えられる。さらに、月と衛星間の電位差の影響を評価するため、異なるエネルギー帯ごとの電子ピッチ角分布を解析し、電子ロスコーン角のエネルギー依存性を調べた。先行研究と同様に、電子のピッチ角分布にエネルギー依存性が見られ、高エネルギーの電子ほど影響が小さい傾向が得られた。この結果を踏まえて、エネルギー依存性の影響が小さい 250-350 eV の電子データを用い、太陽風動圧変動に対する磁気圧の応答を調べると、磁気圧の変化率に地域依存性が見られた。この地域依存性は、30 km 高度での地殻磁場強度分布よりも月面での磁場強度分布とよく対応することが明らかになった。この結果は、太陽風による月地殻磁場圧縮は、主に数 10 km よりも低い高度での荷電粒子の運動に起因することを示唆する。

月超低高度における磁気異常近傍プラズマの観測

齋藤 義文 [1]; 西野 真木 [2]; 横田 勝一郎 [3]; 高橋 太 [4]; 清水 久芳 [5]
[1] 宇宙研; [2] 名大 ISEE; [3] 阪大; [4] 九大・理・地惑; [5] 東大・地震研

Plasma observation at Very Low Altitude around Lunar Magnetic Anomalies

Yoshifumi Saito[1]; Masaki N Nishino[2]; Shoichiro Yokota[3]; Futoshi Takahashi[4]; Hisayoshi Shimizu[5]
[1] ISAS; [2] ISEE, Nagoya University; [3] Osaka Univ.; [4] Kyushu Univ.; [5] ERI, University of Tokyo

The detailed plasma structure around magnetic anomalies on the dayside of the Moon at ˜25km altitude was investigated using Kaguya MAP-PACE data. When Kaguya flew over strong magnetic anomalies at ˜25km altitude in the solar wind, deceleration of the solar wind ions, acceleration of the solar wind electrons, and heating of the ions reflected by magnetic anomalies were observed. Deceleration of the ions and acceleration of the electrons were explained by the existence of the DC electric field over dayside magnetic anomalies generated by the difference in the motion between incident electrons and ions. Although it was found that the reflected ions had higher temperature and lower energy than the incident solar wind ions and it clearly indicated the existence of a non-adiabatic interaction between solar wind ions and lunar magnetic anomalies, the detailed heating mechanism remains unsolved.

Two days before Kaguya impacted the Moon on 9 and 10 June 2009. the perilune altitude became lower than 10km. During this time period, Kaguya was in the Earth's magnetosheath. Since the observation at the lower altitude than 10km will give us additional information to understand the ion heating mechanism, we have analyzed the data obtained at very low altitude <10km around magnetic anomalies. In addition to the deceleration of the ions and acceleration of the electrons in the regions surrounding magnetic anomalies, trapped electrons were observed at the center of the magnetic anomalies. It has been found that the magnetic field structure and/or plasma structure is highly asymmetric around some of the magnetic anomalies. It has also been found that there exists enhanced ion flux observed only in the center part of the magnetic anomalies in some cases. Ion and electron data at very low altitude show more complicated plasma structure than the structure observed at higher altitude.

月昼間側の磁気異常上空約 25km 高度より高高度におけるプラズマ構造は、かぐや衛星に搭載された MAP-PACE によって明らかになった。それによると、太陽風イオンの減速と太陽風電子の加速が同時に観測され、太陽風中のプロトンとアルファ粒子の両方について、イオンの電荷あたりの減速エネルギーは電子の加速エネルギーとほぼ等しい。このことはかぐや上空に上向の静電場が存在することで説明できる。これに加えて、月面方向から飛来するイオンは、バルク速度が太陽風よりも下がり、同時に温度が高くなっていることが明らかとなったが、これらの月面方向から飛来するイオンについては、どのようにしてバルクエネルギーを失い、温度が高くなるのかについて未だによくわかっていない。

かぐやが月面に衝突する直前、2009 年 6 月 9 日と 10 日にはかぐやの高度は最も低いところでは 10km より低い高度になった。この期間、月は地球のマグネトシース領域に位置していたが、10km より低い高度で磁気異常近傍のプラズマを観測すれば、25km 以上の高度の観測ではわからなかった、より低高度におけるイオンの加熱についての情報が得られることを期待して、この超低高度における観測データの解析を試みた。10km 以下の高度の観測データの中には、磁気異常の中心部に月面に両側の繋がった磁力線の領域（trapped electron が観測される）があり、その両側には片側の磁力線のみが月面に繋がった領域（加速された磁力線に沿った電子が観測される）があると解釈できる例があった。これらのデータは、磁気異常によって太陽風が遮蔽される領域の中をかぐやが通過したことを示しており、そこで観測されたプラズマのデータは 25km 高度のデータと整合する。ただ多くの場合、磁気異常領域に入る側と磁気異常領域から出る側で磁場の形状にも、プラズマの分布にも非対称が存在することも明らかとなった。また、10km 以下の高度で観測されたデータの中には、磁場強度の強いところで（主として月面方向から飛来すイオンを計測する質量分析器で）H+イオンの観測される量が多いということも明らかとなった。これに加えて、磁気異常の近傍には、磁気異常の磁場強度が強い程、エネルギーの高い側からよりエネルギーの低いところまでの電子が減少する領域があることも明らかとなった。

月極域探査ローバー搭載用飛行時間計測型質量分析器の開発

福山 代智 [1]; 齋藤 義文 [2]; 横田 勝一郎 [3]; 浅村 和史 [4]
[1] 東大・理・地球惑星; [2] 宇宙研; [3] 阪大; [4] 宇宙研

Development of a time-of-flight mass spectrometer for future lunar polar exploration

Daichi Fukuyama[1]; Yoshifumi Saito[2]; Shoichiro Yokota[3]; Kazushi Asamura[4]
[1] Earth and Planetary Science, The University of Tokyo; [2] ISAS; [3] Osaka Univ.; [4] ISAS/JAXA

Recent observations by lunar explorers have reported the possible existence of ice composed of volatile matter containing H_2O in permanent shadowed craters in lunar polar region, but details such as its abundance and composition are not known. We are developing a mass-spectrometer (Time-Of-Flight Mass Spectrometer: TOF-MS), which we aim to install in a rover landing on the moon of a future lunar polar exploration and will contribute to the elucidation of the composition of volatiles in lunar permanent shadowed craters.

In a TOF-MS, neutral particles are ionized, accelerated in an electric field, and made to fly in a free space. Mass analysis of ions is carried out using mass dependence of flight time. In this method, since the mass resolution is proportional to the flight time of the ions, it is necessary to make the flight path of the ions long to achieve high mass resolution. In order to increase the flight distance without increasing the size of the device, a reflectron-type TOF-MS, which reflects ions by an electric field, is adopted. On the other hand, increasing the number of reflections lowers the detection efficiency because trajectories of ions disperse as the flight distance of the ions increases. Therefore, our instrument is equipped with multiple reflection mode with high mass resolution and one reflection mode with reduced number of reflections and emphasis on sensitivity. These measurement modes are able to be switched for each observation target by only controlling the potential of some electrodes. Redundancy is important in this device because it is assumed to be exposed to shocks of launch and landing on the moon. In order to realize multiple measurement modes, two pulse high voltage modules were used for the acceleration region and the reflection region of this instrument. As a result, this device realized redundancy against failure of the pulse high voltage module.

Currently, a test model is being tested to confirm that it is able to achieve an expected performance.

We will mainly report the performance test results of TOF-MS test model.

近年の月探査機による観測により、月極域永久影における H_2O を含む揮発性物質からなる氷の存在を示唆する観測結果が報告されているが、その存在量や組成等の詳細は不明である。我々は将来の月極域着陸探査ローバーに搭載し、月極域の揮発性物質の組成の解明に貢献する質量分析器（Time-Of-Flight Mass Spectrometer :TOF-MS）の開発を行っている。

TOF-MS は中性粒子をイオン化・電場加速した上で自由飛行させ、飛行時間の質量依存性からイオンの質量分析を行う。本方式において質量分解能はイオンの飛行時間に比例するため、高質量分解能を実現するためには、イオンの飛行経路を長くとる必要がある。機器を大型化させることなく飛行距離を稼ぐため、イオンを電場によって反射させるリフレクトロン方式 TOF-MS を採用した。一方で、イオンの軌道はイオンの飛行距離が長くなるにつれて分散するため、反射回数を増やすと検出効率が低下する。そこで、本機器は高質量分解能の複数回反射モードと、反射回数を抑え感度を重視した 1 回反射モードを搭載し、観測対象ごとにこれらの測定モードを切り替えられるようにした。これらの測定モードは電極に印加する電位の制御のみによって可能である。打ち上げ時の振動や天体への着地による衝撃を受けるローバーへの搭載を想定した本機器において、故障に対する冗長性は重要である。複数の測定モードの実現のため、本機器の加速領域と反射部にはそれぞれ独立したパルス高圧モジュールを用いた。これにより、本機器はパルス高圧モジュールの故障に対する冗長性を実現した。

現在はシミュレーションをもとに製作した試験モデルが設計通りの性能を達成しているかを確認するための実験を行っている。

本発表では主に TOF-MS 試験モデルの性能試験結果を報告する。

Elastic collisions between magnetospheric electrons and neutral H2O molecules in the Enceladus torus by test particle simulation

Hiroyasu Tadokoro[1]; Yuto Katoh[2]
[1] Musashino University; [2] Dept. Geophys., Grad. Sch. Sci., Tohoku Univ.

Water group neutrals (H_2O, OH, and O) in Saturn's inner magnetosphere play the dominant role in loss of energetic electrons and ions because of abundance of the neutrals [e.g., Paranicas et al., 2007; Sittler et al., 2008]. The observations of injected plasmas in the inner magnetosphere suggest that these particles do not survive very long time due to the neutral cloud originated from Enceladus [e.g., Paranicas et al., 2007; 2008]. Thus, the previous studies suggested that the neutral cloud contributes to loss processes of plasma in the inner magnetosphere. However, little has been reported on a quantitative study of the electron loss process due to electron-neutral collisions. Tadokoro et al., [2014] focused on the elastic collision between 1keV electron and neutral H_2O and examined the variation of 1keV electron pitch angle distribution due to elastic collisions with the dense region of H_2O originated from Enceladus using one-dimensional test-particle simulation. They reported that the electrons of ˜11.4% to the total number of equatorial electrons at the initial condition are lost in ˜380sec, corresponding to the co-rotating electron flux tube passes the dense H_2O region in the vicinity of Enceladus. Assuming the uniform azimuth H_2O density structure in the Enceladus torus, they estimated the electron loss rate of 33% during one co-rotation.

In this study, we focus on the elastic collisional loss process with neutral H_2O originated from Enceladus. We show the loss rates through pitch angle scattering of electrons with 500eV-50keV (500eV, 700eV, 1keV, 5keV, 10keV, 20keV, 30keV, 40keV, 50keV) and the comparison of the loss rates between the high (in the vicinity of Enceladus) and low (in the Enceladus torus) H_2O density regions. We also show the calculation errors by making 10 times calculations.

Design of an ion mass spectrometer for the Comet Interceptor mission

Satoshi Kasahara[1]; Shoichiro Yokota[2]; Yoshifumi Saito[3]; Kazushi Asamura[4]; Masafumi Hirahara[5]; Ayako Matsuoka[6]
[1] The University of Tokyo; [2] Osaka Univ.; [3] ISAS; [4] ISAS/JAXA; [5] ISEE, Nagoya Univ.; [6] ISAS/JAXA

Comet-solar wind interaction provides us with opportunities to study plasma structures and phenomena, which are otherwise difficult or impossible to observe in other solar-system objects. Although several flybys and rendezvous have been performed for several comets (e.g., 1P/Halley, 21P/Giacobini-Zinner, 67P/Churyumov-Gerasimenko, etc), simultaneous multi-point measurements have not been achieved so far, and thus the large-scale structures of plasma boundaries around comets are unclear. The Comet Interceptor mission, aiming at a dynamically-new comet or an interstellar object, will provide the first such measurements, in collaboration between ESA and JAXA. In this mission, Japan will provide a daughter spacecraft, whose closest approach will be $<$1,000 km, allowing crossings of several kinds of plasma boundaries. Plasma suite onboard the Japanese daughter spacecraft consists of an ion mass spectrometer and a magnetometer to obtain the details of plasma boundaries as well as other plasma processes around a comet. Here we present the design of ion mass spectrometer onboard Japanese daughter spacecraft of Comet Interceptor.

小天体大気の水素・重水素遠隔観測に向けた吸収セルのフィラメント開発

米本 周平 [1]; 田口 真 [2]; 吉岡 和夫 [3]; 川原 琢也 [4]; 亀田 真吾 [5]; 桑原 正輝 [6]
[1] 東大・理・地球惑星; [2] 立教大・理・物理; [3] 東大・新領域; [4] 信州大・工; [5] 立教大; [6] ISAS/JAXA

Filament development of absorption cell for remote observation

Shuhei Yonemoto[1]; Makoto Taguchi[2]; Kazuo Yoshioka[3]; Takuya Kawahara[4]; Shingo Kameda[5]; Masaki Kuwabara[6]
[1] Earth and Planetary Science,Tokyo Univ.; [2] Rikkyo Univ.; [3] The Univ. of Tokyo; [4] Faculty of Engineering, Shinshu University; [5] Rikkyo Univ.; [6] ISAS/JAXA

The ORIGIN of Earth's water is not clear. Researchers have debated the possibility of comets and asteroids of delivereing the Earth's water.

The deuterium-to-hydrogen ratio (D/H) in water between the asteroids, comets, and Earth's oceans is crucial. Previous D/H measurements have been made for a dozen comets form Oort cloud and three Jupiter family comets. We need to get close to Jupiter family comets with a spacecraft. Therefore, we are developing a smaller and lighter absorption cell than the device that has measured D/H ratio.Using the absorption cell, the opportunity for spacecraft observation for Jupiter family comets will be increased.

The absorption cell is made of glass and contains a filament.Hydrogen molecules or deuterium molecules are filled. When the filaments are activated, H2 is dissociated into atomic H.The H atoms in the cell can absorb the Lyman-alpha line from comets through the resonance scattering. Then, the amount of deuterium and hydrogen can be estimated from the measured values with and without activating the filament.

We have made a prototype hydrogen absorption cell and evaluate its performance. We have two problems with prototypes. The first is that when the filament of the cell is activated, light from 110 nm to 130 nm is emitted. The second is that the filament is broken in several tens of hours. As a cause of the fact that the absorption cell emits light of 110 nm to 130 nm, it is suspected that the hydrogen Lyman alpha line is emitted because emitted electron from hot filament. In addition, we want to extend the life of the filament by adding a rare gas so that the filament does not break in a few tens of hours. We will test these two problems and present a summary of the results obtained.

現在存在している水は地球が冷えた後に彗星あるいは小惑星の衝突によりもたらされたという学説が有力である (Drake et al, 2002).

水の D/H 比は地球の水の供給源を推定するための指標とされる. この学説を検証するために, 彗星やコンドライトの D/H 比が測定されてきた. しかし, カイパーベルトを起源とする木星族彗星についての 3 例の D/H 比測定結果は（1.61+/-0.24) $\times 10^{-4}$,2.0 $\times 10^{-4}$ 未満,(5.3+/-0.7) $\times 10^{-4}$（Hartogh et al., 2011 ,Ceccarelli et al., 2014 ,Altwegg et al., 2015) であり, 傾向がつかめていない. そこで, 私たちは過去の木星族彗星の大型探査機計画で用いられてきた分光器（約 30 kg）や質量分析器 (約 16 kg) よりも, 超小型探査機に搭載可能である小型・軽量（約 1 kg）な吸収セルイメージャーの開発を進めている.

水素と重水素の輝線である Ly-α の波長はそれぞれ 121.567 nm, 121.534 nm で, 約 33 pm の違いがある. これらの輝線を分離して観測できれば, その強度比から D/H 比を得られる.

吸収セルは, ガラスでできた容器（セル）であり, 光を入射, 出射する面には Ly-α を透過するフッ化マグネシウムを使用する. セル内は水素分子・重水素分子で満たされている. フィラメントを加熱していない時は, 水素・重水素の Ly-α は共にセルを通過し, 光検出器まで到達するが, セル内のフィラメントを加熱すると分子が原子になり共鳴散乱を起こすため, 水素の Ly-α は検出器まで到達しなくなる. この現象を用いて, フィラメントの加熱時/非加熱時による Ly-α の光量差から対象の水素・重水素の発光強度を導出できる.

現在私たちは水素吸収セルの試作品を作成し, 性能を評価している. フィラメント加熱時に何らかの要因で光ノイズが生じていることを発見した. これを低減することで, 観測の S/N を向上させられる可能性がある. 光ノイズの発生原因としては, フィラメントの黒体放射, あるいは熱電子もしくは熱エネルギーによる水素原子の励起が考えられる. 原因を実験的に特定した上で, 新しいフィラメント素材の選定, フィラメントに与える電力を検討する. 加えて, フィラメントの寿命にも改善の余地がある. この二点の問題点について, 理論的な検討と試験を進めて得られた結果を発表する.

超小型極端紫外撮像装置に用いる電子回路部の放射線耐性評価

勝瀬 陸 [1]; 吉岡 和夫 [2]; 桑原 正輝 [3]; 疋田 伶奈 [4]; 吉川 一朗 [5]
[1] 東大・新領域・複雑理工; [2] 東大・新領域; [3] ISAS/JAXA; [4] 東大・理・地惑; [5] 東大・理・地惑

Evaluation of radiation tolerance of electronics parts used for the ultra-small mission

Riku Katsuse[1]; Kazuo Yoshioka[2]; Masaki Kuwabara[3]; Reina Hikida[4]; Ichiro Yoshikawa[5]
[1] Complexity Science and Engineering, The University of Tokyo; [2] The Univ. of Tokyo; [3] ISAS/JAXA; [4] the Univ. of Tokyo; [5] EPS, Univ. of Tokyo

In the space environment, as spacecraft is exposed to radiation, the data obtained with instruments would be degraded. For example, the increase in dark current, upset, and change in current consumption would occur.

Recently, the university-made ultra-small spacecraft mission has become popular. As for the mission in this class, we can reduce the cost and time by using commercial products. However, these commercial products are thought to have no radiation tolerance.

We are developing the extreme ultraviolet imager, PHOENIX, onboard the ultra-small satellite, EQUULEUS, which will be launched in 2020. Helium ions in the Earth's plasmasphere emit extreme ultraviolet light (at a wavelength of 30.4 nm) through the solar resonance scattering. PHOENIX will observe it from the moon (Earth-Moon L2 point).

We did the radiation testing of the electronics parts with the equipment using cesium-137. And the radiation tolerance was confirmed.

In this presentation, we will show the gain characteristics and current increase and change of electric noise of semiconductor elements used in PHOENIX instrument with respect to radiation. In addition, we will discuss the applicability of commercial products in the future.

飛翔体搭載機器に用いられる電子機器は、宇宙空間の放射線に曝されることでノイズの増加、ビット反転、消費電流の増加、などの悪影響を受ける恐れがある。

近年、大学の研究室規模で超小型探査機の開発が実現している。超小型の枠組みでは、民生部品を用いて開発にかかる費用と時間を大幅に低減することで、短期間でのミッションの実現を可能にしている。しかし、民生部品は放射線耐性を考慮した設計がなされていないという欠点がある。

我々は、2020 年に打ち上げ予定の超小型衛星 EQUULEUS に搭載される極端紫外撮像機「PHOENIX」を開発している。「PHOENIX」は、地球のプラズマ圏を構成するヘリウム一価イオンが太陽共鳴散乱によって発する極端紫外領域の輝線 (波長 30.4nm) を月近傍から準定常的に観測することで、プラズマ圏の動的描像の大局的な理解することを科学目的としている。

「PHOENIX」は、放射線耐性を考慮していない民生部品を用いて開発されているため、実際の利用環境を再現した試験を通して放射線耐性を確認する必要がある。

我々は、セシウム 137 を用いたガンマ線照射装置で、「PHOENIX」に用いられる電子回路部内に組み込まれた半導体素子の放射線耐性を試験した。「PHOENIX」の予定された運用期間は 2 年で、想定される総吸収線量が 12krad であるため、一時間当たりの照射率は〜7∗10^(-4)krad/h である。本試験では、照射率が〜15krad/h であるため、実際より厳しい放射線環境を設定している。この環境下で、半導体素子の放射線耐性を確認した。

本発表では、累積放射線量の増加によって確認された電流値の増加、半導体素子の利得率特性の変化、電気ノイズレベルの変化について評価した結果を述べる。加えて、放射線照射率の高い木星周辺や、反対に低い火星周辺の環境下での民生部品の応用可能性について議論する。

Proton-oxygen differences in energy spectral evolution during large-scale injections in Saturn's magnetosphere

Kunihiro Keika[1]; Pontus Brandt[2]; Donald Mitchell[2]; Shotaro Sakai[3]
[1] University of Tokyo; [2] JHU/APL; [3] Dept. Earth & Planetary Sci., Science, Univ. Tokyo

It is believed that radial transport with sharp, localized filamentary structures due to inter-change instabilities is the main transport process in Saturn's inner magnetosphere [e.g., Hill et al., 2005, GRL; Paranicas et al., 2016, Icarus; Azari et al., 2019, JGR]. Global injections of energetic particles (higher than 10 keV, non-thermal) were also observed, associated with large-scale reconfigurations of the magnetotail magnetic field probably caused by reconnection [c.f., Mitchell et al., 2015, AGU Monograph]. The pressure of the non-thermal plasma becomes comparable to and dominates thermal pressure outside 9 Rs and 12 Rs, respectively [e.g., Sergis et al., 2010, GRL]. The large-scale injections therefore play an important role in transport and acceleration. Our study focuses most on generation and transport of non-thermal H^+ and O^+ during the large-scale reconfiguration. Observations showed different responses (e.g., relatively high O^+ temperature) to the reconfiguration between the two species [e.g., Dialynas et al., 2009, GRL]. However, the dominant mechanism(s) of selective/mass-dependent acceleration is(are) not fully understood.

Using observations of energetic neutral atoms by the Ion Neutral Camera (INCA) of the Magnetospheric Imaging Instrument (MIMI), we examine the spatio-temporal evolution of energy spectra for hydrogen and oxygen atoms with energies of ˜10 to ˜300 keV. The time sequence of the spectral evolution during large-scale injections is of our particular interest. To characterize the relation of the spectral evolution to the magnetic field dipolarization, we utilize in-situ ion observations by INCA and Charge Energy Mass Spectrometer (CHEMS) and magnetic field measurements by the Cassini magnetometer (MAG). For an example event of large-scale injections on 2 July 2004, energy ranges that make the dominant contribution to ion energy density, which we term 'contributing energies', were higher for O^+ than H^+. This is qualitatively consistent with observations in the Earth's magnetotail [Keika et al., 2018, GRL]. The oxygen-proton difference indicates that O^+ is effectively or selectively energized during the magnetic field reconfiguration in the magnetotail. We discuss how universal the ion acceleration during the magnetic field reconfiguration is to the magnetospheres of different magnetized planets.

ALMAアーカイブデータ解析による木星衛星イオの二酸化硫黄大気の火山噴火成分の検出

古賀 亮一 [1]; 鈴木 達也 [2]; 平原 靖大 [3]; 土屋 史紀 [4]; 鍵谷 将人 [5]; 坂野井 健 [6]
[1] 東北大・理・地物; [2] 名大・環; [3] 名大・院・環境・地球惑星; [4] 東北大・理・惑星プラズマ大気; [5] 東北大・理・惑星プラズマ大気研究センター; [6] 東北大・理

Detection of the volcanic component of Jupiter moon Io's atmosphere by analyzing ALMA archive data

Ryoichi Koga[1]; Tatsuya Suzuki[2]; Yasuhiro Hirahara[3]; Fuminori Tsuchiya[4]; Masato Kagitani[5]; Takeshi Sakanoi[6]
[1] Geophysics, Tohoku Univ.; [2] Earth Sciences, Nagoya Univ.; [3] Earth&Planetary Sciences, Nagoya Univ.; [4] Planet. Plasma Atmos. Res. Cent., Tohoku Univ.; [5] PPARC, Tohoku Univ; [6] Grad. School of Science, Tohoku Univ.

Jupiter's moon Io is the most volcanically active body in the solar system, and it has SO_2 dominated thin atmosphere whose surface pressure is several nbar. Io's SO_2 atmosphere is mainly created by direct input from volcanoes, and by sublimation of the surface frost. SO_2 in the atmosphere are dissociated within ~30 hours, and sulfur and oxygen atoms in the atmosphere are partly escaped from Io's gravity by elastic collision with ions in Io plasma torus (atmospheric sputtering). Recently, the observations when Io was in Jupiter eclipse showed the sublimation is the dominant process which creates Io's atmosphere [Tsang et al., 2016]. However, the enhancement event of escape gasses of O and Na from Io's gravity was also reported [Yoneda et al., 2015; Koga et al., 2018]. The mechanism which increases the escape rate of the neutrals is not understood. The possible trigger is the increase of the exobase caused by the direct input from volcanoes, and the area where atmospheric sputtering occurs. To consider this hypothesis, it is important to detect the emission of atmospheric SO_2 which is ejected from Io's volcanoes.

ALMA (Atacama Millimeter/submillimeter Array) is the radio interferometry which has high spatial and wavelength resolutions. In the observation of Io in 2017, it achieved the beam size of 0.36 arcsec (Io's apparent size is about 1.0 arecsec) and the resolution of 0.21 km/s. We analyzed the ALMA archive data (project code: 2017.1.00670.S) several minutes before Io entered the Jupiter eclipse at 10:02-10:09 UT on March 20, 2017. If Io's atmosphere was created only by sublimation, SO_2 should concentrate only around the equator, where the solar zenith angle is large and the surface temperature is high. However, the actual spectral map shows SO_2 was not only concentrated around the equator (Region 1), but also distributed at high latitude in the northern hemisphere (Region 2). In Region 1, the spectral shape is symmetric and line width is narrow (Full width with half maximum (FWHM) = 0.57 km/s). In Region 2, the spectral shape is asymmetric and line width is broad (FWHM = 0.93 km/s). When we assume the line width is only determined by Doppler broadening because of the thin atmosphere, the atmospheric temperatures was 445 K in Region 1 and 950 K in Region 2. Both temperatures are much higher than sublimation atmosphere temperatures estimated by previous studies (130-180 K). The components in the line of sight of the large-scale atmospheric dynamics driven by pressure gradient broadened the line widths. However, we can not explain the difference of the temperature between Region 1 and 2 only by atmospheric dynamics. Therefore, we considered the atmosphere in Region 2 is composed of the low velocity component which include the sublimation atmosphere and high velocity component emitted directly from volcanoes. We fitted the composited Gaussian function which has two peaks to the observed spectral in Region 2. Difference between low and high velocity components is 0.58 km/s, the ratio of integrated line intensity is 6:1. Line widths (FWHM) of low and high velocity components are 0.76 km/s and 0.42 km/s. The possible reasons that the width of the low velocity component in Region 2 is broader than that in Region 1 are that gases emitted by volcanic input heat the outer atmosphere, and that pressure gradient and wind velocity around hot spot is larger than that around the equator without active volcanic input.

木星衛星イオは太陽系で最も火山活動が活発な天体であり、SO_2 を主成分とした数 nbar の希薄大気を形成している。イオの大気の生成は主に火口から直接噴出すること、及び表面に降り積もった SO_2 霜が太陽の光で温められて昇華することが考えられている。SO_2 大気は 30 時間程度で解離し、イオトーラスのプラズマと弾性衝突することで一部がイオの重力圏外へと散逸する (大気スパッタリング)。これまでは木星影をイオが横切るときの観測 [Tsang et al., 2016] 等によって、イオの大気形成は昇華が支配的とされていた。一方、2015 年にイオ重力圏外への散逸した Na や O の増加のイベントが報告されている [Yoneda et al., 2015; Koga et al., 2018]。この散逸ガスを増やすメカニズムはまだ未解明であるが、イベントを引き起こした要因として火口からの直接噴出による外気圏高度の上昇と、それに伴う大気スパッタリングが起こる面積の拡大が考えられる。この仮説の検証において、噴火で放出された大気成分を直接検出することは重要である。

ALMA (Atacama Large Millimeter/submillimeter Array) は高空間・波長分解能をもつ電波干渉計であり、2017 年のイオ観測時ではビームサイズ約 0.36 秒角 (イオは約 1.0 秒角), 波長分解能 0.21 km/s を達成している。本研究では、2017 年 3 月 20 日のイオが木星陰に入る直前 (10:02-10:09) の観測のアーカイブデータ (project code: 2017.1.00670.S) を解析した。もし、イオの大気が昇華のみで生成されている場合、太陽天頂角が高く表面が温まりやすい赤道周辺のみに SO_2 は集中するはずである。しかし、観測結果のマップ (添付図) から、SO_2 は赤道周辺だけでなく、北半球の高緯度にも分布することが分かった。また、赤道周辺の領域のスペクトルはピークに対称な形をして、線幅が狭かった (半値全幅 0.57 km/s)。一方、高緯度の領域のスペクトルはピークに非対称で、線幅が広い (半値全幅 0.93 km/s) 特徴があった。イオの大気は十

分薄いため、スペクトルの線幅がドップラー広がりに起因するとすると、赤道周辺の SO_2 大気の温度は 445 K、高緯度で 950 K となった。これらの温度は過去の観測で推定されている昇華大気温度 (130-180 K) と比べて有意に高い。大気の圧力勾配力による視線方向に垂直な速度成分の大気の大規模運動が線幅を広げていると考えられる。しかし、この運動では赤道周辺と高緯度の温度の違いを説明できない。本研究では高緯度の領域の大気は昇華大気を含んだ低速の成分と高速で火口から噴出される成分で構成されていると考え、二つのピークをもつガウス関数で観測スペクトルをフィッテイングした。その結果、低速成分と火山噴出成分の速度差は 0.58 km/s、発光強度比は 6:1 であった。また、線幅はそれぞれ半値全幅 0.76 km/s, 0.42 km/s であった。高緯度の領域の低速成分の線幅が赤道周辺の線幅より広い理由として、火口からの直接噴出ガスが周辺の大気を温めていること、火口周辺の方が赤道周辺より大気の密度勾配が大きく、風速が大きくなっていることが考えられる。

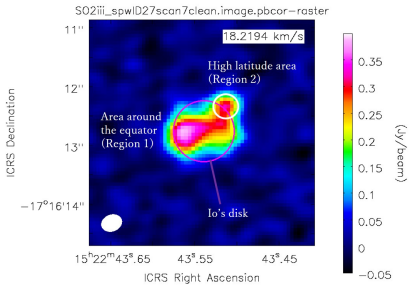

イオプラズマトーラスの突発増光現象におけるエネルギー供給過程の特定

西村 晟八 [1]; 鈴木 文晴 [2]; 吉岡 和夫 [3]; 疋田 伶奈 [4]; 村上 豪 [5]; 土屋 史紀 [6]; 木村 智樹 [7]; 吉川 一朗 [8]
[1] 東大・理・地惑; [2] 東大・新・複雑; [3] 東大・新領域; [4] 東大・理・地惑; [5] ISAS/JAXA; [6] 東北大・理・惑星プラズマ大気; [7] Tohoku University; [8] 東大・理・地惑

Identifying the energy supply process for the Io plasma torus during the sudden brightening events.

Seiya Nishimura[1]; Fumiharu Suzuki[2]; Kazuo Yoshioka[3]; Reina Hikida[4]; Go Murakami[5]; Fuminori Tsuchiya[6]; Tomoki Kimura[7]; Ichiro Yoshikawa[8]
[1] Earth and Planetary Science, UTokyo; [2] Complexity Science, Univ. of Tokyo; [3] The Univ. of Tokyo; [4] the Univ. of Tokyo; [5] ISAS/JAXA; [6] Planet. Plasma Atmos. Res. Cent., Tohoku Univ.; [7] Tohoku University; [8] EPS, Univ. of Tokyo

The terawatt order radiative emission from the Io plasma torus (IPT) has been observed. To balance with this energy loss, ion pick up mechanism is thought to be a major energy input. Sulfur and oxygen atoms, ejected by the Io's volcanic activity, are ionized and subsequently accelerated to near corotation with the Jovian magnetic field. The kinetic energy of the ions then heats the electrons by coulomb collisions. The energy supply only by this process is insufficient to balance with the observed energy emission. Current energetic models for the IPT introduce *ad hoc* non-pickup energy input. Smith et al. (1988) has suggested that radially inward diffusing hot ions could compensate for the missing input energy. The physical chemistry models of the IPT introduced by such as Delamere and Bgaenal (2003, 2011), are implying that hot electrons are important to maintain the energy balance. However, there are no observational evidence for these non-pickup energy supply processes.

In this study, we identify the energy supply process during sudden brightening events of the IPT observed by Hisaki satellite. The durations of the IPT brightenings were measured using the light curves. Most of the durations were shorter than 25 hours. Based on the calculations regarding relaxation time for coulomb collisions, short-lived events suggest that hot electrons (not ions), which energies are several hundreds of eV, should contribute to the IPT brightening events.

ひさき衛星観測との比較を目指した木星内部磁気圏プラズマの動径方向拡散モデルの開発

山口 和輝 [1]; 坂野井 健 [2]; 土屋 史紀 [3]; 木村 智樹 [4]; 古賀 亮一 [5]; 鍵谷 将人 [6]
[1] 東北大・理・地物; [2] 東北大・理; [3] 東北大・理・惑星プラズマ大気; [4] Tohoku University; [5] 東北大・理・地物; [6] 東北大・理・惑星プラズマ大気研究センター

Development of a radial diffusion model of Jovian inner magnetospheric plasma transportation for a comparison with HISAKI data

Kazuki Yamaguchi[1]; Takeshi Sakanoi[2]; Fuminori Tsuchiya[3]; Tomoki Kimura[4]; Ryoichi Koga[5]; Masato Kagitani[6]
[1] PPARC, Tohoku Univ.; [2] Grad. School of Science, Tohoku Univ.; [3] Planet. Plasma Atmos. Res. Cent., Tohoku Univ.; [4] Tohoku University; [5] Geophysics, Tohoku Univ.; [6] PPARC, Tohoku Univ

We developed a diffusion model that enables to examine interaction and radial transport of ions and electron in the Jovian inner magnetosphere, balance of mass and energy of plasmas, and temporal changes. We also aim to verify the observation result of the extreme ultraviolet spectroscope satellite HISAKI using this model.

Jovian first satellite Io has active volcanoes and releases the plasma of the volcanic gas origin to the inner magnetosphere. The plasma is distributed in a donut shape along the revolution orbit of Io by co-rotating with Jupiter, and it is called Io Plasma Torus. 90% of total mass of Jovian magnetospheric plasma is supplied from Io and is transported on the time scale of several tens of days in the radial direction while obtaining energy from the rotation angular momentum of Jupiter. Revealing the mass and energy balance of plasmas in the Jovian inner magnetosphere is an important subject to understand the macroscopic physical phenomena of the magnetosphere.

The radial distribution model of steady state Jovian magnetospheric plasma has been developed based on observation results of Voyager 1, Voyager 2, Cassini spacecraft, but there is no research report on a model capable of tracking time variation of radial distribution.

The purpose of this research is to develop a model that can track the time change of the radial direction transport process of mass and energy of plasma and compare it with observation result of HISAKI.

In this study, a model that can track mass and energy balances of major heavy ions of Io origin (O^+,O^{2+},S^+,S^{2+},S^{3+}) and time evolution of radial transport was developed based on the Fokker-Planck equation. The equation system is based on the mass and energy transport model of steady state magnetospheric plasma developed by Delamere et al. (2005), and it was differentiated by FTCS method. The chemical interaction between ions and electrons is considered by charge exchange, electron impact ionization, electron recombination, Coulomb interaction, and radiation due to electron collision excitation, and radiative rate is calculated from the CHIANTI database based on the method shown in Delamere and Bagenal (2003). The initial values of temperature and density of each ion species and thermal electrons were given in Yoshioka et al. (2018) that obtained from the HISAKI satellite observations in November 2013 when the volcano activity was quiet. The neutral atoms (O,S) were parameterized by the inflow composition ratio of oxygen and sulfur and the total number of neutral particles. For the inner and outer boundary conditions, the spatial differentiation of the density was 0 and the ion temperature was 60 eV at 6 R_J, and plasma density and temperature were fixed with extrapolated values of HISAKI observation results at 30 R_J. In order to verify the validity of the model, the steady state temperature and density of ions and electrons in the region of 6-9 RJ were compared with the observation results of HISAKI. Our model result showed that the density of ions is about 10% less than the observed value, and the temperature is about 20 times greater than the observed value (for example, O_+ temperature exceeded 2 keV). Estimating ion and ion scale heights with the different distribution surfaces between neutrals and ions, we obtained the ion density which is 25% of the observed value and the temperature which is about 10 times greater than the observed value. As a result, the oxygen-sulfur ratio is 2.0, the inflow is 50x10^{-4} (m^{-3}), and the diffusion coefficient is estimated to be 4.2x10^{-8} ($R_J{}^{-2}s^{-2}$) near Io. This result is consistent in the Io plasma whose main atmospheric composition is SO_2. In this presentation, the correspondence between the quantitative inspection results of each parameter and the observation results of HISAKI is described.

惑星分光観測衛星ひさきは衛星イオの火山活動の変化に伴う木星内部磁気圏でのプラズマ増大・減少を捉えた。本研究は、木星内部磁気圏の複数のイオンおよび電子間の相互作用と動径方向輸送を理解することを目的とし、プラズマの質量及びエネルギーの収支と時間変化の追跡が可能な拡散モデルを開発した。モデル結果とひさき衛星の観測と比較を行い、観測に整合的な中性粒子流入量と拡散係数が得られた。

木星第一衛星イオでは活発な火山活動があり、内部磁気圏のプラズマは質量の 9 割がイオの大気から供給される。プラズマは木星と共回転することでイオの公転軌道に沿ってドーナツ状に分布し、イオプラズマトーラスと呼ばれている。プラズマは木星の自転角運動量からエネルギーを得ながら動径方向に数十日の時間スケールで輸送される。この輸送は、遠心力による交換型不安定により駆動されていると考えられており、輸送の過程で、衛星起源の重イオンプラズマは化学的な相互作用によって組成比、エネルギーが変化する [Delamere & Bagenal, 2003]。内部磁気圏におけるプラズマの質量とエネルギーの収支を知ることは、磁気圏のマクロな物理現象を理解する上で重要な課題である。

定常状態の内部磁気圏プラズマの動径方向分布モデルは Voyager1,Voyager2,Cassini 探査機の観測結果に基づいて開発

されている [Delamere et al., 2005]。しかし、動径方向分布の時間変動を追跡できるモデルは研究報告がない。その背景として、これまでの探査機が、イオプラズマトーラスの空間分布を長期観測できなかったことが挙げられる。ひさき衛星は惑星観測専用の宇宙望遠鏡として連続運用されており、木星内部磁気圏の長期観測が可能である。実際に 2015 年 1 月下旬から 4 月上旬の約二か月間にわたって、イオからのプラズマ供給の増加に伴うイオプラズマトーラスの空間分布の変化が捉えられた [Tsuchiya et al., 2018, Yoshioka et al., 2018]。

本研究ではイオ起源の主要な重イオン（O^+,O^{2+},S^+,S^{2+},S^{3+}）の質量およびエネルギーの収支と動径方向輸送の時間発展を追跡可能なモデルを Fokker-Planck 方程式に基づき開発した。方程式系は Delamere et al.（2005）が開発した定常状態の磁気圏プラズマの質量およびエネルギー輸送モデルを基に、Forward Time Central Space（FTCS）法により差分化した。イオン、電子間の化学的な相互作用は Delamere & Bagenal (2003) で用いられている電荷交換、電子衝突電離、電子再結合、クーロン相互作用を採用し、電子衝突励起による体積放射率は CHIANTI データベースを利用して算出した。各イオン種と熱的電子の温度、密度の初期値は、イオ火山活動が静穏であった 2013 年 11 月のひさき衛星観測結果を用いた [Yoshioka et al., 2018]。中性原子（O,S）は流入する酸素・硫黄の組成比と単位時間あたりに流入する中性粒子の総数をパラメータとした。内側境界条件は $6R_J$ で密度の空間微分を 0、イオン温度を 60eV とし、外側境界条件は $30R_J$ で密度、温度ともにひさき観測結果の外挿値で固定した。この設定の下でモデルの妥当性を検証するため、6-9R_J の領域における各イオン種と電子の定常状態の温度、密度をひさき衛星の観測結果と比較した。この結果、定常状態におけるイオンの密度は観測に対し 10%程度しかなく、また温度は O^+ が 2000eV 以上となるなど、観測の 20 倍ほど大きな値となった。木星は自転軸と磁軸が一致していないため、荷電粒子と中性粒子の分布面に約 7° の傾きがある。これは、電子衝突励起などの化学的相互作用に影響を与えると考えられる。今回の発表では新たにこの分布面の傾きを計算に反映させ、また各中性粒子、イオンの相対的スケールハイトを再定義することでイオン密度を観測の 25%、温度を観測の 10 倍程度と、より現実的な 値を得ることができた。

さらに、中性原子の酸素・硫黄比、中性原子流入量、拡散係数をパラメータとし、観測に最も合致する値を求めた。この結果、酸素・硫黄比が 2.0 で、流入量、拡散係数はイオ近傍でそれぞれ $50x10^{-4}$ ($/m^3$)、$4.2x10^{-8}$ ($/R_J{}^2{*}sec$) と見積もられた。この結果は SO_2 を主要大気組成とするイオプラズマにおいて整合的である。本発表では各パラメータの定量的な検証結果とひさき観測結果との対応ついて述べる。

アルマを用いた木星放射線帯変動メカニズムの解明に向けて

北 元 [1]; 佐川 英夫 [2]; 垰 千尋 [3]; 黒田 剛史 [4]; 土屋 史紀 [5]; 三澤 浩昭 [6]; 笠羽 康正 [4]; 藤本 正樹 [7]
[1] 宇宙科学研究所; [2] 京都産業大学; [3] 情報通信研究機構; [4] 東北大・理; [5] 東北大・理・惑星プラズマ大気; [6] 東北大・理・惑星プラズマ大気研究センター; [7] 宇宙研

Investigation of variation mechanisms of the Jovian radiation belt using ALMA

Hajime Kita[1]; Hideo Sagawa[2]; Chihiro Tao[3]; Takeshi Kuroda[4]; Fuminori Tsuchiya[5]; Hiroaki Misawa[6]; Yasumasa Kasaba[4]; Masaki Fujimoto[7]
[1] ISAS/JAXA; [2] Kyoto Sangyo University; [3] NICT; [4] Tohoku Univ.; [5] Planet. Plasma Atmos. Res. Cent., Tohoku Univ.; [6] PPARC, Tohoku Univ.; [7] ISAS, JAXA

Jupiter is now considered as an archetype for gas giants that widely exist in extrasolar systems. At the outermost layer of this giant planet, there is a 300 km-depth of the nearly isothermal atmospheric layer (stratosphere) above the massive troposphere. Jupiter is also known to be a fast rotator (with a period of 9.9 h) with an enormous magnetic field. High energy particles trapped in the magnetic field form a radiation belt around the planet, much stronger than the terrestrial Van Allen's belt. In the case of the Earth, the primary control factor of the radiation belt is the solar wind, while the solar wind is difficult to impact the Jovian radiation belt because of the intense magnetic field.

It is theoretically expected that the driving mechanism of Jovian radiation belt is due to the interaction between the radiation belt and the upper atmospheric dynamics: neutral wind perturbations and diurnal wind system control the radial diffusion and spatial distribution of the energetic particles, respectively. Therefore, precise measurements of Jovian wind field are essential for not only the dynamics of the stratosphere but also the magnetosphere.

ALMA's unprecedented high spatial-spectral resolution enables us to extract the limb emission of the trace gasses in the Jovian upper stratosphere with a few tens m/s sensitivity. It is well known that HCN and CS have been injected into Jupiter by the Shoemaker-Levy 9 impact and they distribute only in the upper atmosphere (p ˜0.4-1mbar). Therefore, the Doppler shift of those molecular emission lines can be used to investigate the dynamics in the upper atmosphere particularly at the limb of the Jovian disk where the line-of-sight direction is equal to the horizontal direction of the atmosphere. We will present the sensitivity of ALMA observation to measuring Jovian stratospheric winds, and discuss its capability of constraining the magnetosphere-atmosphere coupling. A test analysis is carried out using JVO ALMA archive data.

木星は、地球と比較して強力な磁場や10時間の高速自転、太陽系外縁の弱められた太陽風といった諸要素に支配され、地球とは異なった磁気圏を形成している。地球は太陽風による影響を受けるため「太陽風駆動型」と称され、一方で木星は「回転駆動型」と対比されている。

木星放射線帯には太陽系内最大であり、安定した領域だと考えられてきたが、1990年代以降の地上観測によって数日から数週間の時間スケールで変動しているということが明らかになった。理論予測によると、太陽紫外線が熱圏大気を加熱して中性風の擾乱を引き起こし、ダイナモ電場の擾乱が誘発されることにより放射線帯内部で動径拡散が増大と考えられている。更に、熱圏風の昼夜対流により生じる電離圏ダイナモ電場のポテンシャルが朝夕間で異なることにより、磁力線を介して電離圏と結ばれた放射線帯粒子の空間分布が変化することも予想されている。これまでの研究から太陽紫外線と放射線帯の相関関係が明らかとなったが、上層大気の風速変動については解明されていない。従って、上層大気の風速場を観測することは成層圏のダイナミクスだけでなく、放射線帯の時空間変動の解明にも繋がる。

そこで我々はアルマの高空間・周波数分解能に着目した。木星成層圏にはHCNやCSが存在しており、サブミリ波帯で観測が可能である。これらの分子をトレーサーとして、輝線のドップラーシフトから成層圏の風速場を知ることができる。本発表ではアルマの公開データを用いた、木星放射線帯—上層大気結合の検証結果について報告する。

木星放射線帯と磁気圏尾部再結合現象との関連性の探査 - II

三澤 浩昭 [1]; 北 元 [2]; 土屋 史紀 [3]
[1] 東北大・理・惑星プラズマ大気研究センター; [2] 宇宙科学研究所; [3] 東北大・理・惑星プラズマ大気

Examination of the relation between Jupiter's inner magnetosphere and magnetic reconfiguration events - II

Hiroaki Misawa[1]; Hajime Kita[2]; Fuminori Tsuchiya[3]
[1] PPARC, Tohoku Univ.; [2] ISAS/JAXA; [3] Planet. Plasma Atmos. Res. Cent., Tohoku Univ.

http://pparc.gp.tohoku.ac.jp/index.html

It is known that Jupiter's synchrotron radiation (JSR) has information on dynamics of the deep inner magnetosphere. We have made JSR observations more than a decade, and has showed that JSR generally shows short term variations by more than several tens percent with the time scale of days to weeks. A plausible causality of such the short term variations is due to solar UV/EUV variations initially proposed by Brice and McDonough (Icarus, 1973) and observationally confirmed by several groups including us, which is so to speak an externally driving process. However, this scenario cannot be always applicable to any short term JSR variations, rapid flux variations with the time scale within a few days (hereafter RFV), and any other processes are required.

As a process which might explain RFV, an internally driving process, so-called 'substorm like event' is known (see Louarn et al., JGR, 2014). This phenomena is interpreted as a magnetic reconfiguration event occurred in the Jupiter's magnetotail region. Although it is revealed that major magnetic reconfiguration events generally affect the whole magnesphere from 10 to 80-120 Rj (Jupiter's radii), however, it has not been known whether the events affect the deep inner magnetosphere within a few Rj.

In order to reveal unknown dynamics of RFV, we have tried to examine relationship between the fast JSR variations and magnetic reconfiguration events. In this study we have used Jupiter's particular radio wave component in the hectrometer wave range (HOM) as an indicator of RFV (cf. Misawa et al., sgepss2018), and have compared them with JSR total flux data observed with the Kashima 34m radio telescope of NICT at 2.3GHz and radio imaging data observed with the GMRT, India at 1.4GHz. A preliminary result shows a positive correlation between JSR variations and occurrence of the particular HOM. In the presentation, we will show results of the observational comparison and will discuss possible linkage processes.

木星氷衛星探査衛星 JUICE, 日本からの貢献 ー プロジェクトの概況、現状、そして展望

笠羽 康正 [1]; 関根 康人 [2]; 塩谷 圭吾 [3]; 浅村 和史 [4]; 笠井 康子 [5]; 春山 純一 [6]; 松岡 彩子 [7]
[1] 東北大・理; [2] 東大・理・地惑; [3] 宇宙研; [4] 宇宙研; [5] NICT; [6] JAXA; [7] JAXA 宇宙研

Jupiter Icy Moons Explorer (JUICE), with the contribution from Japan:Overview, recent status, and perspectives

Yasumasa Kasaba[1]; Yasuhito Sekine[2]; Keigo Enya[3]; Kazushi Asamura[4]; Yasuko Kasai[5]; Junichi Haruyama[6]; Ayako Matsuoka[7]
[1] Tohoku Univ.; [2] Earth & Planetary Sci., Univ. of Tokyo; [3] JAXA/ISAS; [4] ISAS/JAXA; [5] NICT; [6] JAXA; [7] ISAS/JAXA

JUpiter ICy moons Explorer (JUICE) is ESA's first L-class mission and will perform detailed observations of Jupiter and three of its large icy moons, Europa, Ganymede, and Callisto, suing the eleven onboard instruments. Japan is a junior partner of the JUICE mission and is participating into the development of four instruments (PEP, RPWI, GALA, and SWI) and into the science teams of six instruments (the above four plus JANUS and J-MAG).

This paper will present the overview, recent status, and perspectives of this unique project and the contribution from Japan. Toward the planned launch year 2022, JUICE is going to provide a unique and first opportunity for Japanese planetary science community to be involved in Outer Solar System exploration. We will also provide the links to the
on-going and planned outer planetary missions in the international level.

JUICE (Jupiter Icy Moon Explorer) は、木星系磁気圏、大気、氷衛星フライバイ観測および氷衛星ガニメデの周回観測が目的である。現在、2022 年の打上に向け急速に開発中で、2030 年に木星系到着、2032 年にガニメデ周回軌道投入、約８か月後の 2033 年 6 月に終了する。本講演は、この欧州最大の惑星探査ミッションへの日本からの貢献について、プロジェクトの概況、現状、そして展望を報告する。接続する進行中・計画中の国際的外惑星探査の状況も述べる。

Development of a low-energy energetic neutral atom analyzer (PEP/JNA) for JUICE mission

Kazushi Asamura[1]; Yoshifumi Saito[2]; Manabu Shimoyama[3]; Yoshifumi Futaana[3]; Yoshizumi Miyoshi[4]
[1] ISAS/JAXA; [2] ISAS; [3] IRF; [4] ISEE, Nagoya Univ.

We are developping a low-energy (10eV-3keV) energetic neutral atom analyser (PEP/JNA) which is to be onboard European JUICE spacecraft. Ganymede has its own intrinsic magnetic moment. There is considered to be a magnetosphere around Ganymede because of interactions between plasma in the Jovian magnetosphere and Ganmede's magnetic field. However, its characteristics is different from the terrstrical one, since Alfven mach number of upstream plasma flow (corotational plasma flow around Jupiter) is less than 1 (sub-sonic). JNA (Jovian Neutral Analyzer) will reveal characteristics of the Ganymede's magnetosphere by measurement of scattered and sputtered particles generated by precipitation of plasma particles onto Ganymede's surface. Measurement of these particles will provide spatial distribution of plasmas in remote sense, since electric/magnetic field do not affect trajectories of neutral particles. For the instrument development, the flight model is under manufaturing. We will discuss current status of JNA.

Development of KOSEN-1 CubeSat for Jupiter's decametric radio observation

Kazumasa Imai[1]; Nobuto Hirakoso[2]; Taku Takada[3]; Kentarou Kitamura[4]; Masafumi Imai[5]; Kazumasa Imai KOSEN-1 Team[6]; Charles A. Higgins[7]; James R. Thieman[8]; Kazumasa Imai NASA Radio JOVE Team[6]
[1] NIT, Kochi; [2] NIT,Gunma; [3] Kochi-CT; [4] NIT, Tokuyama College; [5] University of Iowa; [6] -; [7] Middle Tennesee State University; [8] University of Maryland Baltimore County

Since the discovery of Jupiter's decametric radio emissions in 1955, important details of its radiation mechanism have not yet been determined. In order to investigate the beaming structure of Jupiter's radio emission and to clarify aspects of the emission mechanism, we are developing a 2U-size CubeSat for observation of Jupiter's radio waves and observe simultaneously in outer space and on the Earth.

Our application was selected on Dec. 12, 2018, as a CubeSat candidate for JAXA's innovative satellite technology demonstration program. The 2U-CubeSat, named KOSEN-1, is planned to be launched by a JAXA Epsilon rocket at the end of 2020. After the launch of KOSEN-1, we will deploy a half-wave dipole antenna at 20.5MHz. The Software Defined Receiver (SDR) will be used to receive Jupiter radio waves over a 2MHz band width. An onboard GPS module will be used to maintain a time accuracy within 1 millisecond between the satellite and the ground station. Selected short duration radio data events (Jupiter S-bursts) will be saved to data storage by the onboard computer (Raspberry Pi Zero compatible Computer Module 1) and transmitted to the ground station at the communication speed of 9600bps by using the 430MHz Amateur radio band.

The measurement of the delay time between the CubeSat and ground observatories by the correlation analysis of Jupiter's S-bursts is proposed to reveal the beaming structure of Jupiter's radio emissions. The worldwide ground-based observations together with the KOSEN-1 satellite will be supported by the NASA Radio JOVE project, an education and outreach program for planetary radio astronomy. The elucidation of the radiation mechanism of Jupiter radio waves, which is the ultimate goal of Jupiter radio research, may lead to a better understanding of particle-wave energy generation mechanisms and their applications. This mission is believed to be significant based on the potential scientific contribution to this subject.

The KOSEN-1 project is supported by the Coordination Funds for Promoting AeroSpace Utilization of the Ministry of Education, Culture, Sports, Science and Technology (MEXT), JAPAN.

Effects of the IMF direction on ion escape mechanism under a weak intrinsic magnetic field condition at Mars

Shotaro Sakai[1]; Kanako Seki[1]; Naoki Terada[2]; Hiroyuki Shinagawa[3]; Ryoya Sakata[1]; Takashi Tanaka[4]; Yusuke Ebihara[5]

[1] Dept. Earth & Planetary Sci., Science, Univ. Tokyo; [2] Dept. Geophys., Grad. Sch. Sci., Tohoku Univ.; [3] NICT; [4] REPPU code Institute; [5] RISH, Kyoto Univ.

It is considered that Mars had kept the warm and wet climate before ˜4 billion years. However, atmosphere and water are lost by certain processes, resulting in that present Mars only leave thin atmosphere. One candidate of the escape mechanism is the ion outflow from the upper atmosphere associated with the magnetic field. It is expected that ancient Mars had a global intrinsic magnetic field because there exists the crustal magnetic field in present Mars, and thus investing the effect of intrinsic magnetic field on the ion escape leads to understanding the climate change of Mars from past through present.

The planetary intrinsic magnetic field is significantly important in considering the atmospheric escape from planets. The strength of intrinsic field particularly affects the interaction between the solar wind and terrestrial-type planets (e.g., Seki et al., 2001), and it would change the escape mechanism. The direction of interplanetary magnetic field (IMF) significantly changes the magnetospheric configuration, influencing the atmospheric escape rate and mechanism. Sakai et al. (2018) investigated the effect of a weak intrinsic magnetic field at the Martian equatorial surface on the escape mechanism. It was shown that the existence of the weak field results in an enhancement of the ion escape rate. A parker-spiral IMF was however used in order to obtain the escape rate in this earlier study. This study investigates effects of the IMF direction on the ion escape, when Mars has a weak intrinsic magnetic field. Three IMF conditions, namely, the northward, southward, and Parker-spiral IMFs under present solar wind conditions are compared based on multispecies magnetohydrodynamics simulations. In the northward IMF case, molecular ions escape from the high-latitude lobe-reconnection region, where ionospheric ions transported upward along the open field lines. Oxygen ions originated either in ionosphere or oxygen corona escape from a broader ring-shaped region in the magnetotail. In the southward IMF case, escape flux of heavy ions increases significantly and have two peaks around the equatorial tail flanks in dawn and dusk. The draped IMF can penetrate into the subsolar ionosphere by erosion and the IMF is mass-loaded as it is transported through the dayside ionosphere. The mass-loaded draped IMF is carried to the tail, contributing to the ion escape. The escape channels in the northward and southward IMF cases are quite different from in the Parker-spiral IMF case. The escape rate is higher in the southward IMF than in the northward IMF case. In the northward IMF case, a weak intrinsic dipole forms the magnetosphere configuration similar to Earth, quenching the escape rate, while the southward IMF causes the erosion in the subsolar region, promoting the ion escape from upper atmosphere.

References:

Sakai, S., et al. (2018). *Geophys. Res. Lett.*, *45*, 9336-9343. https://doi.org/10.1029/2018GL079972

Seki, K., et al. (2001). *Science*, *291*, 1939-1941. https://doi.org/10.1126/science.1058913

Atmospheric compositions in the ionosphere/thermosphere on Mars observed by NGIMS and IUVS on MAVEN

Nao Yoshida[1]; Naoki Terada[2]; Hiromu Nakagawa[3]
[1] Geophysics, Tohoku Univ.; [2] Dept. Geophys., Grad. Sch. Sci., Tohoku Univ.; [3] Geophysics, Tohoku Univ.

It is well known that the vertical profile of the composition of a planetary atmosphere is characterized by the compositional boundary, called the homopause, below which gases are well-mixed by eddy diffusion (homosphere) and above which they are diffusively separated according to their own scale heights by molecular diffusion (heterosphere). Since each atmospheric species has a scale height corresponding to its molecular mass in the heterosphere, the mixing ratio of lighter species is expected to increase with altitude above the homopause. The fractionation between the homopause and the exobase determines the relative abundance of species escaping to space [Jakosky et al., 2017]. In addition, the location of homopause altitude influence the thermospheric composition and thereby the species escaping to space [Imamura et al., 2016]. The variations of the atmospheric composition in the thermosphere were poorly constrained due to the complex observing geometry at diverse locations, seasons, and local times of in-situ observations. The relative flux ratios of cold ion outflow, O_2^+:O^+:CO_2^+, from the Martian atmosphere were analyzed using ion mass analyzers [Carlsson et al., 2006; Ludin et al., 2009; Inui et al., 2018]. In Inui et al. [2018], the ratio of O_2^+:O^+:CO_2^+ is almost the same as the density ratio at around 260 km altitude in the Martian ionosphere. Thus, the source altitude of the heavy ions is suggested around 260 km or below. To understand the heavy ions escaping from the Martian atmosphere, it is important to know the atmospheric composition in the upper atmosphere and its variation.

In our previous studies, we investigated that the dayside N_2/CO_2 ratio at 140 km altitude in the Martian thermosphere derived from MAVEN Image UltraViolet Spectrograph (IUVS) during the period from October 2014 to May 2018. We found that the N_2/CO_2 at 140 km altitude significantly varied in the range of 0.02 to 0.20, which shows an annual sinusoidal trend. The higher value appears during aphelion and the lower value during perihelion. In addition, we found a clear latitudinal dependence in Northern summer season. The higher value appears in southern winter hemisphere and the lower value in northern summer hemisphere. In order to reveal the drivers of N_2/CO_2 variations at 140 km, we have examined the effects of surface N_2/CO_2, thermospheric temperature, and homopause altitude. Our results imply that the N_2/CO_2 variation at 140 km is mainly caused by the variation of homopause altitude. Inferred homopause altitude derived from IUVS observation shows that the dayside homopause altitude is located between 60 and 140 km and it has an anti-correlation with the trend of N_2/CO_2 at 140 km. We suggested that a stronger heating in the lower atmosphere due to a closer Sun-Mars distance could cause increase in the homopause altitude and decrease in the mixing ratio of N_2 in the upper atmosphere.

In this paper, we investigate dayside number densities of both neutrals (CO_2, N_2, and O) and ions (CO_2^+, O_2^+, and O^+) species at the exobase (˜200 km) using data from MAVEN Neutral Gas and Ion Spectrometer (NGIMS) to consider the relationship between thermosphere and ionosphere. By combining with our IUVS result, we show the relative importance of effects of external forcing (such as solar wind, solar EUV, SEP etc.) and lower atmospheric phenomena (solar insolation, dust loading) on the upper atmospheric composition.

Development of the hydrogen absorption cell imager for observation of planetary coronas

Masaki Kuwabara[1]; Makoto Taguchi[2]; Kazuo Yoshioka[3]; Takuya Kawahara[4]; Shingo Kameda[5]; Shuhei Yonemoto[6]
[1] ISAS/JAXA; [2] Rikkyo Univ.; [3] The Univ. of Tokyo; [4] Faculty of Engineering, Shinshu University; [5] Rikkyo Univ.; [6] Earth and Planetary Science,Tokyo Univ.

Hydrogen atoms in the planetary exospheres resonantly scatter the solar H Lyman-alpha radiation (121.567 nm) and form planetary hydrogen coronas. By measuring this emission, a density distribution of the hydrogen atom can be estimated. An absorption cell technique is an efficient tool for remote sensing of the planetary coronas and can measure not only density but also temperature distributions. These distributions give us crucial information to estimate quantitatively the escape rate of hydrogen atoms from the present planetary atmosphere. Furthermore, the technique could be suitable for future missions with ultra-small spacecraft because of its smallness, lightness, and simplicity. The performance of the absorption cell is strongly dependent on parameters such as filament shape, applied power, infill gas density, optical path length, and beam path of incident light. New hydrogen absorption cells have been developed for optimization of these parameters, and dependences of their performance on the parameters have been evaluated using an ultra-high spectral resolution Fourier transform spectrometer installed at the DESIRS beamline of Synchrotron SOLEIL in France. From the results of experiments, we have confirmed that the filaments should be thin and that the appropriate gas pressure and applied power should remain, respectively, in the range 100-300 Pa and 1-3 W. In addition, the new cell can be constructed with a weight less than 2 kg including electronics and in an outer envelope smaller than 2U (1U = 10 x 10 x 10 cm^3). Such a compactness is suitable for ultra-small space missions. However, further evaluations of the performances are required. In this presentation, the remaining issues and the current status of the development are presented.

中間赤外ヘテロダイン分光観測から得られた火星中間圏での2018年全球ダストストームによる東西風加速

宮本 明歩 [1]; 中川 広務 [1]; 高見 康介 [1]; 黒田 剛史 [2]; 村田 功 [3]; 寺田 直樹 [4]; 吉田 奈央 [5]; 鳥海 克成 [6]; 笠羽 康正 [2]; 青木 翔平 [7]
[1] 東北大・理・地球物理; [2] 東北大・理; [3] 東北大院・環境; [4] 東北大・理・地物; [5] 東北大・理・地物; [6] 東北大・理・惑星大気; [7] BIRA-IASB

Zonal wind acceleration in the Martian mesosphere during the 2018 global dust storm derived from mid-IR heterodyne spectroscopy

Akiho Miyamoto[1]; Hiromu Nakagawa[1]; Kosuke Takami[1]; Takeshi Kuroda[2]; Isao Murata[3]; Naoki Terada[4]; Nao Yoshida[5]; Katsushige Toriumi[6]; Yasumasa Kasaba[2]; Shohei Aoki[7]
[1] Geophysics, Tohoku Univ.; [2] Tohoku Univ.; [3] Environmental Studies, Tohoku Univ.; [4] Dept. Geophys., Grad. Sch. Sci., Tohoku Univ.; [5] Geophysics, Tohoku Univ.; [6] Geophysics, Tohoku Univ; [7] BIRA-IASB

About the mesospheric winds on Mars, a few of remote sensing observations from ground-based telescopes have been available. Sonnabend et al. [2012] and Moreno et al. [2009] observed at the same altitude as this study and about 50 km respectively showed the retrograde wind at the equator, but the latter suggested a large discrepancy between observed winds and those predicted by a Mars general circulation model (MGCM). We have no explanation about the discrepancy so far. Just below it, recent observations have revealed unexpectedly high abundance of water in the middle atmosphere (1.0˜0.1 Pa), which could affect the atmospheric escape of water to space [Maltagliati et al.,2013]. Heavens et al. [2018] also found that the water vapor abundances in the middle atmosphere are further enhanced during the global dust storm. However, the middle atmosphere during global dust storm is not yet addressed, even though it is proposed that an intensified meridional circulation may transport water vapor effectively [Kuroda et al., 2009; Shaposhnikov et al., 2019]

On June 2018, a global dust storm occurred on Mars. It lasted for more than two months till August. In order to understand the mesospheric response during the dust storm, we have performed the direct measurement of mesospheric zonal winds and temperature on June and September 2018 by our mid-infrared heterodyne spectrometer with an ultra-high spectral resolution, ˜10^7. We used CO_2 non local thermodynamic equilibrium (non-LTE) emission lines at 10 micron from the mesosphere, peaking at ˜80 km (˜0.15 Pa) altitude [Lopez et al., 2011]. It allows us to derive the zonal wind velocity and kinetic temperature at altitudes around 80 km. The former was directly derived from line-of-sight Doppler shift of emission core, and the latter was derived from Doppler width of emission lines. Observations were executed in June (during the dust storm) and in September (decaying phase of dust storm).

We identified that kinetic temperature was changed from 150 K in June (solar longitude, Ls = 197) to 125 K in September (Ls = 242), i.e., decrease with ˜25 K in the middle atmosphere during the descending phase of the storm. We also found that zonal wind velocity was the retrograde wind and changed from ˜223 m/s in June to ˜235 m/s in September, respectively. Those results suggest strong retrograde zonal wind during the global dust storm. The uncertainties of them were ˜34% for kinetic temperature and ˜44% for zonal wind, due to the fitting & pointing errors and wavelength calibration uncertainty.

The decrease of kinetic temperature after the storm time was not reproduced by MGCMs, possibly due to the assumed vertical distributions of dust in the models (cut-off altitude: below ˜80 km and probably not high enough). On the other hand, retrograde wind found in this study shows a reasonable agreement with the previous observations [Moreno et al., 2009; Sonnabend et al.2012]. Although Moreno et al.[2009] did not detect retrograde wind during global dust storm, it showed the increase of wind velocity between normal dust(tau=0.3) and regional dust storm(tau=0.5). However, our result indicates a larger value comparing with previous studies with values ranging from 160 to 200 m/s. This result implies that the global dust storm may intensify the easterly zonal wind in the mesosphere. Meanwhile, Sonnabend et al. [2012] suggests latitudinal variation of wind velocity is about 270 m/s.

In order to clarify the mechanism to accelerate the zonal wind during the global dust storm, we are now comparing the observed features with simulations by a MGCM [Kuroda et al., 2005, 2013, 2015]. We will show the contributions of the meridional advection, vertical advection and eddies on the acceleration of zonal wind due to the global dust storm in the middle atmosphere.

近年の衛星観測によって、モデルでは再現することが出来ない水蒸気遊離層が火星中間圏 (1.0˜0.1 Pa) に発見され、宇宙への水の高速消失を駆動していることが明らかになった [Maltagliati et al.,2013]。また Heavens et al. [2018] は、中間圏の水蒸気量が全球ダストストーム期間中にさらに増加することを観測している。Kuroda et al. [2009]; Shaposhnikov et al. [2019] では強められた子午面循環が水蒸気をより効率的に高高度に輸送している可能性が示唆されているものの、全球ダストストーム期間中の中間圏大気循環の理解は不足しており仮説を立証出来ない。数少ない観測として、Moreno et al. [2009] では静穏時の高度 50km 付近の中間圏赤道域において 60-70 m/s 程度の東風を示しており、火星大気大循環モデル (MGCM) が予測する東風風速に比べて 10-50 m/s 程度強い。また Sonnabend et al. [2012] では本研究と同高度で 270 m/s 程度の東風緯度変化を観測しているが、これについては未だ説明出来ていない。

そこで本研究では、ダストストーム期間中における中間圏の循環を理解するため、2018 年 6 月から 8 月まで続いた全球ダストストーム期間中に 10 μ m 帯の non-LTE CO_2 輝線を高分解能分光観測 [Nakagawa et al.,2016] することで、6 月と 9 月における高度˜80 km (˜0.15 Pa)[Lopez et al., 2011] の温度と風速を導出することに成功した。温度は発光輝線のドップラー幅から導出し、風速は輝線コアのドップラーシフトから直接的に導出している。

解析の結果、中間圏温度は 6 月 (Ls=197) で 150 K、9 月 (Ls=242) で 125 K と、ダストストームが落ち着くにつれて約 25 K 温度が減少したことが分かった。風速については 6 月に 223 m/s、9 月に 235 m/s とダストストーム期間中で強い東風を検出している。ここで温度と風速導出におけるフィッティング誤差、観測時の指向誤差、CO2 レーザー波長の不確定性による誤差は、それぞれ温度で約 34%、風速で約 44%と見積もられている。

一方 MGCM では、6 月で 129 K(光学的厚さ 1.2)、9 月で 135 K(光学的厚さ 0.3) と予測され、本研究で得られた全球ダストストームが落ち着くにつれ観測された温度減少は再現することが出来ない。高度˜80km におけるダストが MGCMs 中では再現されていないために、ダストが太陽光を吸収することによる背景場の加熱が考慮されていない可能性が考えられる。本研究で得られた風速場は、風向き (東風) は先行研究 [Moreno et al., 2009 , Sonnabend et al.,2012] と比較しておおよそ整合的である一方で、その風速強度は先行研究と比べて 160-200 m/s 程度強い結果を示唆している。本講演では、中間圏において全球ダストストームが東風を加速させた可能性を調べるため、観測結果と MGCM [Kuroda et al., 2005, 2013, 2015] による予測を比較し、全球ダストストームによる子午面循環項・鉛直移流項・渦乱流拡散項の中間圏東西風加速への寄与について評価する。

火星探査機MRO搭載熱赤外センサMCSで観測された気温と水氷雲の正相関

上田 真由 [1]; 野口 克行 [1]; 林 寛生 [2]
[1] 奈良女大・理・環境; [2] 富士通 FIP

Positive correlation between temperature and water ice clouds in the Martian atmosphere observed by MRO-MCS

Mayu Ueda[1]; Katsuyuki Noguchi[1]; Hiroo Hayashi[2]
[1] Nara Women's Univ.; [2] Fujitsu FIP

Mars is the fourth planet from the Sun and its colder climate than Earth causes condensation of water vapor to generate water ice clouds. Water ice clouds can influence temperature field by scattering/reflecting the visible light and absorbing/emitting infrared. Previous analyses showed negative correlation between air temperature and water ice cloud [Lee et al, 2009; Wilson and Guzewich, 2014]. We have focused on the relationship between air temperature and water ice cloud opacity observed by Mars Climate Sounder (MCS) onboard Mars Reconnaissance Orbiter (MRO). We calculated zonal correlation coefficients between air temperature and water ice cloud by using five Mars Years' MRO-MCS dataset and found that negative correlation was dominant both in the dayside and the nightside as shown in the previous studies. In part of the middle and high latitude regions, however, we found positive correlation in temperature and water ice cloud opacities. We investigated their zonal structures and found zonal wavenumber 1 and 2 disturbances. We also show the result of Mars Climate Database (MCD) developed by the LMD group in France.

火星は地球の外側に位置する第4惑星であり、地球に比べて寒冷な惑星である。そのため大気中の水蒸気は一部凝結し水氷雲の形で存在している。雲は可視光を散乱・反射、地表からの赤外線を吸収・射出することで気温場に影響を与え得る。本研究は、米国の火星探査機 Mars Reconnaissance Orbiter（MRO）搭載の 熱赤外センサ Mars Climate Sounder（MCS）で得られたデータを用いて、火星大気における気温と水氷雲の相関に着目する。これまでの研究では、火星大気の気温と水氷雲の間には負相関の関係が観測的に見つかっていた [Lee et al, 2009; Wilson and Guzewich, 2014]。しかし、５火星年に及ぶ MRO-MCS データを用いて、気温と水氷雲の東西方向の分布に対して相関係数を求めたところ、確かに負相関を示すデータが多く見られたものの、中高緯度域の一部において高い正相関が見つかった。先行研究と相反するこの正相関の関係を説明する手がかりを得るために、気温と水氷雲の経度・緯度分布と経度・気圧分布を詳細に解析した。その結果、正相関が見つかった領域において気温や水氷雲の分布に東西波数1〜2の構造が存在することが分かった。講演ではフランス・LMD のグループによって開発された火星大気気候モデル Mars Climate Database (MCD) の結果とも比較しながら、この東西構造の成因について議論を行う。

火星古気候の大気・水圏結合モデリング：Valley network 再現に向けて

黒田 剛史 [1]; 鎌田 有紘 [2]; 鳥海 克成 [3]; 笠羽 康正 [1]; 寺田 直樹 [4]; 中川 広務 [5]
[1] 東北大・理; [2] 東北大・理・地物; [3] 東北大・理・惑星大気; [4] 東北大・理・地物; [5] 東北大・理・地球物理

Modeling of the coupled atmosphere-hydrosphere of the Martian paleoclimate: Towards the reproduction of valley networks

Takeshi Kuroda[1]; Arihiro Kamada[2]; Katsushige Toriumi[3]; Yasumasa Kasaba[1]; Naoki Terada[4]; Hiromu Nakagawa[5]
[1] Tohoku Univ.; [2] Geophysics, Tohoku Univ.; [3] Geophysics, Tohoku Univ; [4] Dept. Geophys., Grad. Sch. Sci., Tohoku Univ.; [5] Geophysics, Tohoku Univ.

Though the current Mars is a dry planet, the early Mars during the Noachian and Hesperian boundary (3.85-3.6 Ga) is thought to have been a water-rich planet like the present Earth. The isotopic ratios detected from Martian meteorites showed the evidence of surface pressure of higher than 0.5 bars in ˜4.1 Ga [Kurokawa et al., 2018] and surface water abundance of ˜550 m global equivalent layer around that time [Kurokawa et al., 2016], which should indicate that the surface liquid water made the observed fluvial traces. Also, the topographic evidences of the existence of long-term fluvial system in that time, called as valley networks (VNs), have been observed to represent the past water distributions on Martian surface.

Due to the weak solar luminosity (˜75% of the current value) of early Mars, 3-dimensional numerical studies using Mars global climate models (MGCMs) had shown that the reproduction of surface temperature of above 273K (melting point of water) would be difficult with only the radiative effects of thick (up to 7 bars) CO_2 atmosphere, water vapor and clouds [Forget et al., 2013; Wordsworth et al., 2013]. To solve this contradiction, preceding studies have shown that adding other molecules such as SO_2 [Mischna et al., 2013] or H_2 [Ramirez et al., 2014; Ramirez, 2017] into the radiative schemes would make sense, but no study has performed with 3-dimension including the spatial changes of surface parameters such as liquid water surface (ocean/lake).

We present the results of a newly-developed 3-dimensional Paleo MGCM (PMGCM) assuming the CO_2/H_2O/H_2 atmosphere under the, with surface pressures between 0.3 and 7 bar. The PMGCM also has a hydrologic cycle module, which includes ocean thermodynamics, water vapor advection/convection/condensation/precipitation processes, and surface fluvial activities (e.g. fluvial and sediment transport) with high resolution.

For atmosphere including 3% H_2, the PMGCM simulation with a surface pressure exceeding 1.5 bar indicated that the early Martian surface environment would have been 'cool' (surface temperatures exceeding 273 K during summer to allow seasonal melting of snow-ice deposits, and low enough during winter to produce considerable snow precipitation and accumulation), and 'wet' (characterized by precipitation and seasonal melting of snow/ice), with enough fluvial sediment transport in the low to middle latitudes to reconcile Martian VNs within a relatively short time (less than tens of million years).

However, the simulated distributions of VNs had several discrepancies from the observations. One possible reason is the existence of Tharsis bulge. In the early Martian history, the formation time of Tharsis (the largest volcanic plateau in the Solar system) is under debate, and the presence or absence of Tharsis would be an important parameter in the discussion of the global water circulation in early Mars. Then we also performed the PMGCM simulation with surface topography before the Tharsis load. Our preliminary results with a 1.5 bar CO_2 atmosphere including 3% H_2 showed the reproduction of the clement surface environment and matured surface runoff systems consistent with observed VN systems without Tharsis bulge, while not consistent with Tharsis.

In addition, the sensitivity of different cumulus convection schemes on the simulated precipitation would affect the reproduction of VNs. We are comparing the results between the Relaxed Arakawa-Schubert scheme [Moorthi and Suarez,1991], which is often used in a terrestrial GCM, and the Kain-Fritsch scheme [Kain and Fritsch,1993], which calculates cloud structures in more detail. In the simulation under the terrestrial conditions, we could obtain similar results in both schemes, although there were slight differences in cloud amounts and precipitation. In the presentation we report the results in the early Mars conditions and evaluate the quantitative differences in both schemes.

Structures of planetary-scale waves at Venusian cloud top revealed by an cloud-tracking method tolerant to streaky features

Yusuke Nara[1]; Takeshi Imamura[2]
[1] GSFS, Univ. Tokyo; [2] The University of Tokyo

Ultraviolet (UV) images of Venus show various features of clouds due to inhomogeneously distributed UV absorbers in the cloud layer (Nara et al., 2019). Cloud tracking has been widely used to derive atmospheric motion. As for Venus atmosphere, long term variations of super-rotation (Kouyama et al., 2013), properties of atmospheric waves (e.g. Kouyama et al., 2015; Limaye, 1988), and a relationship between the cloud morphology and wind velocities (Del genio & Rossow, 1990) have been studied.

The atmosphere in the high latitudes of Venus are considered to be unstable due to the strong latitudinal shear of the mean zonal wind associated with mid-latitude jets. A momentum transport caused by such regions is essential to understand the mechanism of super-rotation. However, the discussions of these studies are limited to low latitudes due to the difficulty in cloud tracking in high latitudes, where streak features are predominant. Because the displacement of such streaks along the streak direction cannot be identified, uncertainties in estimated cloud motion vectors become large (Ikegawa & Horinouchi, 2016).

To solve this problem, we developed a method to increase the accuracy of cloud tracking by eliminating streaks from the images. The algorithm finds the orientation of streaks in an image making use of the nature that the brightness gradient takes a minimum along streaks, and then remove the streaks by differentiating the image along the estimated orientation.

Using UV (365 nm) images obtained by UVI on Akatsuki, we deduced velocity fields with cloud tracking proposed in this study. Spectral analysis of the time series detected significant periodicity associated with planetary-scale waves even in high latitudes. We present horizontal structures of the planetary-scale waves and associated momentum transports.

金星の衛星間電波掩蔽観測立案に向けたデータ同化による研究

杉本 憲彦 [1]
[1] 慶大・日吉物理

Data assimilation study for the Venus future mission of radio occultation measurement among small satellites

Norihiko Sugimoto[1]
[1] Physics, Keio Univ.

http://user.keio.ac.jp/~nori/

At the altitudes of approximately 60-70 km in the Venus atmosphere, there is a unique phenomenon called "cold collar" where the temperature of the polar region is higher than that of the surroundings (latitudes of about 60-80 degrees). The Japanese Venus Atmospheric GCM For the Earth Simulator (AFES-Venus) succeeded in the reproduction of cold collar for the first time (Ando et al., 2016). However, the temperature difference between the pole and the surroundings is small compared with that observed. Recently, using the Local Ensemble Transform Kalman Filter (LETKF), we have succeeded in developing the Venus AFES LETKF Data Assimilation System (VALEDAS, Sugimoto et al., 2017). In this study, we investigated the reproducibility of the cold collar by the data assimilation of French Venus Atmospheric GCM (IPSL Venus GCM) in which the cold collar is realistically reproduced (Garate-Lopez & Lebonnois, 2018). We prepared idealized observation data assuming radio occultation measurement among small satellites. We will report the reproducibility of the cold collar by changing the conditions such as observation point, observation number, and time interval. In the results, the cold collar was reproduced when three vertical profiles of temperature observations at 85 degrees north every 6 Earth hours are assimilated. Therefore, such kind of future mission would be promising. Furthermore, there is a bias of the horizontal mean temperature between AFES-Venus and IPSL Venus GCM. Thus, we subtracted a bias using linear interpolation. In this presentation, we will present the results for the reproducibility of the cold collar after the bias correction and discuss effectiveness of the radio occultation measurement among small satellites.

金星大気の高度約 60-70 ☒では、極域が周辺に比べて温度が高くなっており緯度約 60-80 度では低温になる、コールドカラーと呼ばれる現象が存在する。金星大気大循環モデル (AFES-Venus) では、コールドカラーの再現に初めて成功した (安藤他, 2016) が、実際の観測で得られる値に比べて極とコールドカラーの温度差は小さかった。本研究では、より温度差を良く再現するフランスの金星大気大循環モデル (IPSL Venus GCM) のデータ (Garate-Lopez & Lebonnois, 2018) を、局所アンサンブル変換カルマンフィルター (LETKF) を用いた金星大気データ同化システム (VALEDAS；杉本他, 2017) に同化し、コールドカラーの再現可能性を調べた。金星の衛星間電波掩蔽を想定した擬似観測データとして、観測地点、観測数、時間間隔等の条件を変えた一連の実験を行い、コールドカラーの再現性を評価した結果を報告する。北緯 85 度の 3 地点で温度の鉛直分布の観測が 6 時間ごとに得られた場合にコールドカラーの再現は成功し、これは衛星間電波掩蔽観測が有効であることを示唆している。さらに、実験の結果から AFES-Venus と IPSL Venus GCM との間には温度バイアスが存在することを確認した。このため、両者の水平平均温度を比較し、同高度で水平平均温度が等しくなるように線形補間を用いてバイアス補正を行なった。本発表では、バイアス補正後のコールドカラーの再現性と衛星間電波掩蔽観測の有用性についても詳しく議論する。

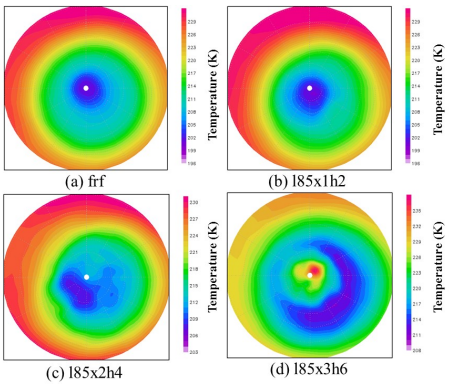

Comparative analysis of the the Rossby wave at the Venusian cloud top observed by Venus Express/VMC and Akatsuki/UVI

Masataka Imai[1]; Toru Kouyama[1]; Takeshi Horinouchi[2]; Shigeto Watanabe[3]; Atsushi Yamazaki[4]; Manabu Yamada[5]; Shin-ya Murakami[6]
[1] AIST; [2] Hokkaido University; [3] Cosmosciences, Hokkaido Univ.; [4] ISAS/JAXA; [5] PERC/Chitech; [6] ISAS/JAXA

Planetary-scale waves at the Venusian cloud-top cause periodic variations in both winds and ultraviolet (UV) brightness. The prominent planetary-scale UV features (sometimes called as the 'Y-feature') might be related to the prominence of these waves, and they hold an important clue to understanding the atmospheric dynamics of Venus.

We analyzed the periodicities in the 365-nm brightness and cloud-tracking winds observed by Akatsuki/UVI. From June to October in 2017, we found the continuous temporal change in the amplitude of 5-days periodical signals. It can be attributed to the temporal evolution of the Rossby wave (Imai et al., submitting), and the corresponding deformation of planetary-scale UV features was captured. The observed Rossby wave was accompanied by the equatorially symmetric planetary-scale vortices. The amplitude of winds amplified gradually over ˜20 days and attenuated over ˜50 days. Following the formation of the Rossby wave vortices, the brightness variation emerges to form rippling white cloud belts in the 45^o–60^o latitudes of both hemispheres.

Our next target is understanding the source mechanism of the Rossby wave observed at the cloud top. By using the Venusian atmospheric general circulation model, Sugimoto et al. (2014) analyzed the temporal evolution of kinetic energy of some wave modes associated with baroclinic instabilities, and they observed several tens of days amplification and longer attenuation. In order to investigate generalities in the temporal evolution of the Rossby wave, we have started to analyze the Venus Express/VMC images in which the prominent Rossby wave signal was reported by Kouyama et al. (2015). We have already captured a similar temporal change in the amplitude of 5-day mode from January to May 2008. In this presentation, we will show the comparative results of the Rossby wave event captured by Akatsuki and Venus Express.

A circumpolar stratospheric telescope FUJIN-2 aiming at identification of a UV absorber in the Venus atmosphere

Yukiko Shirafuji[1]; Makoto Taguchi[2]; Masataka Imai[3]; Yukihiro Takahashi[4]; Mitsuteru SATO[5]; Toshihiko Nakano[6]; Yasuhiro Shoji[7]
[1] Physics, Rikkyo Univ.; [2] Rikkyo Univ.; [3] AIST; [4] Cosmosciences, Hokkaido Univ.; [5] Hokkaido Univ.; [6] Space Engineering, Tohoku Univ.; [7] JAXA

FUJIN-2 is a project to study phenomena in the planetary atmospheres and plasmas by an optical telescope suspended by a balloon up to the polar stratosphere at an altitude around 32 km. FUJIN-2 can observe planets for a long continuous period in a wide wavelength range. Seeing is expected to be 0.1" or less at that altitude, smaller than the diffraction limited spatial resolution of a visible telescope with an aperture of 1 m. Since FUJIN-2 floats above the peak density of the ozone layer, it is possible to observe wavelengths of 280 nm by FUJIN-2. On the other hands the balloon-borne telescope has a disadvantage that its launch depends on the weather condition. We regard that the above merits of the balloon-borne telescope surpass those of the other observation platforms even the disadvantage of balloon observation is admitted.

Venus is covered with thick sulfuric acid (H_2SO_4) clouds throughout the altitude range of 45-70 km. The cloud layer, not the ground surface, absorbs solar radiation and heats the atmosphere. At an altitude of 64 km, 50% of the solar radiation is scattered and absorbed [Tomasko et al., 1980]. The Venus atmosphere also has a special general circulation called as a super rotation, which circulates the entire planet to the west. The wind speed of the super rotation reaches 100 m/s at an altitude of 70 km, 60 times faster than the rotation speed of the solid body.

Attempts to reproduce the high velocity wind by a numerical model are an indispensable approach to theoretically explain the super rotation, and so far a large number of studies have been carried out. However, insufficient understanding about the solar heating makes it difficult to build a sophisticated model which reflects the realistic solar heating and distributions of chemical species. The main reason for this is that an absorber of a broad absorption band in the wavelength range of 320 - 500 nm is still unidentified. The ultraviolet absorption band for the wavelength region shorter than 320 nm is well explained by absorption due to SO_2 centered at 283 nm. However, the absorption in the wavelength region longer than 320 nm cannot be explained by SO_2. Absorbing materials containing S (sulfur) have been proposed to explain the absorption in these several decades. Recently, it is shown that S_2O or OSSO are the most promising candidates for reproducing the edge of the absorption band at 400 - 500 nm. Some researchers propose that microorganisms are also a candidate of the unknown absorber.

The first target of FUJIN-2 is to identify the unknown absorber in the Venus atmosphere. Since the absorption ranges from NUV to the visible region which can be observed from the ground, we have to examine how precisely we can resolve the absorption structure by a ground-based observation. A test spectroscopic observation of Venus was performed with the Pirka telescope in Nayoro City, Hokkaido. As a result, an absorption spectrum at wavelengths shorter than 310 nm could not be acquired, because the signal intensity was weak in the spectral region. In addition, we could not detect the characteristic absorption spectrum of S_2O in the atmospheric absorption spectrum of Venus, though the spectrum clearly showed absorption in the wavelength range shorter than 550 nm.

A Cassegrain telescope with a cler aperture diameter of 400 mm has been under development for FUJIN-2. FUJIN-2 is equipped with the same spectroscopic and imaging observation system used for the observation at Nayoro. Attitude of the gondola is 3-axis stabilized by two pairs of control moment gyros, while only azimuth of the gondola was controlled for FUJIN-1. In order to confirm the performance of the attitude control and guiding system a ground-based test experiment is planned to be carried out in Taiki-cho, Hokkaido in November 2019.

High-resolution spectroscopy of Venus' dayside at 3-4 micron with IRTF/iSHELL

Takao M. Sato[1]; Hideo Sagawa[2]
[1] HIU; [2] Kyoto Sangyo University

Venus is completely shrouded by massive sulfuric acid clouds in altitudes of 50-70 km. Their distribution in space and its temporal change are the key to understand several fundamental subjects in the atmosphere of Venus, such as the energy balance i.e., thermal structure, atmospheric waves' propagation which closely links to the mechanism of the super-rotating atmospheric circulation, and the sulfur-related atmospheric chemistry.

One of observational approaches to the clouds is to retrieve cloud top altitude, by measuring CO_2 absorptions in sunlight reflected from Venus. Since CO_2 is thought to be uniformly mixed in the atmosphere, lower reflectivity observed in CO_2 absorption results from a longer path length to clouds, meaning lower cloud top altitude. Altimetry of Venus' cloud top has been conducted using data provided by Pioneer Venus Orbiter, Venera 15, Venus Express, and Akatsuki. The cloud top has an equatorially symmetric structure and the upper cloud boundary is vertically diffuse in the low and middle latitudes and gets sharper at higher latitudes. No considerable local time and long-term variations have been detected before.

In order to improve climatological knowledge on the clouds, we carried out a high-resolution spectroscopy of Venus' dayside at wavelengths of 3.20-3.48 micron and 3.57-4.18 micron with IRTF/iSHELL on August 5-7, 2018 (UT). Taking the full advantages of its high spectral resolution of R ~75,000, IRTF/iSHELL provides its capability of detecting changes of the CO_2 absorption depths due to the cloud-top altitude variation. This spectrally resolved observations will provide another independent measure of the cloud top altitude to be compared with the results obtained by the narrow-band filter imaging of Akatsuki/IR2. In this presentation, we will show several processed spectra and what can be retrieved from them with radiative transfer calculation.

あかつき/IR1が捉える金星雲全球変動

高木 聖子 [1]
[1] 北海道大学

The global variation of Venus cloud investigated from IR1 onboard AKATSUKI

Seiko Takagi[1]
[1] Hokkaido Univ.

Venus is our nearest neighbor, and has a size very similar to the Earth's. However, previous observations discovered an extremely dense (90 bar at the surface) and CO_2-rich atmosphere, with H_2SO_4 thick clouds. The Venus cloud consists of H_2SO_4 main cloud deck at 40-70 km, with thinner hazes above and below. The upper haze on Venus lies above the main cloud surrounding the planet, ranging from the top of the cloud (70 km) up to as high as 90 km.

Near infrared (0.986 um) dayside image of Venus has taken by solid state imaging (SSI) of the Galileo spacecraft (NASA). It appears almost flat, there are some small scale features with a contrast of 3 % [Belton et al., 1991]. In Takagi and Iwagami. (2011), it may be calculated that the source of the contrast of the order of 3 % in near infrared Venus dayside image is due to variation in the cloud optical thickness.

On December 7, 2015, AKATSUKI (JAXA) approached Venus and the Venus orbit insertion was successful. After the Venus orbit insertion, many 0.90 um Venus dayside images were taken by the 1 um near infrared camera (IR1) onboard AKATSUKI.

In this study, Venus cloud variations are investigated from 0.90 um Venus dayside images taken by IR1 camera globally. Further, meteorological some changes that contribute to cloud variation are examined in using radiative transfer calculation. Furthermore, I will introduce observation plan with PIRKA telescope at NIR wavelength of Hokkaido University.

金星は地球と同程度の大きさと質量を持つ一方で、二酸化炭素を主成分とする分厚い大気は地表面で 90 気圧にも達し、地表面温度は約 500 度という灼熱の世界である。また、硫酸を主成分とする雲の層 (高度 40-70 km) と固体微粒子の層 (もや層, 70-90 km) が浮かび、金星全球を一様に覆っている。

金星探査機あかつき (JAXA) は、2015 年 12 月に金星周回軌道投入に成功した。あかつきは、紫外から中間赤外 (283-10000 nm) の多波長同時撮像観測により、硫酸雲の 3 次元的な動きを詳細に捉えようとしている。搭載近赤外カメラ IR1 は、大気の窓領域である近赤外波長光 [Allen and Crawford, 1984] における撮像観測により、雲全体の光学的厚さの増減を金星表面の明暗として捉える [Takagi and Iwagami. 2011]。木星探査機 Galileo/SSI (NASA) により得られた金星昼面近赤外画像 (0.986 um) では、金星表面の明暗はわずか 3 %と示されている [Belton et al., 1991] が、IR1 はかつて Galileo/SSI が得たものと整合的な昼面画像を多数取得している。

本研究では、IR1 が取得した昼面画像から、雲の明るさとその変動を全球的に把握する。また、雲変動に寄与する金星の気象変化について、放射輸送計算を用いて考察する。さらに北海道大学が所有するピリカ望遠鏡を用いた同波長領域観測計画を紹介する。

ハワイ IRTF/iSHELL 赤外分光データによる木星大赤斑上空を含む熱圏温度観測

神原 歩 [1]; 北 元 [2]; 坂野井 健 [3]; 笠羽 康正 [4]; 鍵谷 将人 [5]
[1] 東北大・理・惑星研; [2] 宇宙科学研究所; [3] 東北大・理; [4] 東北大・理; [5] 東北大・理・惑星プラズマ大気研究センター

Observations of the Jovian thermospheric temperature including the GRS by IRTF/iSHELL

Ayumu Kambara[1]; Hajime Kita[2]; Takeshi Sakanoi[3]; Yasumasa Kasaba[4]; Masato Kagitani[5]
[1] pparc, Tohoku Univ.; [2] ISAS/JAXA; [3] Grad. School of Science, Tohoku Univ.; [4] Tohoku Univ.; [5] PPARC, Tohoku Univ

It is known that the thermospheric temperature of all giant planets including Jupiter is several hundred kelvins higher than that expected from solar heating [Yelle and Miller, 2004]. At mid- to low-latitudes, although the direct atmospheric heating caused by precipitating particles and the energy transportation from the high-latitude auroral region have been considered, it is not enough to explain. Another candidate for the heating is energy transportation by atmospheric waves from the lower atmosphere. Perturbations of temperature due to such atmospheric waves have been confirmed by the observations of the Galileo probe [Young et al., 1997]. Then, we focused on the Great Red Spot. As the Great Red Spot is considering to be an anticycronic storm in the troposphere, atmospheric waves such as atmospheric gravity waves and acoustic waves may be likely to occur in the GRS. By detection the enhancement of temperature in the upper atmosphere above the GRS, we can suggest the energy transport between the lower atmosphere and the upper atmosphere. Recently, O'Donoghue et al. [2016] revealed the heating in the thermosphere above the Great red spot from the intensity ratio of two emission lines (3.383um/3.454um) of the vibrational-rotational spectrum of thermospheric H_3^+ taken by IRTF /SpeX (R˜2500) in December 2012. They estimated that the temperature above the GRS is 1644+/-161K, and that on surrounding mid- to low-latitude region is 900+/-42K. However, the infrared spectrum observed by SpeX might be contaminated by CH_4 line due to its low-resolution capability.

In this study, we carried out the thermosphere temperature observation in the Jovian mid-latitude region near the GRS by IRTF/iSHELL on January 9 and 11, 2017. On Jan. 11, This observation was performed with the iSHELL's Lp1-mode (3.265-3.657um). We installed 15 arcsec slit in the east-west direction and observe the region above the GRS and the surrounding regions simultaneously. This observation acquired the Jovian data and the sky data alternately in 30 sec. Similar to the past study by O'Donoghue et al. [2016], we adopted the intensity ratio of two emission lines of H_3^+ (3.3839um/3.4548um), and estimated the temperature precisely distinguished from CH_4 lines by iSHELL's higher wavelength resolution (R˜75000). As a result, we estimated the thermospheric temperature above the GRS to be 988+/-115K, and that in the surrounding regions to be 889+/-77K, showing about 100K increase above the GRS. On Jan. 9, This observation was performed with the iSHELL's Lp4-mode (3.83-4.14um). We installed 25 arcsec slit in the north-south direction and moved in the east-west direction to observe the region including the GRS. This observation acquired the Jovian data and the sky data alternately in 60 sec. The data reduction was performed with NASA's data reduction tool Spextool ver. 5.0.3beta. In LTE, we estimated the thermospheric temperature by using the intensity ratio (3.9039um/3.9530 um) of the H_3^+ ro-vibrational emission lines. As a result, we obtained the map of Jovian temperature from observation on Jan. 9. The observation on Jan. 11 confirmed the temperature above the GRS is higher than that in the surrounding regions. This may suggest the existence of energy transport from the lower to the upper atmosphere above the GRS. The observation on Jan. 9 was able to take spatial variation of Jovian temperature including the GRS. In this presentation, we report the result of careful reduction.

木星を含む巨大惑星の熱圏は、太陽極端紫外線による加熱による予測温度より数 100K 高温であることが知られている [Yelle and Miller, 2004]。中低緯度での比較的低エネルギー降下粒子による大気直接加熱や、高緯度でのオーロラ領域加熱の低緯度への輸送が高温となっている説明として考えられているがよくわかっていない [Waite et al., 1983]。その他の要因として、下層大気で励起した大気重力波・音波等よるエネルギー輸送がその原因として提唱されている。そのような大気波動による温度の擾乱がガリレオ探査機の観測によって確認されている [Young et al., 1997]。そこで本研究では木星の大赤斑に着目した。大赤斑は対流圏の高気圧性の嵐であると想定されていることから、この領域では大気重力波や音波等の大気波動が発生しやすい可能性がある。大赤斑上の上層大気温度上昇を捉えることで、下層大気-上層大気間のエネルギー輸送現象を明らかにすることが期待される。最近、O'Donoghue et al. [2016] が IRTF 赤外分光装置 SpeX(R˜2500) による H_3^+ 発光の２つの輝線強度（3.383um/3.454um）から熱圏大気温度を推定した結果、大赤斑上で 1644+/-161K、その他中低緯度領域では 900+/-42K と、大赤斑上での加熱を示唆する結果を報告した。

ただし先行研究では波長分解能が低いため、近傍波長 CH_4 の発光輝線が分離できず、温度推定に誤差が残っている可能性が指摘されている。そこで我々は 2017 年 1 月 9、11 日にハワイ・マウナケア山頂にある IRTF のエシェル赤外分光装置 iSHELL を用いて、大赤斑近傍での熱圏大気温度観測を実施した。11 日の観測は、Lp1-mode (3.265-3.657um) を用い、空間方向に 15arcsec のスリットを、大赤斑を含む東西方向に配置し、一つの撮像フレーム内に大赤斑と大赤斑以外の中低緯度領域の情報を同時にとらえた。観測では 30 秒間で木星データ、スカイデータのデータ取得を交互に行った。

熱圏温度推定は、O'Donoghue et al. [2016] と同じ H_3^+ 発光輝線 (3.3839um/3.4548um) を用いた。ここで、3.4548um の輝線近傍に CH_4 輝線が存在するため、精密にその影響を差し引く必要がある。この波長差は最も近接しているものでおよそ $3*10^{-3}$um であり、iSHELL の高波長分解能（R~75000）で分離することができる。この特長を生かして 3.4548um の発光輝線と CH_4 輝線の分離を実現し、より正確な温度推定を可能とした。我々のこれまでの解析結果から、大赤斑の熱圏温度は 988+/-115K、その周囲の同緯度域で 889+/-77K と見積もられ、大赤班上の熱圏温度は周囲より高い傾向があることが明らかになった。また 9 日の観測は iSHELL の Lp4-mode(3.83-4.14um) を用いて、空間方向に 25arcsec のスリットを南北方向に設置し、東西方向に移動させ、大赤斑を含む領域で観測した。観測では木星データ、スカイデータを 60 秒間で交互に取得した。解析において、校正や物理量変換は NASA 提供のデータ補正・校正ツール Spextool ver. 5.0.3beta を用いた。熱圏温度推定には LTE を仮定し、H_3^+ の回転振動励起発光輝線の強度比 (3.9039um/3.9530um) を用いて行った。その結果、大赤斑を含む領域での温度マップを作成し、木星熱圏温度の空間分布を得ることができた。11 日の観測の事実からは大赤斑で発生した大気重力波・音波の熱圏への伝搬の存在の可能性が示唆される。9 日の観測では大赤斑を含む木星温度の空間変動をとられることができた。本講演では、木星の熱圏温度場の観測・データ解析の詳細と、その評価について検討した結果を報告する。

High dynamic-range observation using a low-scattered light telescope PLANETS: design and feasibility study

Masato Kagitani[1]; Takeshi Sakanoi[2]; Toshihisa Suzuki[3]; Yasuhiro Hirahara[4]; Yasumasa Kasaba[5]
[1] PPARC, Tohoku Univ; [2] Grad. School of Science, Tohoku Univ.; [3] Geophysics, Tohoku Univ.; [4] Earth&Planetary Sciences, Nagoya Univ.; [5] Tohoku Univ.

High dynamic-range (HDR) observation is one of the key technique to reveal composition, distribution and dynamics of plasma and neutrals in the vicinity of planets and their moons in our solar system, e.g. water plumes on Europa and Enceladus, volcanic plumes on Io, escaping plasma and neutrals from Venus and Mars, and so on. A low-scattered light telescope, PLANETS (Polarized Light from Atmospheres of Nearby Extra-Terrestrial Systems) would be an 1.8-m off-axis telescope on Mt. Haleakala, Hawaii under collaboration with Japan, USA, Germany, Brazil, and France. The off-axis optical system enables us to achieve HDR measurements without diffraction by support structure of secondary mirror. We present feasibility study of monitoring water plumes on Europa, neutral torus close to Enceladus, and ionosphere on Mars using PLANETS telescope.

To test feasibility of HDR under actual condition of wavefront error was made which includes by an optical system as well as by atmospheric turbulence, modeling the propagation of light though the system was made based on Fraunhofer (far-field) calculations with help from PROPER library (Krist 2007). The optical system consists of an entrance pupil (1.85 m), primary mirror, a deformable mirror, an occulting mask, a Lyot mask on a pupil, and a detector on image plane. We gave wavefront error made by atmospheric turbulence (Fried length is 25 cm for best 10% seeing condition) and the optical system represented with power spectral density. Then, dynamic range of point spread function was calculated for several cases of surface roughness of the primary mirror, 1 to 8 nm r.m.s., and number of control points for active wavefront compensation by a deformable mirror, 7 to 24. Finally we calculated brightness distribution of background continuum, and derived signal-to-noise ratio for each observing target assuming expected brightness and band-width of spectroscopy. For O2+ 561 nm and N2+ 391 nm emissions from Martian ionosphere and O 630 nm emission from Enceladus torus, sufficient signal-to-noise ratio is expected for 2-hour integration by employing wavefront compensation with 7x7 deformable mirror and small roughness of primary mirror, 2-nm r.m.s. Whereas for O 630 nm emissions from water plumes on Europa, wavefront compensation by 24x24 deformable mirror is needed to achieve sufficient signal-to-noise ratio for 2-hour integration.

We also present latest design of the telescope structure. The most part of the telescope structure is reuse of prototype of Kyoto 3.8-m telescope (Kurita and Sato, 2009) which employs commercial truss component for architecture. The structure is characterized by its light-weight and high-stiffness. The primary thin mirror (100 mm thick on edge) is supported by 36 points from bottom. The support structure is under examination by comparing an active support using force-control actuators against whiffle-tree with warping harnesses which both enable to compensate low-frequency wavefront error of the primary mirror. Latest design of the telescope as well as support structure of primary mirror will be presented.

惑星大気観測のためのPLANETS望遠鏡の主鏡支持機構の開発状況

鈴木 駿久 [1]; 鍵谷 将人 [2]; 坂野井 健 [3]; 笠羽 康正 [4]; 平原 靖大 [5]
[1] 東北大・理・地球物理; [2] 東北大・理・惑星プラズマ大気研究センター; [3] 東北大・理; [4] 東北大・理; [5] 名大・院・環境・地球惑星

Development status of PLANETS telescope main mirror support system for observing planetary atmosphere

Toshihisa Suzuki[1]; Masato Kagitani[2]; Takeshi Sakanoi[3]; Yasumasa Kasaba[4]; Yasuhiro Hirahara[5]
[1] Geophysics, Tohoku Univ.; [2] PPARC, Tohoku Univ; [3] Grad. School of Science, Tohoku Univ.; [4] Tohoku Univ.; [5] Earth&Planetary Sciences, Nagoya Univ.

PLANETS (Polarized Light from Atmospheres of Nearby Extra-Terrestrial Systems) telescope is a 1.8m off-axis telescope, which is developed by Tohoku University and international collaboration with Hawaii, Germany, Brazil. It is going to be installed in Japan in 2020, and it is aimed that it will be transferred to Haleakala observatory, which is one of the world's best astronomical observation sites. The main target of PLANETS telescope is faint atmosphere and plasma emission near bright body, such as plume of Europa and Enceladus, Io volcanic eruption and torus, atmospheric escape of Mars and Venus. To perform these observations, it is necessary that diffraction and scattering light is effectively decreased and it gets a good contrast between bright body and faint emission. PLANETS telescope is one of the biggest off-axis telescopes performing in night time, and there is no obstacle of secondary mirror and spider in the light path. The off-axis design enables us to observe high contrast observation. Moreover, to understand such atmospheric and plasma phenomena, long-time continuous monitoring observation is essential, so PLANETS telescope can be continuous observation because it is own instrument. In this presentation, we report development status of main mirror support system which is important to be high contrast observation.

The main mirror of PLANETS telescope is Clearceram Z-HS with 1.8m aperture and 80mm of average thickness. Comparably thin glass with multipoint active supports can enable to decrease polishing process and cost. In this study, we led optimal support load distribution when main mirror is supported by 27 or 36 points and decided maximum load and load error to satisfy observation requirement, which is more than 0.90 of strehl ratio. As a result, maximum support load of each main mirror is about 20kg and support load precision is less than +/- 30g when main mirror is supported by 36 points.

We are developing the main mirror axial support system and evaluate performance collaborated with Tohoku University, Kyoto University, Nagoya University.

We examine two options of the main mirror axial support system, one is force actuator active support with loadcell and the other is whiffletree active support with warping harness referred to TMT telescope and Seimei telescope (Williams et al., 2008). In this study, we tested performance evaluation of force actuator support with loadcell by using one prototype of supporting system. The force actuator structure is that linear actuator which is combined by ball screw and stepping motor moves one end of compression spring and another end of spring transmits thrust to back surface of mirror via cylinder. Spring compression height changes by changing linear actuator length, so it can control thrust of spring. We adopted wave spring CMS40-H9 by SMALLEY company. From resolution of linear actuator and spring constant, it was decided that the maximum thrust is 30kg and resolution is 16g.

Next, we tested repeatability, time stability and hysteresis of prototype force actuator. We measured thrust of cylinder via spring by loadcell with changing linear actuator length. However, we used a substitute wave spring of which maximum thrust was about 10kg in the experiment because CMS40-H9 couldn't get during the test. As a result of test, it was revealed that maximum hysteresis was about 200g between gradually increasing and decreasing thrust. The error of hysteresis was larger than requirement accuracy +/- 30g, but it is thought that error can decrease by closed loop control which feeds back loadcell measuring value. Moreover, we tested time stability of thrust. Time stability of thrust during 30 seconds was less than +/- 5g, and it satisfied requirement precision. In the future, we will perform the same test by using CMS40-H9 to consider the requirement accuracy of telescope support. Moreover, we will compare force actuator with whiffletree and decide supporting system.

PLANETS（Polarized Light from Atmospheres of Nearby Extra-Terrestrial Systems）望遠鏡は，口径 1.8m の非軸望遠鏡であり，東北大学がハワイ，ドイツ，ブラジルとの国際協力のもと開発を進めている．2020 年に国内でファーストライトを迎える予定で，将来的には世界有数の好観測地であるハワイ州マウイ島のハレアカラ観測所への移設を目指している．PLANETS 望遠鏡の観測対象は，エウロパやエンケラドスのプリューム，イオの火山噴出，火星や金星の希薄大気からの電離圏・外圏大気散逸現象など，明るい天体周りの微弱な大気やプラズマの発光現象である．これらの観測を実現するためには，明るい天体からの光の回折と散乱を効果的に抑え，周辺に広がる微弱な発光とのコントラストを上げる必要がある．PLANETS 望遠鏡は夜間使用の望遠鏡としては世界最大級の非軸光学系であり，光路上に副鏡やその支持構造による回折の影響がない．したがって，コロナグラフと補償光学とを組み合わせることで，高コントラストの観測が期待できる．また，先に挙げた大気やプラズマの発光現象を理解するには，数ヶ月から数年に及ぶ長期間のモニタ観測が必要であり，まとまった観測時間を確保できる PLANETS 望遠鏡は，大気変動現象の解明に不可欠である．本発表では，高コントラスト観測を実現する上で重要な主鏡の支持機構についての検討と開発状況について報告する．

PLANETS 望遠鏡の主鏡は，直径 1.8m，平均厚さ 80mm のガラスセラミック（CLEARCERAM）である．比較的薄い硝材を多点で能動的に支えることにより，研磨に必要な工程を短くし，コスト削減を狙う．不適切な支持による鏡面誤差の増大は，像の乱れのみならず，コロナグラフと組み合わせた観測のコントラストを低下させ，重大な支障をきたす．本研究では，主鏡裏面を 27 点および 36 点で支持する場合の最適な支持力分布を導出し，ストレール比が 0.90 以上である観測要求を満たす波面誤差に抑えるために必要な最大支持力とその誤差を検討した．その結果，36 点支持の場合，1 点あたりの最大支持力約 20kg に対して+/- 30g 以下の誤差で制御を行う必要があると判明した．

我々は，東北大，京都大，名古屋大と共同で，主鏡の光軸方向の支持構造の開発と要素試験を実施している．主鏡の光軸方向の支持構造は，フォースアクチュエータとロードセルを組み合わせた能動支持 (Iye et al., 2004) に加えて，TMT 望遠鏡やせいめい望遠鏡を参照しウィッフルツリーにワーピングハーネスを組み合わせた支持 (Williams et al., 2008) を検討している．本研究では，特にフォースアクチュエータとロードセルを組み合わせた支持について， 1 点の支持構造の試作品を用いて性能評価を行った．フォースアクチュエータは，ボールスクリューとステップモータを組み合わせたリニアアクチュエータが圧縮バネの一端を上下させ，バネのもう一端がシリンダーを介してミラーの裏面に推力を伝える構造になっている．リニアアクチュエータの長さを変えることで，ばねの作動高さが変化し，推力を制御することができる．圧縮ばねには SMALLEY 社のウェーブスプリング CMS40-H9 を採用した．ウェーブスプリングは，自然長や作動高さが通常のばね（コイルスプリング）より短いことや，ばねの軸に対して垂直方向に発生する余分な力（サイドフォース）が低減されるという特徴がある．リニアアクチュエータの分解能とバネ定数から求められる最大推力と分解能はそれぞれ 30 kg と 16g となる．

次に製作したフォースアクチュエータの再現性，時間安定性，およびヒステリシスを評価する試験を行った．リニアアクチュエータの長さを変えながらバネを介したシリンダーの推力をロードセルによって測定した．ただし，本実験で用いたウェーブスプリングは実験時に入手できた代替品を用いたため，最大推力が約 10kg であった．試験の結果，推力を徐々に大きくした場合と徐々に小さくした場合とで，最大で約 200g のヒステリシスが生じることが分かった．ヒステリシスによる誤差は要求精度である+/- 30g よりも大きい値であるが，負荷の大きさを変更する際に同じ経路を通る方法や，ロードセルの値をフィードバックする閉制御にすることで誤差を抑えられると考えられる．また推力の時間安定性についても測定を行った．30 秒間における安定性は，推力誤差+/- 5g 以内であり，要求精度を満たすことが分かった．今後，最大推力 30kg を満たすウェーブスプリングでも同様の試験を行い望遠鏡支持の要求仕様を満たすかどうか検討を行う．そしてウィッフルツリーにワーピングハーネスを組み合わせた支持と比較・検討を行い，支持方法を決定する．さらに主鏡の支持点数の決定，各支持点の負荷の変化と波面誤差の関係について調べ，波面誤差を要求精度以内に抑えるように主鏡を能動的に支持する方式を検討する．